Engineered Science
DOI: https://dx.doi.org/10.30919/es8d808

Silver Nanowires: From Synthesis, Growth Mechanism, Device Fabrications to Prospective Engineered Applications

Longxia Yang,[1,#] Xianjun Huang,[2,*,#] Huating Wu,[1,#] Yuanlong Liang,[2] Mao Ye,[3] Wencong Liu,[2] Faling Li,[1] Tao Xu[3,*] and Haicheng Wang[1,*]

Abstract

Due to their excellent electrical conductivity, thermal conductivity, and comprehensive performance on optoelectronics, flexible electronics, and mechanics, silver nanowires (Ag NWs) have attracted much attention and achieved diverse functions comparing other one-dimensional nanomaterials. Ag NWs-based conductive films are considered the most promising substitute for indium tin oxide (ITO) film because they could be expected to solve the problem of scarcity of indium resources and the disadvantage of the unsuitability for bending. A variety of synthesis routes of Ag NWs have been studied, and some applications of Ag NWs-based conductive films have been explored. Plenty of excellent progress had been achieved. However, it remains to find a preferable synthetic route for homogeneous Ag NWs with high yields and to explore the synthesis mechanism of Ag NWs in depth from the thermodynamics and kinetics processes. In this review, we provide a comprehensive summary of the recent progress of Ag NWs from synthesis, growth mechanism, and device fabrications to prospective engineered applications.

Keywords: Silver nanowires; Synthesis; Reaction mechanism; Device fabrication; Engineered applications.
Received: 27 September 2022; Revised: 07 December 2022; Accepted: 23 January 2023.
Article type: Review article.

1. Introduction

One-dimensional (1D) nanomaterials, such as nanotubes, nanowires, nanorods, nanofibers, *etc*.[1-3] have become a research hotspot in the 21st century because of their excellent optical, electrical, thermal, magnetic, and mechanical properties.[4-6] Particularly, silver nanowires (Ag NWs), have inherited silver's high electrical conductivity (6.3×10^7 S/m), excellent thermal conductivity (429 W/(m·K)), and high electro-catalytic efficiency due to their small diameter and high aspect ratio. Furthermore, Ag NWs can exhibit excellent light transmission properties and flexible bending resistance. Therefore, Ag NWs-based conductive films are considered the most promising substitute for indium tin oxide (ITO) film, because they could be expected to solve the problem of scarcity of indium resources and the disadvantage of the unsuitability for bending.

By now, some other kinds of conductive materials, such as carbon nanotubes (CNTs),[7,8] graphene,[9,10] conducting polymers,[11] liquid metals,[12,13] metal nanowires,[14] *etc*. have been investigated intensively. CNTs show moderate conductivity, excellent mechanical properties, chemical stability, and relatively low production costs. However, the commercialization of CNT electrodes is hampered by the lack of scalable and controlled deposition onto flexible substrates. Graphene is reported to have high intrinsic in-plane conductivity and high Fermi velocity with impressive mechanical bendability. Nevertheless, the deposition temperature is high and the yield is low. As for conducting polymers, such as poly(3,4-ethylenedioxythiophene): and polystyrene sulfonate (PEDOT: PSS), which are potentially low cost and have good mechanical ductility, the conductivity

[1] *State Key Laboratory of Advanced Materials for Smart Sensing, China GRINM Group Co. Ltd., Beijing 100088; GRIMAT Engineering Institute Co. Ltd., Beijing 101407; General Research Institute for Nonferrous Metals, Beijing, 100088, P. R. China.*
[2] *School of Electronic Science and Engineering, National University of Defense Technology, Changsha, 410073, P. R. China.*
[3] *SEU-FEI Nano-Pico Center, Key Lab of MEMS of Ministry of Education, Southeast University, Nanjing 210096, P. R. China.*
 # These authors contributed to this work equally.
**Email:* huangxianjun001@163.com (X. Huang), xt@seu.edu.cn (T. Xu), hcwang@grinm.com (H. Wang)

is rather relatively poor. Although liquid metals are metallic conductors with infinite deformability, their chemical stability, unstable electrical contact with other metals, and control of movement are not negligible.[15]

Ag NWs could be obtained with good synthetic scalability, reproducibility, and compatibility with low-cost, large-area, and solution-based manufacturing processes.[16] Nowadays, there are plenty of routes for the synthesis of Ag NWs, and then Ag NWs-based conductive films can be fabricated on rigid or flexible substrates with curved surfaces by scraping, spraying, and spin coating.[17-21] Ag NWs and Ag NWs-based films could be applied in flexible optoelectronic devices,[22,23] electromagnetic shielding,[24,25] intelligent sensors,[26,27] flexible transparent heaters[28-30] and so on.

It should be noted that the synthesis of large-scale and uniform Ag NWs is crucial for the successful application and wide popularization of Ag NW-based devices. For this point, many researchers dedicated their efforts toward the synthesis of Ag NWs with uniform size, high aspect ratio, and high yields in recent years. For example, Xia and coworkers have reported a variety of work on silver nanostructures,[31-34] which promoted the development of preparation and application of Ag NWs. Growing attention is focused on the use of soft and hard template methods, a range of wet-chemical techniques (such as hydrothermal, solvothermal, and polyol-based synthesis), and the electrospinning method.[35-40] Particularly, polyol-based synthesis is a relatively dominant route due to its plenty of advantages such as high quality, easy to control, and industrial applicability. Ag NWs obtained by these methods have a wide range of aspect ratios (up to ~5000). It has been proved that the morphology and yield of Ag NWs are affected by many factors, such as reaction temperature, concentration and injection rate of $AgNO_3$, salt mediator, concentration and molecular weight of PVP, *etc*. Up to now, one preferable synthesis route with high-yield homogeneous Ag NWs still needs to be explored.

Researchers have attempted to gain insight into the synthesis mechanism of Ag NWs. Some reviews had summarized that the morphology and size will affect the performance of Ag NWs-based devices.[16,41] Controllable synthesis of Ag NWs is essential but the control mechanism is not described comprehensively in previous reviews. The synthesis mechanism of Ag NWs from the thermodynamics and kinetics process should be addressed further.

The successful large-scale applications of Ag NWs are still hindered by some challenges, such as geometric controllability, electronic and mechanical stability, reducing contact resistance, and device manufacturing simplicity.[42,43] Many researchers are actively addressing these problems, paving the way for the industrial development of Ag NWs. Some work had been recently reported about reducing the insulation coating of nanowires by solvent cleaning or acid treatment, in order to reduce the contact resistance.[44,45]

Most conventional electromagnetic shielding composites are opaque, while Ag NWs films are considered the most promising transparent electromagnetic interference shielding materials due to their good electrical conductivity, high light transmittance, and easy manufacturing.[46,47] Especially in some aerospace optical systems, such as optical windows and electronic displays,[48] transparent electromagnetic shielding films can meet the requirements of electromagnetic functionality and optical visibility at the same time, so that their signal detection and optical observation functions can be guaranteed. With the rapid development of flexible electronics, transparent film heaters based on Ag NWs are also widely used in the field of smart windows[49,50] and personal health management.[51] For example, S.H. Ko *et al*.[52] used the transparent conductive film of Ag NWs (about 100 nm in diameter and about 100 μm in length) as electronic skin, which can effectively monitor the bioelectric signals of the heart, brain, muscle, and other parts. In this review, we further discuss the application of Ag NWs in optoelectronic devices, including photovoltaic, light emitting devices, and touch screens; electromagnetic applications, such as electromagnetic shielding, frequency selective surfaces, and transparent antennas; and also applications in transparent heaters, strain sensors, color changing soft robotics and other devices for wearable electronics.

Offering a comprehensive review article to cover all aspects of Ag NWs with highlights on recent progress in this growing field is of great significance for its further development. To this end, this review aims to critically summarize the recent progress of Ag NWs from synthesis to prospective Engineered Applications. Firstly, various synthetic strategies are summarized, focusing on soft and hard templates method, hydrothermal/solvothermal methods, polyol methods, and electrospinning methods. Following that, the growth mechanism of Ag NWs (primarily via polyol strategies) and the factors affecting the morphology of Ag NWs are highlighted. Subsequently, several fabrication methods to form Ag NWs thin film structures and strategies to reduce contact resistance are briefly introduced. Thereafter, various applications of Ag NWs and their composites are presented, including optoelectronic devices, electromagnetic applications, and other applications in transparent heaters, strain sensors, and so on. Finally, we conclude this review by summarizing the current process and offering some personal insights into the existing challenges and future opportunities

in this promising field.

2. Synthesis Methods

2.1 Template Method

The template method can prepare nanomaterial with desired aspect ratio and get highly directional arrangement nanowires easily. The template is convenient to synthesize and determines the quality of the final synthesized nanowires.[53] The template method is mainly divided into hard template methods, such as carbon nanotubes method, mesoporous silica method, and AAO template method, and soft template methods, such as cetyltrimethylammonium bromide (CTAB) method and ionic liquids method.

2.1.1 Hard Template Method

The hard template method can get highly directional arrangement nanowires easily, which have outstanding electrochemical detection sensitivity[54] and optical properties.[55] Anodic aluminum oxide (AAO) is the most frequently used hard template for Ag NWs arrays synthesis because it contains uniform nanometer-size holes with a wide range of hole diameters and the density of the pores can be easily controlled by changing the oxidation conditions.[56-58] Zhang *et al*.[59] successfully synthesized single-crystalline Ag nanowire arrays based on the use of AAO templates at 970 °C as shown in Figs. 1a-d. They added CuO as a supplement to improve the infiltration height by improving the wetting behavior between the molten Ag and AAO templates and used sodium hydroxide (NaOH) solution in a high-pressure autoclave to remove the AAO templates without destroying the Ag nanowire arrays.

Mesoporous silica materials have also been utilized as a kind of template due to their potential of producing very thin NWs.[60] For example, Kim and coworkers[61] synthesized Ag NWs using a mesoporous silica SBA-15 as the template. The obtained nanowires (4 μm long and 7 nm in diameter) are free from bundling and thus can be separated as single nanowires. Silver-filled carbon nanotubes (CNTs) can be generated using capillary action when molten silver[62] or silver salt precursors (subsequently thermalized by an electron irradiation beam)[63] are pulled into the cavities of CNTs. Following the same path, Borowiak-Palen *et al*.[64] optimized a wet chemistry technique to fill single-walled CNTs (SWCNTs) with silver with 80%, and they proposed that there may be a new transition that arises due to hybridization between Ag and carbon. Transmission electron microscopy (TEM) images of Ag-filled SWCNTs are shown in Figs. 1e-h.

Hard templates have advantages in the preparation of ultrathin nanowires and provide good control over the size, shape, and overall morphology of nanowires because of their predesigned well-distributed, and uniform aperture and channel length. However, a series of troublesome procedures are required to remove these templates, and the purification step can lead to a significant loss of the generated nanowires, resulting in a lower yield of Ag NWs and damage to the nanowires, especially those with high aspect ratios. Generally speaking, hard template methods are not suitable for large-scale industrial production.

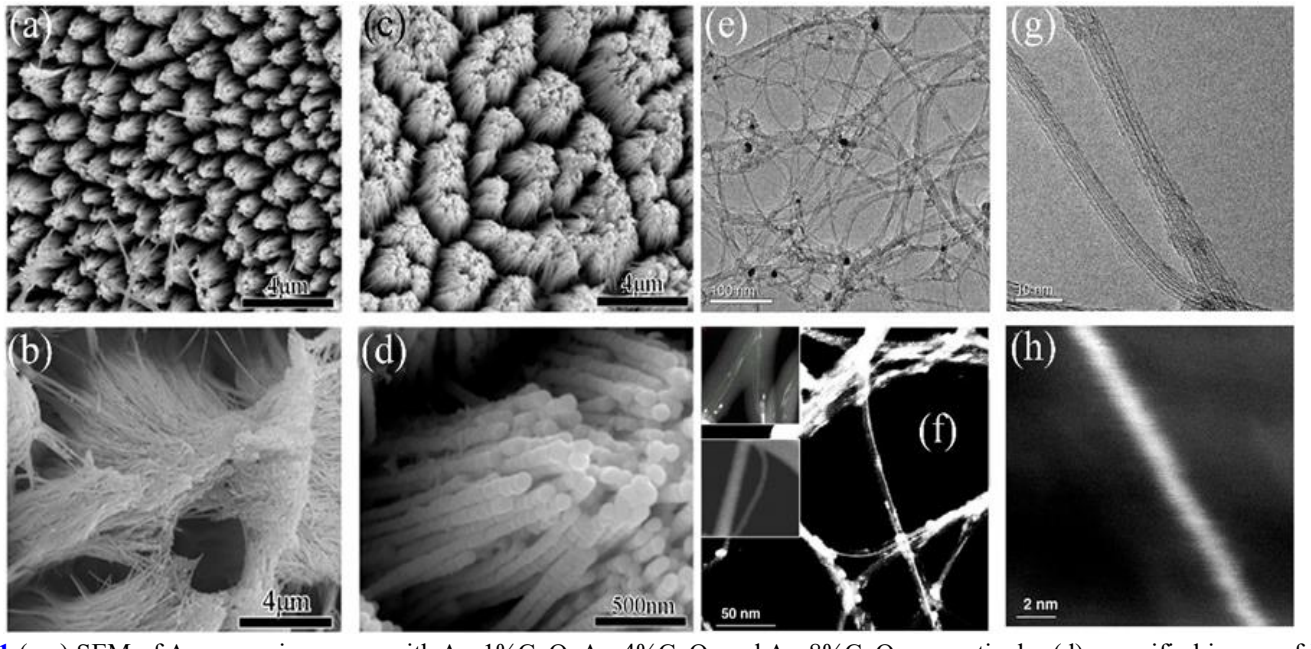

Fig. 1 (a-c) SEM of Ag nanowire arrays with Ag-1%CuO, Ag-4%CuO, and Ag-8%CuO, respectively; (d) magnified image of Fig. 1c; Reproduced with the permission from [59], Copyright 2019 Acta Materialia Inc, TEM images of Ag filled SWCNTs: (e, g) dark field images; (f, h) high magnification images. Reproduced with permission from [64], Copyright 2006 IOP Publishing.

2.1.2 Soft Template Method

Soft template methods utilize chemicals such as surfactants, micelles, and polymers which are dispersible/dissolvable in solvents and can be absorbed into the growing crystals. They kinetically control the growth rates through their adsorption and desorption from the crystal surface. The synthesized nanowires can be easily purified from the solvent phase, resulting in improved efficiency and scalability.

DNA is a good template because of its self-assembly properties and special double helix structure, which gives DNA the appropriate mechanical properties to form the desired shape, alignment, and junctions. In addition, DNA has molecular recognition properties, which improve the selectivity of Ag ions to form supramolecular structures. The idea of using DNA as a template to construct Ag NWs was first introduced by Braun.[65] Various methods for the fabrication of DNA-templated nanowires and the mechanism of templating are concluded in detail in a number of reviews.[66,67] The mechanism of growth can be summarized as nucleation at DNA binding sites, followed by gradual growth of spherical particles and slow transformation into smooth nanowires, as is shown by Fig. 2a. Murphy *et al*. successfully synthesized silver nanorods and nanowires (Figs. 2b-c) using rodlike micellar CTAB as templates.[68,69] The aspect ratio of the generated nanowires can be modulated by the shape and size of CTAB, as well as the molar ratio of precursors, salts, and surfactants.[69] In another interesting example, self-assembled nanotubular J-aggregates of amphiphilic cyanine dyes were used as chemically active templates, as shown in Fig. 2d.[70] Ag ions were reduced by photo-excited electrons in the cyanine dyes to form polycrystalline Ag NWs with a diameter of less than 7 nm. Hong *et al*.[71] reported the synthesis of atomic-sized and highly stable single-crystalline Ag NWs using a soft template in the ambient aqueous phase. The ultrathin silver wires with a width of 0.4 nm grew to micrometer lengths in the pores of self-assembled calix[4] hydroquinone nanotubes (CHQs) by electro/photochemical redox reactions. CHQ moieties have a rich π-electron density, which enables CHQ nanotubes to trap metallic silver ions in their pores with high affinity through cation-π interactions (Fig. 2e).

In addition, ionic liquids,[72] sodium dodecyl sulfate (SDS),[73] β-cyclodextrin (β-CD),[74] dithiodipropionic acid (DTDPA)[75] and biological molecules (Peptide Nanotubes,[76,77] proteins[78]) have also been used as soft templates to produce Ag NWs. However, Ag NWs synthesized by soft template methods usually have low yields, irregular morphology, and low aspect ratios.

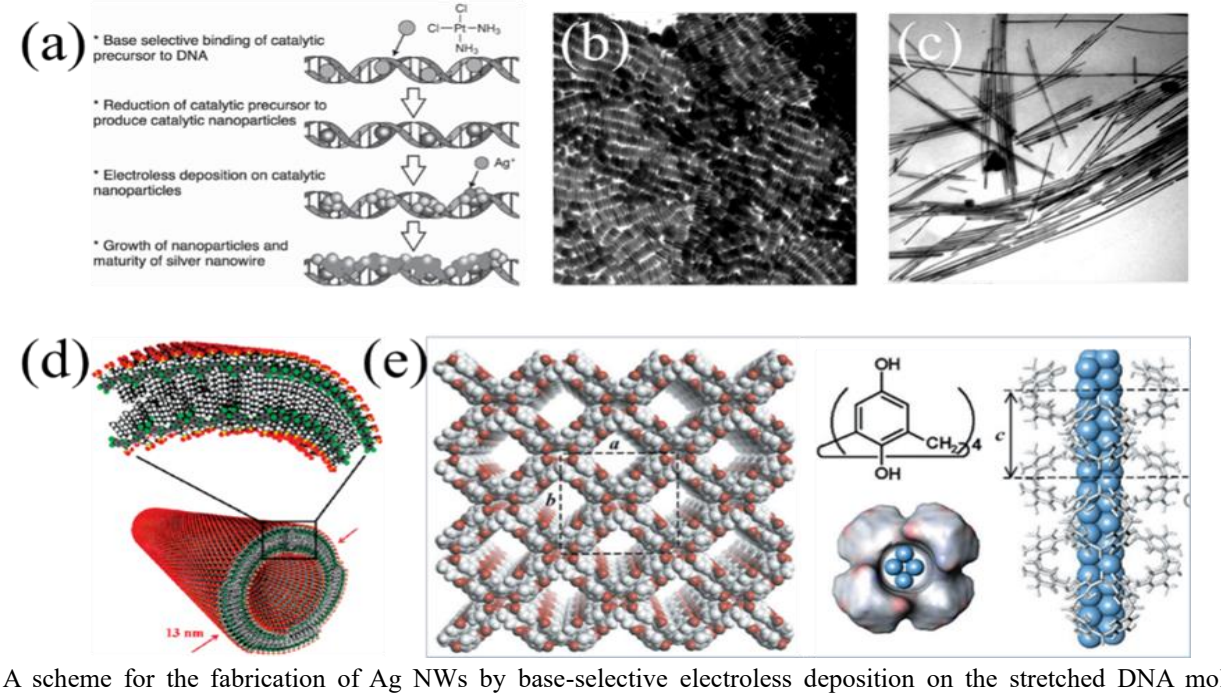

Fig. 2 (a) A scheme for the fabrication of Ag NWs by base-selective electroless deposition on the stretched DNA molecule. Reproduced with the permission from [67], Copyright 2017 The Society of Polymer Science, Japan(SPSJ); TEM image of shape-controlled (b) Silver nanorods and (c) Ag NWs using pH~11, scale bar = 100 nm. Reproduced with permission from [68], Copyright 2001 Royal Society of Chemistry; (d)Illustrating the self-assembled double-walled nanotubular J-aggregates dyes with an outer diameter of 13 nm. Reproduced with permission from [70], Copyright 2010, American Chemical Society (e) CHQ nanotube templates and an Ag NW inside the nanotube, the space-filled models (blue) represent the Ag NWs. Reproduced with permission from [71], Copyright 2001, The American Association for the Advancement of Science.

2.2 Hydrothermal/Solvothermal Method

The hydrothermal method is an encouraging method for the synthesis of Ag NWs because this method is green and does not require any surfactants or polymers. The high temperature and pressure conditions of the hydrothermal method contribute to the crystallization of silver in aqueous solutions. Although this hasn't been widely applied nowadays because of some disadvantages such as too long reaction time, the hydrothermal method can produce ultra-long Ag NWs of length up to 500 µm with uniform morphology to some extent. In 2005, Wang and co-workers[79] directly reduced the freshly prepared AgCl colloids with glucose at 180°C for 18 h and thus prepared Ag NWs with a diameter of about 100 nm and up to 500 µm in length. Glucose is a type of soft reducer and the reaction between silver chloride and glucose can be formulated as shown in equation (1):

$$2AgCl + CH_2OH\text{-}(CHOH)_4\text{-}CHO + H_2O = CH_2OH\text{-}(CHOH)_4\text{-}COOH + 2HCl + 2Ag \quad (1)$$

But silver chloride colloidal solution aggregates with heating and forms precipitates. In order to avoid this problem, Bari *et al.*[80] used polyvinylpyrrolidone (PVP) to make the hydrosol homogenous. In the presence of PVP, there were a lower number of particles and the size of most of the generated nanowires is uniform. The synthesis process involves drop wise addition of NaCl aqueous solution for better control of the reaction. The lengths of the Ag NWs are in the range of 200 to 500 µm and the average diameters are 45–65 nm as shown in Figs. 3a-b.

Some researchers also use the polyol-solvothermal method to prepare Ag NWs in a one-pot way with a shorter time period. For example, Ag NWs, ~220 µm (even larger than 400 µm) in length and ~55 nm in diameter were synthesized via a polyol-solvothermal reaction at 130°C for 8 h using ethylene glycol (EG), high molecular weight PVP (Mw=1 300 000) and

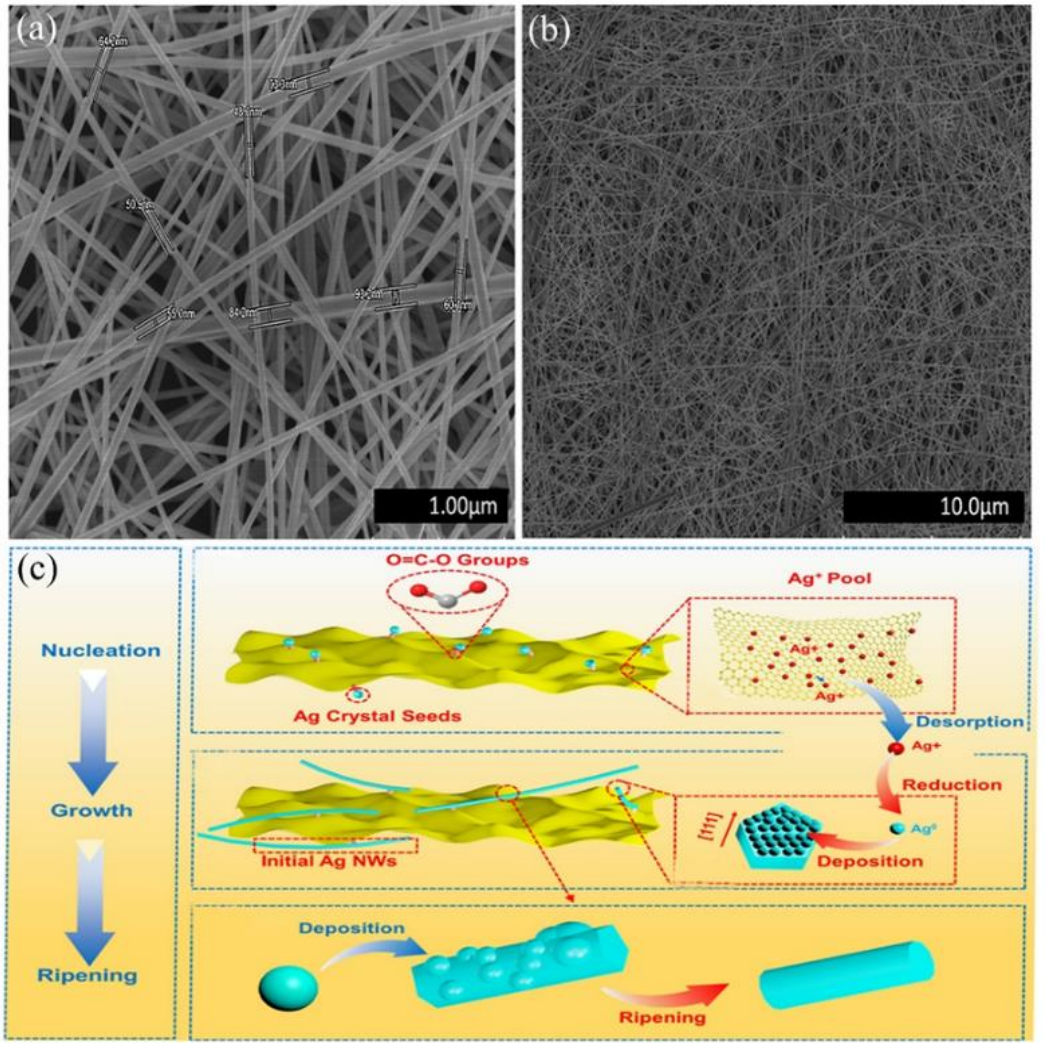

Fig. 3 (a, b) The SEM images of uniform, ultra-long, and thin Ag NWs prepared by the hydrothermal method at 160 ℃ – 22 hours of reaction. Reproduced with permission from [80], Copyright 2016 The Royal Society of Chemistry; (c) Schematic showing the proposed nucleation, growth, and ripening mechanism of Ag NWs film induced by graphene. Reproduced with permission from [92], Copyright 2021 Elsevier Ltd.

$FeCl_3$.[81] Li *et al*.[82] prepared ~120 μm in length, ~40 nm in diameter Ag NWs by using NaCl + KBr modulation and reacting at 170 °C for 2.5 h. The growth mechanism of the polyol-solvothermal method is similar to the polyol method.

Some researchers also investigated modified hydrothermal/solvothermal processes by using novel reducing agents,[83-85] novel solvents,[86] or novel reaction conditions.[87,88] Kim's research group[89] found that Ag NWs change in diameter as a function of pressure and prepared Ag NWs with diameters in the range of 15–30 nm and lengths up to ~20 μm under high pressure of 200 psi. They also synthesized ultra-thin Ag NWs with sub-15 nm diameters and aspect ratios of 1000 through a water-based high-pressure (190 psi) hydrothermal method in the presence of a tetrabutylammonium dichloro bromide organic salt and glucose-reducing agent.[90] Azani and co-workers[91] used a simple solvothermal method to synthesize uniform Ag NWs with controllable diameter (17, 20, 35, 70, and 100 nm) and high aspect ratio (>1000) by using different concentrations and kinds of salts: KBr, NaCl, tetra butyl ammonium chloride and 1-butyl-3-methylimidazolium chloride. In another research, graphene-induced Ag NWs were controllable and fabricated via a one-step hydrothermal route.[92] As shown in Fig. 3c, the O=C-O groups of G400 graphene provide an in-situ nucleation site to capture Ag nuclei as crystal seeds. Moreover, the oxygen functional groups of graphene act as an "Ag^+ pool" to store and slowly release Ag^+, avoiding a large amount of nucleation in a short time and preventing oxidation from Ag^+ to Ag_2O.

The solvothermal method can enhance the shape-controlled synthesis of Ag NWs and improve the growth rate compared to the hydrothermal route. However, for high-yield applications, there are still some challenges such as heavy reactor, long processing time, and uneven heating at different positions in the oven.[88]

2.3 Polyol Method

After being developed for about three decades, the polyol method is now widely recognized to synthesize Ag NWs for its plenty of advantages: low cost, high quality, easy to control, and, most importantly, higher industrial applicability at large scale. In a typical synthesis, polyol, capping agent, and silver precursor are needed. EG ($HOCH_2CH_2OH$) is the most popular polyol used in this process, which acts as a reducing agent and solvent. The most frequently used capping agent and precursors are PVP and silver nitrate. Silver precursors influence the thermodynamics of the reaction as well as the kinetics of reduction.[93] Polyol method was firstly applied to synthesize Ag NWs by Xia's group,[94] who developed the polyol method from the initial introduction of exotic seeds[94] to the later self-seeding process.[95] After that, researchers conducted extensive and in-depth studies on the preparation of Ag NWs by polyol method, which developed in the direction of high purity, high aspect ratio, and small diameter. However, it is still a little bit difficult to control the reaction parameters well to achieve a shape-controlled synthesis of uniform Ag NWs with high aspect ratios.

Reducing the diameter and increasing the length of Ag NWs have been proven to be an effective way to improve their optoelectronic performance by decreasing light attenuation. Based on the properties of individual nanowires, nanowire networks with smaller diameters (usually <20 nm) will provide higher transmittances at a given sheet resistance (R_s).[96] Ag NWs with a diameter of 20 nm and an aspect ratio larger than 1500 had been prepared by Ye *et al*. using a polyol method under a nitrogen-protected atmosphere.[97] The reaction system was heated to 180 °C and then lowered to 160 °C for 2 h. This way of lowering the temperature of the subsequent reaction stages promoted the uniform nucleation of Ag nanoparticles and was able to obtain Ag NWs with high purity (about 94.5%). Wiley *et al*.[98] used NaCl and NaBr as synergistic control agents to prepare Ag NWs with different diameters by adjusting the concentration of Br^- (Figs. 4a-d). When NaBr was added at 2.2 mM, Ag NWs with a diameter of 20 nm and an aspect ratio of 2000 could be produced. Yang and co-workers[99] reported a modified polyol synthesis of Ag NWs based on the use of benzoin-derived radicals in 2018. The strong reductant benzoin-derived radicals can speed up the reduction process, and the allowed relatively low reaction temperature facilitated the adsorption of Br^- on Ag (100) and limited their lateral growth, resulting in unprecedented ultrathin (13 nm) Ag NWs with aspect ratios up to 3000, as shown in Figs. 4e-h.

Besides the one-step synthesis method mentioned above, there are other methods called successive multistep growth (SMG) to synthesize very long Ag NWs. During this process, very long Ag NWs are grown by repeating the chemical reaction while suppling the chemical sources in a carefully controlled condition. As the growth times increase, the length of the Ag NWs increases. Lee *et al*. successfully synthesized ultra-long nanowires of >500 μm length with the SMG method while maintaining the same NW diameter (100-150 nm).[100] Subsequently, they conducted a systematic parameter study and enabled the synthesis of Ag NWs at a large scale.[101]

2.4 Electrospinning Method

Electrospinning is a versatile and viable technique for generating nanofibers, which could be used to produce ultra-

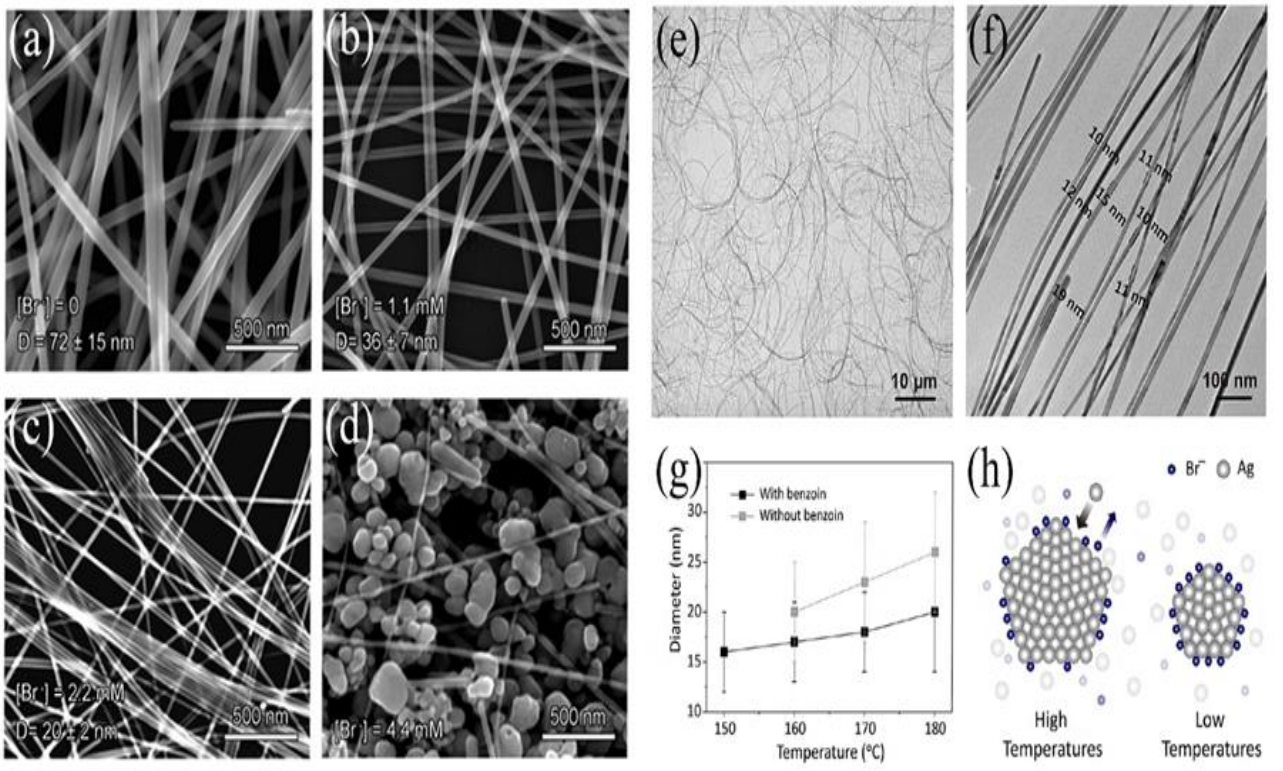

Fig. 4 Typical high-resolution SEM images of purified products obtained from different concentrations of NaBr: (a) 0, (b) 1.1, (c) 2.2, and (d) 4.4 mM. Reproduced with permission from [98], Copyright 2015 American Chemical Society. (e, f) TEM images with different magnifications of Ag NWs (13 nm in diameter) were synthesized using a standard procedure with an optimized concentration of bromide ions; (g) The nanowires became thicker with the increased growth temperature (150−180 °C), independent of the existence of benzoin; (h) Schematic illustration showing cross sections of Ag NWs grown at high temperatures and low temperatures, respectively. The Ag (100) surface is tightly bound by Br− ions at low temperatures, impeding lateral growth. Reproduced with permission from [99], Copyright 2018 American Chemical Society.

long Ag NWs of up to several centimeters.[102] The electrospinning process is based on a strong electric field, in which solution droplets are electrified to produce jets which are then stretched and elongated to produce fibers, followed by solvent evaporation and fiber solidification.[103]

To produce electrospun Ag NWs, the insulating polymer portion is removed by thermal decomposition, followed by the reduction of the silver element from the precursor. For example, Zhang *et al*. successfully prepared ultra-long silver microfibers with a minimum diameter of 310 nm, using a combination of centrifugal electrospinning and annealing in addition to the help of PVP (Figs. 5a-b).[40] Huang and co-workers fabricated PAN/Ag nanofibers by reduction of electrospun PAN/$AgNO_3$ composite using heat and formic acid vapor treatment.[104] Liu *et al*. prepared an Ag NW membrane by electrospinning Poly(acrylonitrile-co-phenylethylene) (P(AN-S)) solution with $AgNO_3$ and silver mirror reaction.[105] Although higher annealing temperature benefits the growth of silver crystals, it may result in morphology damage and breakage of the nanofibers. Besides, the complicated post-treated procedures at high temperatures might limit the fabrication of Ag nanofiber webs on a flexible polymer substrate. Chen *et al*. synthesized Ag nanofibers via electrospinning and ultraviolet (UV) treatment with the photodecomposition of poly(methyl methacrylate) (PMMA) and the photoreduction of silver trifluoroacetate precursor.[106] However, this method still results in morphology damage of the nanofibers and mixing by-product silver nanoparticles. In addition, ultra-long Ag nanofibers can be formed by directly using a suspension of Ag NPs (40 ± 5 nm) dispersed in ethylene glycol as an ink, followed by coalescing of Ag NPs during thermal annealing at 150 °C in the air (Figs. 5c-d).[107] However, the performance of this method is limited by the difficulty of preparing high-concentration Ag NP suspensions. The electrospinning method generally has outstanding advantages in low-cost production, in preparing ultra-long Ag NWs, and in forming Ag NWs networks directly.[108,109] However, for this process, some obstacles still need to be resolved, such as difficulties in achieving fiber diameter uniformity, hard to create thinner silver fibers (less than 100 nm), and preparing silver fibers with a smooth surface. Low productivity, high electric field, complicated post-treatment

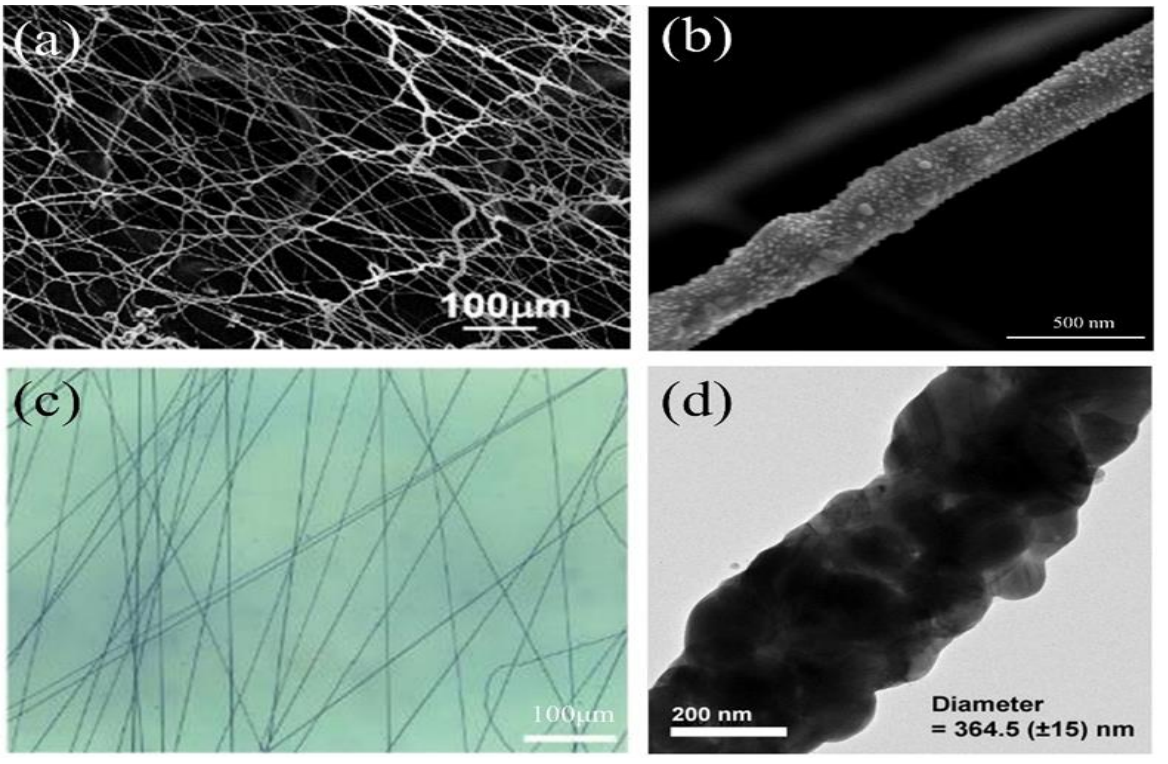

Fig. 5 (a) SEM image of annealed silver fibers with PVP: $AgNO_3$ weight rations of 6:15 and (b) SEM image of a single Ag nanofiber. Reproduced with permission from [40], Copyright 2022 the authors. (c) Optical micrograph of Ag nanofibers (20s electrospinning time) and (d) TEM image of a single Ag nanofiber. Reproduced with permission from [107], Copyright 2017 The Author(s).

procedures, and mixing by-product silver nanoparticles in Ag NWs have also hindered the development of the electrospinning method.

From what is discussed above, every synthesis method has its advantages, and at the same time, has its disadvantages. These points are summarized in Table 1.

Table 1. Summary of the advantages and disadvantages of different synthesis methods.

Synthesis method	Advantages	Disadvantages
Hard template	Distributed uniformly Highly directional arrangement Preparing ultrathin nanowires Controllable size, shape, and overall morphology	Troublesome follow-up process not suitable for large-scale industrial production
Soft template	Easy preparation process Efficiency and scalability Preparing ultrathin nanowires	low yields irregular morphology low aspect ratios
Hydrothermal/solvothermal method	Can produce very long Ag NWs Uniform morphology	Too long reaction time Heavy reactor Uneven heating at different positions in the oven
Polyol method	Low cost High quality Easy to control High industrial applicability at large scale	Nearly no defectiveness Non-uniform diameter Difficult to produce diameters of less than 100 nm
Electrospinning method	Low cost Preparing ultra-long Ag nanofiber Forming Ag NWs network directly	Rough surface Low productivity High electric field Complicated post-treatment procedures Mixing by-product silver nanoparticles in Ag NWs

3. Polyol Synthesis Mechanism

Different synthesis corresponds to different reaction mechanisms. For polyol method is now widely used for most cases, here, we discuss the mechanism of the polyol method as an illustration.

In 2003, Xia *et al*.[110] proposed several pieces of evidence that directly supported the five-fold twinned crystal structure of Ag NWs. The authors presented selected-area electron diffraction (SAED) pattern (Fig. 6a), a TEM image taken from a microtomed sample of Ag NWs (Fig. 6b), an HRTEM image of the end of an Ag NW (Fig. 6c) and SEM image taken from a sample of Ag NWs after it had been sonicated for 1h (Fig. 6d). The five-fold twinned structure of Ag NWs had also been proved by subsequent publications. Furthermore, Xia *et al*.[111] concluded that the chemical reactions involved in the synthesis of Ag NWs appeared to be fairly simple and could be easily found in chemistry textbooks. However, the nucleation and growth mechanisms behind the simple chemical reactions are extremely complex. It must be emphasized that, until today, we are still far from an in-depth understanding of the mechanism of Ag NWs by polyol synthesis at the atomic scale. The polyol synthesis mechanism of Ag NWs is expected to follow the mechanism proposed by LaMer and co-workers (Fig. 6e),[112] which is based upon an extensive study of the solution-phase synthesis of monodisperse sulfur colloids.

In a typical polyol synthesis, it can be divided into three distinct stages in a rough way: 1) the generation of silver atoms, 2) nucleation and evolution into seeds, and 3) the growth step leading to the formation of the nanowires. Firstly, Ag atoms are obtained from the reduction of Ag precursor. After that, Ag atoms will nucleate and grow into Ag nanoparticles by homogeneous or heterogeneous nucleation when their concentration reaches a saturation value. These Ag nanoparticles include a certain number of multiply twinned particles (MTPs), and the MTPs can act as the seeds of Ag nanorods or Ag nanowires because of their relatively low surface energies. However, it is often multiple factors that jointly determine the morphology of the final products in the process of synthesizing Ag NWs.[113] Therefore, clarifying the specific roles of different additives in the synthesis of Ag NWs and precisely controlling the reaction conditions are crucial to obtain Ag NWs with good morphology. This section focuses on the formation mechanism of Ag NWs and discusses the factors affecting the morphology of Ag NWs from the aspects of chemical additives and experimental conditions.

3.1 Redox Process and Generation of Silver Atoms

The investigation of the oxidation process of EG in the reaction is of key importance to reveal the reaction mechanism and the factors influencing the oxidation production of EG, such as temperature and atmosphere, which can have far-reaching effects on the nucleation and growth kinetics. Fiévet *et al*.[114] firstly proposed that metal atoms are possibly obtained by polyol reduction through the reaction as follows:

$$HOCH_2CH_2OH \rightarrow CH_3CHO + H_2O \quad (2)$$

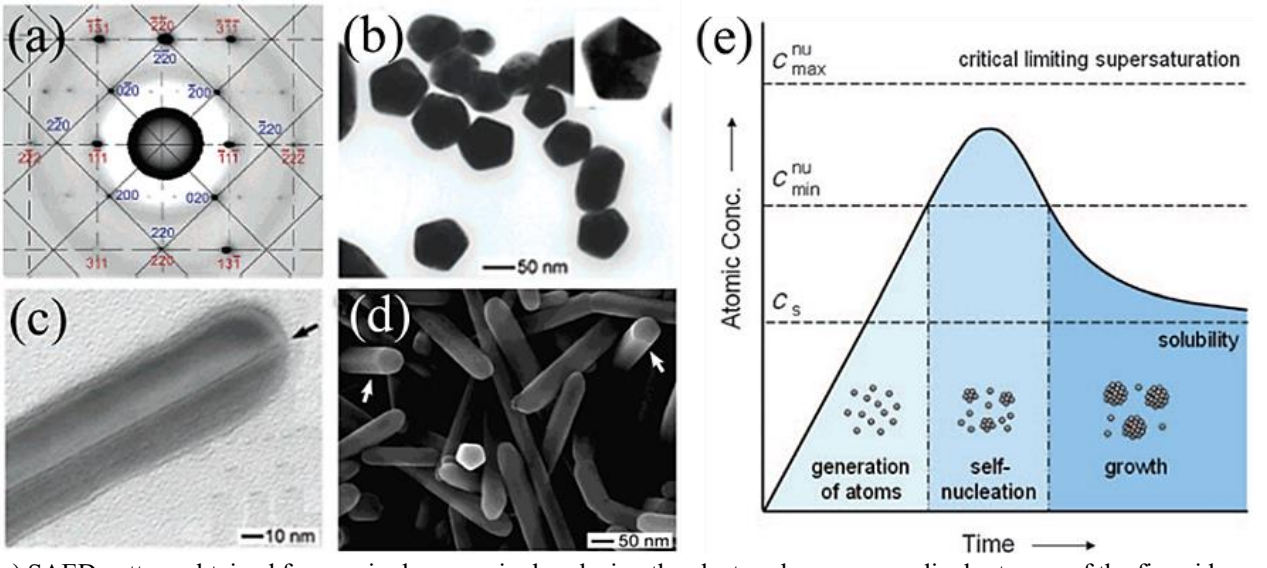

Fig. 6 (a) SAED pattern obtained from a single nanowire by placing the electron beam perpendicular to one of the five side surfaces; (b) TEM images taken from a microtomed sample of nanowires; (c) HRTEM image taken from the end of a nanowire, showing the presence of a twinned plane along the longitudinal axis; (d) SEM image taken from Ag NWs that had been broken by sonication to show their cross sections. Reproduced with permission from [110], Copyright 2003 American Chemical Society; (e) Plot of atomic concentration against time, illustrating the generation of atoms, nucleation, and subsequent growth. Reproduced with permission from [111], Copyright 2009 WILEY-VCH Verlag GmbH & Co. KGaA, Weinheim.

$$2M^{+}+2CH_3CHO \rightarrow CH_3COOCCH_3+2M+2H^{+} \quad (3)$$

Xia *et al*.[115] considered glycolaldehyde (GA), a stronger reductant than ethylene glycol is responsible for the polyol reduction in air through the following reaction:

$$2HOCH_2CH_2OH+O_2 \rightarrow 2HOCH_2CHO+2H_2O \quad (4)$$

when EG is saturated with argon, however, no such reaction was observed. Identifying glycol-aldehyde as a reducing agent helps explain why temperature differences of <5°C can profoundly impact reaction products, and only precise temperature control can achieve good reproducibility. Once the metal particles formed, they can in turn accelerate redox reactions via autocatalytic growth.[115] Therefore, tight control over the concentration of Ag precursor to slow down the generation of Ag atoms is very critical, because it will allow one to produce penta-twinned Ag NWs with reduced lateral dimensions and high yields. This can be achieved by choosing an appropriate concentration of Ag precursor, injecting the precursor at a relatively slow rate, or using a salt mediator to release Ag^{+} slowly.

3.2 Nucleation

Xia's research group[111] proposed the following nucleation mechanism: as the atomic clusters grow to a critical size, structural fluctuations become so energetically costly, resulting in the formation of a well-defined structure--a seed. In general, the seeds can take the form of a single-crystal, single-twined, or multiply-twined structure, as illustrated in Fig. 7. The key to obtaining only one nanocrystal shape to the exclusion of the others is to strictly control the nucleation process. The formation of the multiply twinned particles has been explained by several possibilities. Zhang *et al*.[116] suspected that both the stacking fault and intrinsic equilibrium structures of lower energy led to the twinned structures. In general, the structure formation is determined by a combination of thermodynamic and kinetic factors.[117] However, it is still unclear whether the silver is first reduced to atoms before further nucleation, or whether the unreduced silver binds first to produce seeds, which are then reduced in a second step.[111]

3.2.1 Thermodynamic Control

Ag NWs have a fivefold twined structure with a decahedral seed.[110] Decahedral has been demonstrated to be the most thermodynamically stable seed because it is almost completely bound by the lower energy {111} facets.[117] Ag nano-decahedrons might be assembled from five tetrahedrons step by step as shown in Fig. 8a.[118] Ag nanoparticles first grow into tetrahedrons, then the tetrahedrons assemble subsequently into

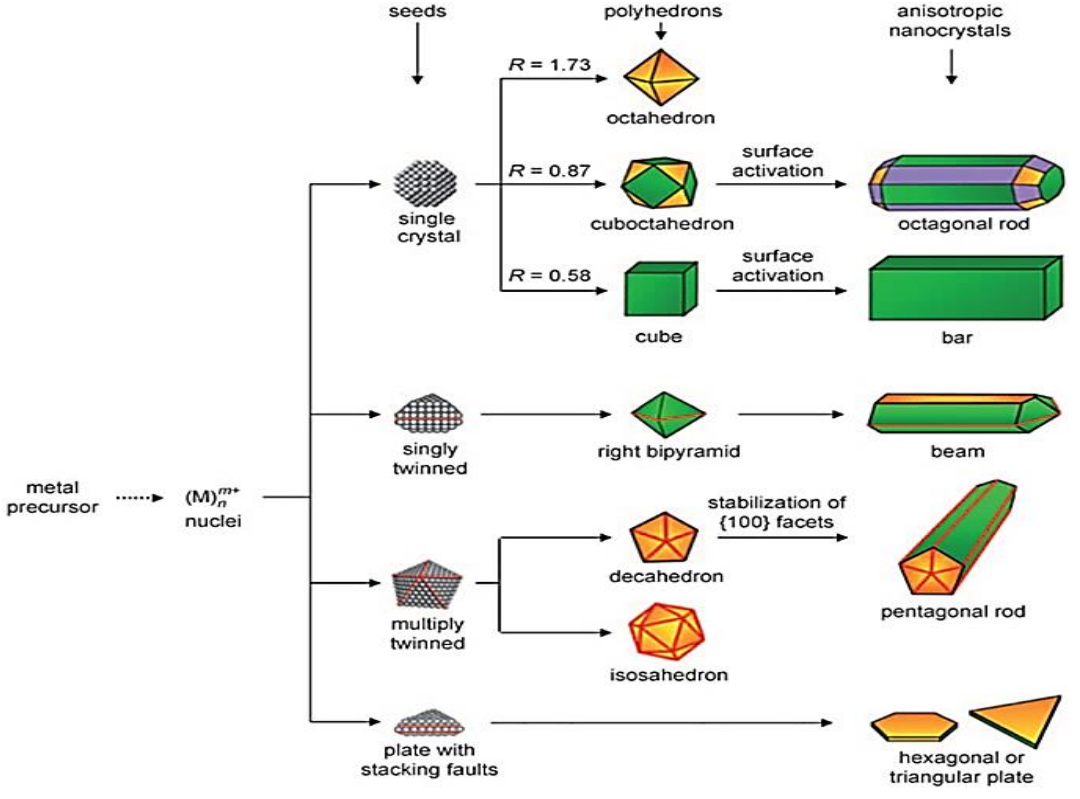

Fig. 7 Reaction pathways leading to Ag nanocrystals of different shapes. The green, orange, and purple colors represent the {100}, {111}, and {110} facets, respectively. Twin planes are delineated with red lines in the drawing. The parameter R is defined as the ratio between the growth rates along the <100>and <111> directions. Reproduced with permission from [111], Copyright 2009 WILEY-VCH Verlag GmbH & Co. KGaA, Weinheim.

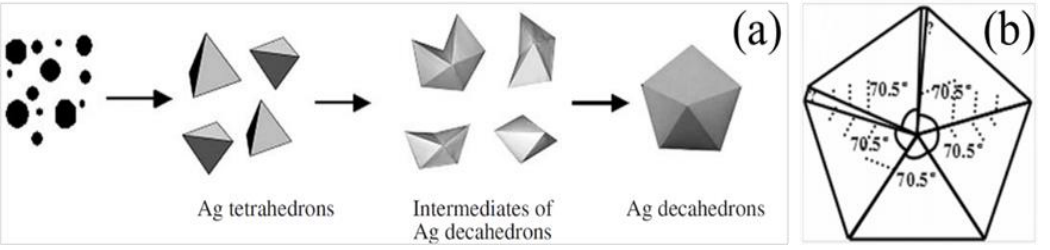

Fig. 8 (a) The schematic diagram of the plausible growth approaches of Ag nanodecahedra. Reproduced with permission from [111], Copyright 2006 Elsevier B.V.; (b) Pentatetrahedral twin model of Ag decahedral seeds.

the Ag decahedrons. Decahedral seed can be considered as a combination of five tetrahedron units sharing a common edge while leaving a gap of 7.5° because each tetrahedral has an internal angle of 70.5° theoretically (Fig. 8b).[32] The gap leads to many distortions and defects, which represent the highest energy locations on the fivefold twinned particle surface that would be more favorable for atom deposition, allowing the decahedra to grow preferentially along the axial direction as pentagonal nanowires whose sides are bounded by {100} facets.[31]

3.2.2 Kinetic Control

The essence of kinetic control is to control the generation rate of silver atoms and concentration of seeds by varying the reduction rate of precursor.[111] When metal atoms generate slowly, it's favorable for the formation of multiply twined seeds because they can remain small in size for a long period of time. The final nanostructures of silver are determined by the rate of seed formation, the structure of the initial seed, the rate of addition of metal atoms to the seed faces, and the capping agent. The formation and addition rate of silver atoms is sensitive to the kinetics of reduction, which depends on the reducing agent.[115]

3.2.3 Oxidative Etching

When $AgNO_3$ is used as a precursor, nitric acid (HNO_3) is formed during the synthesis. HNO_3 has a high oxidative etching effect on multiply twinned silver seeds and will prevent the homogeneous nucleation of Ag atoms via the following reactions:[119]

$$3Ag+4HNO_3 \rightarrow 3AgNO_3+NO+2H_2O \quad (5)$$

$$4NO+3O_2+2H_2O \rightarrow 4HNO_3 \quad (6)$$

Moreover, O_2 is present throughout the entire reaction process when syntheses are conducted in air, which can result in a powerful etchant for both the nuclei and seeds with a combination of ligands.[120] The defect zones in a decahedral seed have the highest energy and thus their atoms are most susceptible to being attacked by the etchant, oxidized, and then dissolved into the solution. Conversely, oxidative etching is favorable to forming single-crystal seeds because they are more resistant to oxidative etching. The oxidative etching effect is not only able to selectively solubilize twinned structures but also competes with the reduction of metal precursors to affect nucleation and growth. Thus, by utilizing oxidative etching, the research community has achieved more precise control over the nucleation and growth of metal nanocrystals in solution-phase synthesis.[121] In order to reduce the amount of oxidative etchant in the system, Xia *et al.* introduce trace ions such as Fe^{2+}/Fe^{3+}[122] and Cu^{+}/Cu^{2+}[123] to promote the growth of nanowires. Molecular oxygen present during initial seed formation can adsorb and dissociate on the Ag seeds, blocking sites for further Ag deposition. Fig. 9a illustrated the proposed mechanism by which Fe^{2+} removes atomic oxygen from the surface of Ag. Reduction by ethylene glycol (EG) competes with oxidation by atomic oxygen to form an equilibrium between Fe^{3+} and Fe^{2+}. The mechanism of Cu-salt to remove atomic oxygen was similar (Fig. 9b). Fivefold twined seeds can also be saved by performing the experiment under inert gas conditions.

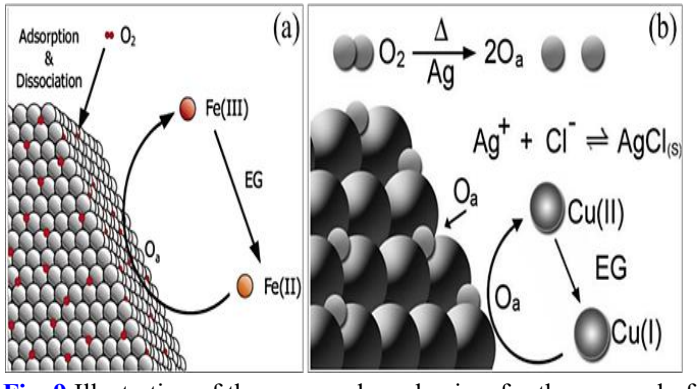

Fig. 9 Illustration of the proposed mechanism for the removal of atomic oxygen from the surface of silver nanostructures by (a) Fe(II), Reproduced with permission from [122], Copyright 2005 American Chemical Society; (b) Cu(I). Reproduced with permission from [123], Copyright 2008 Royal Society of Chemistry.

3.3 Growth

The growth mechanism generally follows the model proposed

by LaMer,[112] suggesting that nucleation and growth are two completely separate steps. The separating of nucleation and growth steps in polyol synthesis allows greater control over the size, aspect ratio, and shape of the resulting nanostructures.[32] Following the nucleation step, the larger Ag nanoparticles are able to grow at the expense of smaller ones through Ostwald ripening. The majority of larger Ag nanoparticles could directly grow into pentagonal nanorods with uniform diameters, and eventually form uniform nanowires, by ensuring a slow reaction rate to slowly supersaturate the silver nuclei present in the solution and avoiding oxidative etching. Since the lateral growth of the decahedron increases the strain energy considerably, the atoms prefer to be added axially parallel to the twin planes, leading to the elongation of the decahedra into nanowires.

Although the growth mechanism of Ag NWs can be explained by LaMer and Ostwald ripening theory, and the silver nanostructures involved in all steps of this process have been confirmed by numerous researchers, the growth process is still elusive to some extent.

3.3.1 The Role of PVP

Because of the polar nature of polyol media, PVP has been ubiquitously used in the shape-controlled synthesis of metal nanostructures.[124] PVP is mainly considered as a capping agent through selectively facet-binding, or steric stabilizer preventing the product from agglomeration.[125] The exact molecular structure of the capping agent on the surface of the nanocrystals is difficult to probe, resulting in the unclear definite role of PVP. However, it is believed that the resulting habit of the crystal can be explained by its selective adsorption on specific crystallographic facets of the particle. It is believed that the anisotropic growth can be explained by the selective adsorption of PVP on specific crystallographic surfaces of the fivefold twin crystal. It had been verified that the growth rates of specific facets in Ag nanostructures depend on the capping agent.[126] Fichthorn *et al*.[127] reported a multi-scale theoretical framework for kinetic Wulff shape predictions and they use it to probe the kinetic influence of PVP in the synthesis of Ag nanocrystals. The results showed that the adsorbed PVP films can regulate the flux of Ag atoms to be greater towards Ag {111} than Ag {100}. PVP binds more strongly to the {100} facets (the side surfaces of an Ag NW) than {111} facets (the ends of an Ag NW) of Ag, leading to the anisotropic growth,[110] as shown in Fig. 10a. An investigation of X-ray photoelectron spectroscopy demonstrated that the PVP molecules were adsorbed on the surface of the Ag NWs through Ag: O coordination.[128] In the polar group of the PVP repeated unit, the lone pair of electrons from the nitrogen and oxygen atoms can be donated to the sp hybrid orbital of the Ag^+ ions to build complex compounds.[129] Fig. 10b shows how a repeating unit of a PVP molecule binds to an Ag^+ ion. These two coordination types can effectively reduce the chemical potential and further make the PVP-bound Ag^+ ion more susceptible to reduction by EG.

The concentration of PVP is of great importance to the final morphology of Ag nanostructures. Excessive use of PVP is detrimental to the formation of decahedral seeds and may also lead to the capping of all surfaces of twin crystals, including {111} facets, and thus the selectivity of PVP is lost.[110,130] On the other hand, if the molar ratio of PVP/$AgNO_3$ is relatively lower, PVP will not be enough to completely passivate the side surfaces of nanowires, resulting in loose control over the growth process.[131] Therefore, a suitable PVP/$AgNO_3$ molar ratio is particularly important, however, no definite molar ratio can be taken as ideal.[113,132,133]

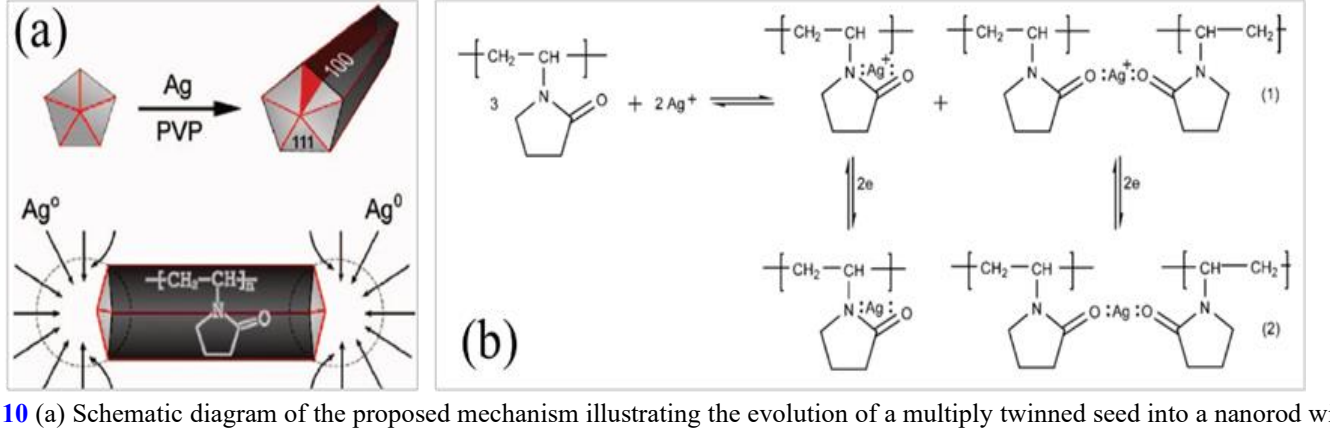

Fig. 10 (a) Schematic diagram of the proposed mechanism illustrating the evolution of a multiply twinned seed into a nanorod with the assistance of PVP, where silver atoms diffuse towards the ends of the nanorod and the side surfaces are completely passivated by PVP; Reproduced with the permission from [110], Copyright American Chemical Society 2003 (b) Possible coordination and reaction process for PVP and Ag^+ ions. Reproduced with permission from [129], Copyright 2004 WILEY-VCH Verlag GmbH & Co. KGaA, Weinheim.

The molecular weight (M_w) of PVP also affects the nanowire morphology significantly. Zhang *et al*.[134] investigated the performance of PVP with different M_w (29,000, 40,000, and 1,300,000) on the synthesis of Ag NWs by the polyol method. They obtained uniform Ag NWs with good morphology and high production in the presence of PVP M_w=1,300,000. It has been suggested that longer PVP chains can result in longer and thinner Ag NWs,[134-136] thus PVP with M_w=1 300 000 is frequently used to synthesize high aspect ratio Ag NWs. Zhang *et al*.[137] found that high M_w PVP in the synthesis resulted in uniform Ag NWs with a high aspect ratio, while low M_w PVP resulted in non-uniform low aspect ratio Ag NWs. They concluded that the presence of high M_w PVP can help to obtain high aspect ratio Ag NWs because high M_w PVP can decrease the number of Ag seeds in the mixture by lowering the reduction rate of $AgNO_3$, which led to the formation of high-aspect-ratio Ag NWs.

It had been discovered that the hydroxyl end groups of PVP could also serve as a very mild reductant for the kinetically controlled synthesis of Ag nanoplates with yields as high as 75%.[138] Jharimune *et al*.[139] further revealed that the molecular weight (M_w), monomer concentration (C_m), and end-group properties of PVP can affect the shape-control of polyol method synthesis. They synthesized Ag NWs and nanocubes using PVP with hydroxyl and aldehyde end groups through a two-step reduction process, respectively. However, it is not clear whether PVP plays the role of reductant in the common synthesis process of Ag NWs by polyol method.

However, PVP introduces insulating layers around each nanowire, which cannot be easily removed using the common washing process, thereby deteriorating the optical properties and electrical conductivity.[140] To remove the PVP ligands, various welding strategies,[141,142] $NaBH_4$ treatment[143] and electrochemical cleaning strategies[144] have been exploited. Han *et al*.[145] provided an idea to directly prepare nanowires with a thin capping layer. They used mixed PVP (linear PVP and branched PVP) instead of commercial PVP as the capping agent, producing high-quality Ag NWs with negligible Ag nanoparticles and a thin (~1 nm) capping layer.

3.3.2 The Role of Salt Mediators

The addition of both anions and cations facilitates the synthesis process and plays a critical role in the formation of Ag NWs. Derakhshi *et al*.[146] found that $FeCl_3$ has a crucial role in the synthesis of Ag NWs and the aspect ratio of nanowires can be tuned by $FeCl_3$ concentration. Zhan *et al*.[147] used $FeCl_3$ as a reaction promoter to synthesize Ag NWs at a high concentration of Ag precursor. Wang *et al*.[148] proposed that the Cu^{2+} present in the solution could be reduced to Cu^+ by EG. The Cu^+ could not only decrease the etching of Ag seeds during the nucleation process but also increase the adoption rate of Ag^0 on the surface of Ag NWs during the growth process. Hence, by simply varying the concentration of Cu^{2+}, Ag NWs with different sizes could be produced.

The nucleation step may be helped by the presence of foreign seeds in the solution because the heterogeneous nucleation[149] approach always gives Ag decahedral seeds with small sizes. Various metal salts, such as $PtCl_2$[35,150] and AgCl,[17] have been used for the initial nucleation of silver seeds in earlier years. The presence of a trace amount of halide ions in the solution can also facilitate heterogeneous nucleation and stabilize them against aggregation. Especially, an abundance of Cl^- or Br^-ions will form AgCl or AgBr colloids and thus can release Ag^+ gradually to prevent the excessive concentrations of silver cations.[151,152]

Schuette *et al*.[153] demonstrated that during the synthesis of Ag NWs from polyols, the early addition of NaCl led to the rapid formation of AgCl nanocubes, which induced heterogeneous nucleation of Ag on their surface. The smaller AgCl nanocubes are more potent heterogeneous nucleating agents, providing higher selectivity and narrower NW diameter distribution for the growth of Ag NWs. Chang *et al*.[154] varied Ag NWs mean diameters with added chloride ion, which can bind the side-wall facets, inhibiting growth in diameter. The addition of chloride ions caused the diameter of the Ag NWs to decrease from 100 nm to about 55 nm. When the molar ratio of $[Cl^-]/[Ag^+]$ exceeds 0.05, the diameter of NWs stops decreasing, which indicates saturation of adsorption. In general, it is difficult to decrease the diameter of Ag NWs below 30 nm in the presence of Cl^- only. Cui and coworkers[17] reported that the introduction of Br^- ions helped the growth of thinner nanowires, from 50−100 nm to 30−50 nm. Xia and coworkers[152] successfully synthesized Ag NWs with diameters below 20 nm and an aspect ratio greater than 1000 with the employment of Br^- ions through a facile polyol method (Figs. 11b-c). As shown in Fig. 11a, the Br^- ions are able to effectively passivate the side {100} facets of pentagonal Ag NWs like PVP, and thereby prevent them from lateral growth. The possible competition between PVP and halide ions required further studies. However, it is inevitable to produce nanoparticles as side products when using Br^- ions only. Particles could even become the predominant product with increasing Br^- ions.

Notably, the combination of Cl^- and Br^- ions could be effective in producing Ag NWs with both small diameters and high purity. By changing the ratio of Br^- to Cl^- while keeping the number of halide ions constant, Zhang *et al*.[155] found that Br^- can promote the nucleation of AgBr nanocubes and limit

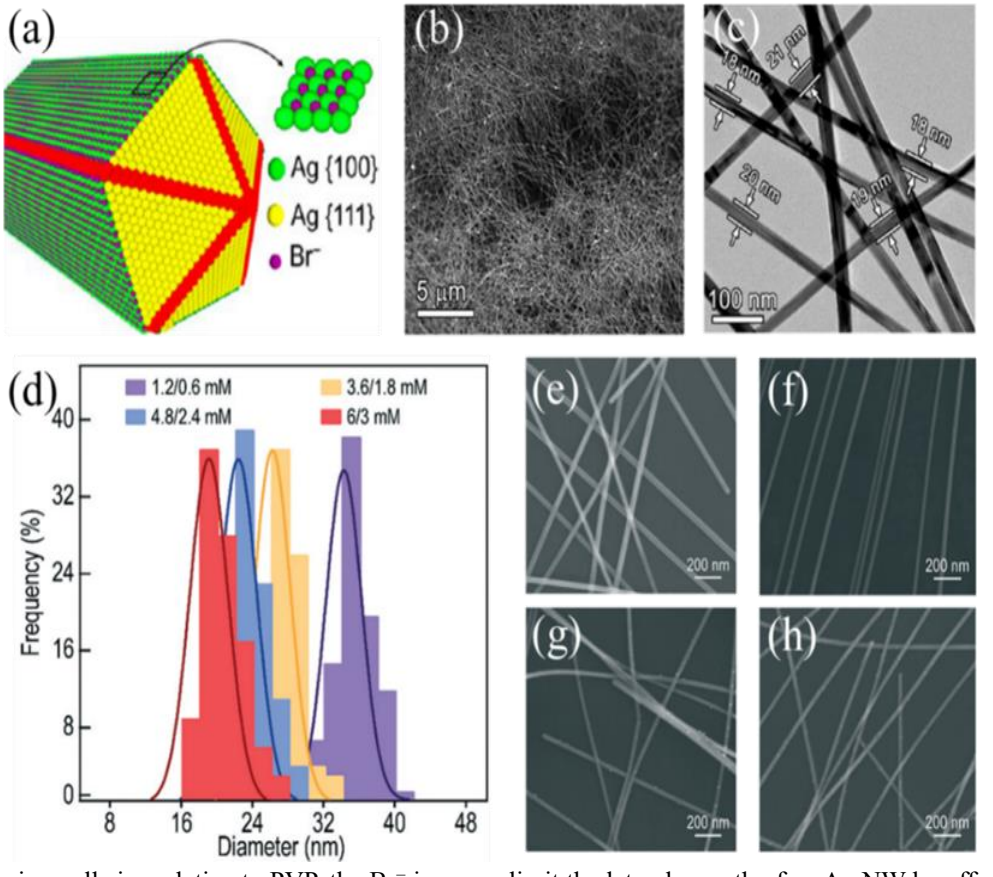

Fig. 11 (a) Due to their small size relative to PVP, the Br^- ions can limit the lateral growth of an Ag NW by effectively capping the {100}; facets on the side surface; (b) SEM and (c) TEM images of Ag nanowires obtained with a reaction time of 35 min; Reproduced with the permission from [152], Copyright 2016 American Chemical Society (d) A diameter histogram and (e–h) SEM images of the Ag NWs obtained at different NaCl/NaBr ratios of (e) 1.2/0.6 mM, (f) 3.6/1.8 mM, (g) 4.8/2.4 mM and (h) 6/3 mM. Reproduced with permission from [156], Copyright Royal Society of Chemistry.

the lateral growth of Ag nanowires in the bromide-mediated polyol method. Zhu *et al*.[156] proposed that the uniformity and purity of the Ag NWs depended on the Cl^-/Br^-molar ratio, with the optimum point being 2:1. They synthesized Ag NWs with tunable diameters from 35 to 19 nm and aspect ratios of up to 1500 via adjusting the total concentration of Cl^- ions while keeping the Cl^-/Br^-ratio constant (Figs. 11d-h). Rui *et al*.[157] found that for the case of Cl^- and Br^- co-additives, a mixed silver halide crystal of $AgBr_{1-x}Cl_x$was formed rather than the AgBr/AgCl mixture.

3.3.3 Other factors Influencing the Polyol Synthesis of Ag NWs

Hemmati *et al*. provided an overview of polyol Ag NWs synthesis and outlook for a green process.[133] The factors that affect the morphology and size of synthesized Ag NWs include reaction temperature, $AgNO_3$ concentration and its preparation and injection rate, PVP concentration and molecular weight, salt mediator, mixing type, and rate were reviewed. In addition, reaction time, atmosphere, heating rate, and stirring rate may also influence the synthesis of Ag NWs. In a study by Hemmati *et al*.,[158] a parametric study was performed on the polyol synthesis of Ag NWs, they found that four parameters (temperature, $AgNO_3$ concentration, PVP concentration, and $CuCl_2$ concentration) are the most important factors affecting Ag NWs yield.

The concentration of $AgNO_3$: The concentration of $AgNO_3$ is vital to the yield and morphology of Ag NWs. Gebeyehu *et al*.[159] synthesized Ag NWs with different concentrations of $AgNO_3$ (i.e. 20.6, 30.5, 60.4, and 90.3 mM), and the experimental results showed that Ag NWs tend to become shorter and wider as the concentration of $AgNO_3$ increases. In addition, too high or too low a concentration of $AgNO_3$ led to large amounts of nanoparticles. This is consistent with what is reported elsewhere.[130,160] When $AgNO_3$ at a high concentration was added, the Ag^+ concentration was high in a volume of the same unit, leading to an increase in the possibility of molecular collisions and thus the increase of chemical reaction rate. The addition of 30.5 mM $AgNO_3$ produced uniform Ag NWs with a mean diameter of 22±2 nm

and lengths of 50±5 μm.[159]

Temperature and reaction time: A suitable reaction temperature is an essential condition for the synthesis of Ag NWs with favorable morphology. It had been reported that Ag NWs cannot form when the reaction temperature was lower than 110°C.[110] Authors thought that twin regions of MTPs play an important role in the formation of Ag NWs with favorable shape and the reactivity of these twin regions is increased by melting at relatively high temperatures, which means that the lower reaction temperature is not sufficiently enough to activate twin regions of MTPs for growth of Ag NWs. Xia *et al*.[35] found that no Ag NWs were obtained at 100°C, only low aspect ratio Ag nanorods were obtained at 185°C, while high aspect ratio Ag NWs could be obtained at a reaction temperature of 160°C. They concluded that the low temperature could not provide enough energy to activate the specific facets and transfer silver atoms to the surface of the growth Ag seeds required for the anisotropic growth of Ag NWs. It is well known that at high temperatures in the air, EG changes to GA, which can easily reduce Ag ions to Ag atoms.[115] The rate of GA formation increased with temperature, making the reducing power of EG increase with temperature. As a result, the as-prepared Ag NWs become wider and shorter as the reaction temperature increases. Meanwhile, the increased temperature favors the accelerated generation of Ag atoms. Therefore, Ag atoms are deposited not only on {100} but also on {111}, thus allowing more Ag atoms to form Ag nanoparticles instead of being deposited on MTPs. Plenty of reports are consistent with this.[161,162] Wiley and coworkers[96] determined the extent of Ag^+ to Ag^0 conversion as a function of time and temperature, as shown in Fig. 12c. When at lower temperatures, nucleation rates are lower, and more silver precursors are left per nuclei, making Ag NWs grow longer and wider (Figs. 12a-b). They reported that the reduction rate was greater at higher reaction temperatures, which in turn likely supported a higher nucleation rate. The lower reaction temperature and longer synthesis time can enhance the length of nanowires with a vital difference while a quick synthesis leads to results in a low aspect ratio. For example, Jiu *et al*.[163] synthesized Ag NWs >60 μm and even 100 μm in length with a uniform ~60 nm diameter at low temperature (130°C) and for a longer time (12 h). However, the overreaction of Ag NWs (more than 12 h) would lead to an increase in diameter and a decrease in length.

Stirring rate: Stirring homogenizes Ag^+ ion concentration and reduces the possibility of aggregation throughout the whole solution. Stirring also homogenizes the diameter and length of the synthesized nanowires. The increase in stirring

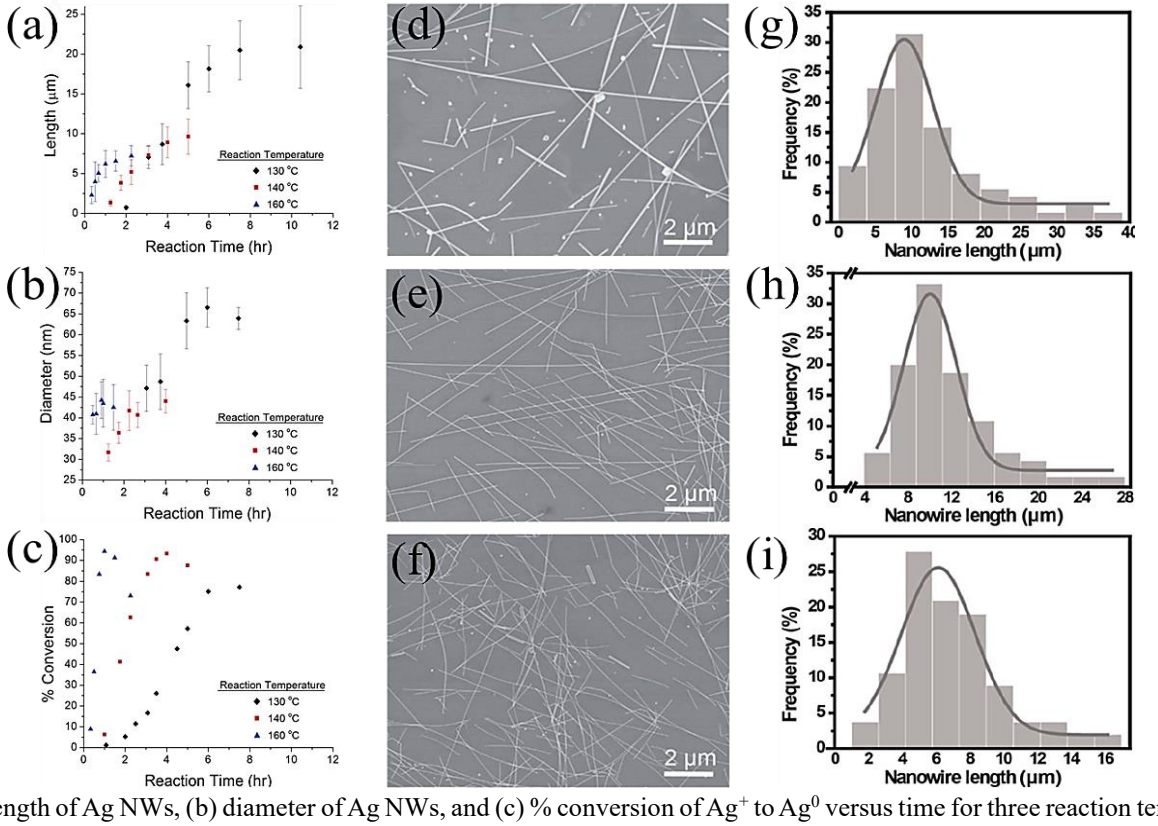

Fig. 12 (a) length of Ag NWs, (b) diameter of Ag NWs, and (c) % conversion of Ag^+ to Ag^0 versus time for three reaction temperatures; Reproduced with the permission from [96], Copyright, Copyright RSC Publishing. SEM images and length distribution of Ag NWs prepared at different stirring speeds: (d, g) at 0 rpm, the yield of Ag NWs is low, (e, h) at 200 rpm, high yields of Ag NWs are formed, and (f, i) at400 rpm, Ag NWs with short length are formed. Reproduced with permission from [162], Copyright RSC Publishing.

rate decreases the possibility of Ag atoms being deposited on MTPs. As a result, these MTPs grow as thinner and shorter nanowires.[151] Jiu *et al*.[163] investigated the effect of stirring on nanowires and synthesized Ag NWs by adjusting the stirring speed (0–700 rpm) during the process. The nanowires obtained without stirring were three times larger than those with stirring. Liu *et al*.[162] examined the effect of stirring speeds on the Ag NWs synthesis, three different stirring speeds (0, 200, and 400 rpm) for the same reaction time and temperature were carried out, as shown in Figs. 12d-i. The Ag NWs at 200 rpm exhibit thinner diameter, longer length, and higher purity. Ag NWs with lengths in the range of 20-100 μm and a maximum length of 230 μm have been successfully synthesized at a low temperature of 110°C with low stirring speeds.[164] In addition, vigorous stirring increases the exposure of nanostructures to oxygen, which significantly enhances the oxidative etching process, thereby removing the formed MTPs that are essential for nanowire growth.[165]

4. Fabrication Methods of Ag NWs Thin Film

The thin film structure of Ag NWs could have excellent electrical and thermal conductivity, optical transmittance, mechanical flexibility, and even good stretchability. For gaining these superior properties, it is crucial to develop a low-cost, high-throughput, large-area, reliable, and simple fabrication method to form Ag NWs networks on flexible substrates using ideal nanowires.[16,23,132,166,167] Kinds of fabrication methods are available for transferring Ag NWs network to the flexible substrates, such as drop casting, Meyer rod coating, spin coating, spray coating, screen printing, and vacuum filtration, *etc*. Different fabrication methods have their own advantages and disadvantages, which are summarized in Table 2. Several frequently used fabrication methods are introduced in this section.

4.1 Drop Casting

Drop casting is the simplest method for producing Ag NWs thin films, which simply requires dropping a definite concentration of Ag NWs solution onto the substrate and then evaporating the solvent.[168,169] As illustrated in Fig. 13a, the drop-casting procedure can be applied to fabricate flexible polymer solar cells based on polyimide (PI)/Ag NWs

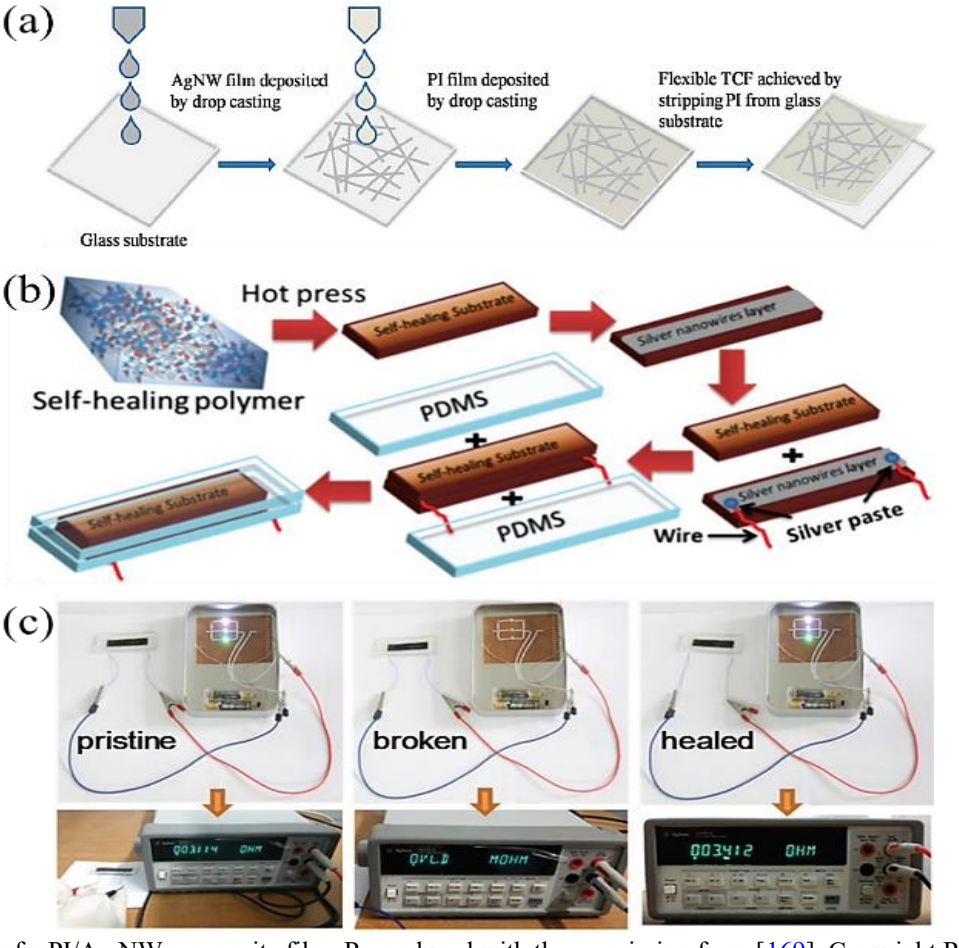

Fig. 13 (a) Fabrication of a PI/Ag NW composite film; Reproduced with the permission from [169], Copyright RSC Publishing, (b) The fabrication process of Ag NW-based and sandwich-structured strain sensors; (c) Photographs showing the lighting of LED bulb and resistance of pristine, broken, and healed respectively. Reproduced with permission from [171], Copyright RSC Publishing.

composite. The Ag NWs with a high aspect ratio of 2820 could be deposited into a photodiode device by simple drop-casting without any post-processing steps at room temperature.[170] Jiang *et al*. developed a flexible self-healing sandwich-structured strain sensor with Ag NWs by drop casting method.[171] They demonstrated that Ag NWs can be well dispersed on the surface of reinforced self-healing polymer composites. The 3D Ag NWs network can be broken following the breakage of the self-healing conductive composite and established again after the self-healing of the composites.

Table 2. Summary of the advantages and disadvantages of different fabrication methods.

Fabrication method	Advantages	Disadvantages
Drop casting	The simplest method	Uncontrollable thickness "Coffee ring" effect
Meyer rod coating	Scalable capability Controllable film thickness	Nearly no defectiveness
Spin Coating	Small-area uniform Simple Fast Low cost	Unsuitable for industrial production Waste of material Limited control over film thickness
Spray Coating	Large area uniform Scalable capability The coating on almost any type of substrate Obtaining patterned films with shadow masks	Contaminated Waste of ink Lower edge resolution
Screen Printing	Scalable capability Low cost Versatile pattern designs Little waste	Strict requirements for ink
Vacuum Filtration	Little waste Controllable film thickness and areal density Simply to obtain ultrathin and uniform Ag NW networks	Unsuitable for industrial production

However, the drop-casted film thickness is hard to be controllable. In addition, due to the surface tension of the solution and the self-aggregation of nanowires, it is easy to lead to the inhomogeneous distribution of Ag NWs during the drying process, i.e., the "coffee ring" effect. Yu *et al*. proposed a modified drop casting process for transferring the Ag NWs coating from the glass substrate to the crosslinked poly(acrylate) overcoat using a UV-curable polymer and peeling-off method, which improves the inhomogeneous to a certain extent.[172] Furthermore, the coffee ring effect can be ameliorated by several strategies, such as using the Marangoni effect, anisotropic particles, or surfactants.[173]

4.2 Meyer Rod Coating

Meyer rod coating is widely used to prepare Ag NWs networks and can be scaled up to a roll-to-roll process.[174-177] In this process, Ag NWs solution is directly applied to the surface of the substrate by sweeping and spreading out with a Meyer-rod bar. The thickness of the Ag NWs film can be adjusted by repeating the coating steps[178] and tuned by varying the distance between the substrate and the rod. Moreover, the solvent type and evaporation rate, solution concentration and dispersibility, interactions between solution and substrates, and slit size of the Meyer rod are also critical to the film homogeneity.[44] The faster evaporation rate of solvent (compared with the drop-casting method) can effectively prevent the uneven thickness and local agglomeration of Ag NWs caused by the coffee ring effect.

In 2010, Hu *et al*. fabricated Ag NW films of 80% transmittance and 20 Ω/sq sheet resistance by using the Meyer rod coating method.[17] Kang *et al*. also used the Meyer rod coating method and applied photopatterning steps to embed the Ag NWs into a UV-patternable polymer matrix to form an anode electrode in OLED, which obtained excellent device performance.[179] As demonstrated by Cho *et al*., the Meyer rod coating method can also enable the alignment of Ag NW arrays by the shear-induced hydrodynamic force generated by dragging (Fig. 14).[180] They enhanced the Ag NW adhesion to the substrate via electrostatic force by pretreating the PET substrate with poly-L-lysine (PLL), because of the strong ionic interaction between the amine functional groups of PLL and PVP-capped Ag NWs. Based on the highly cross-aligned Ag NWs network, flexible, transparent, and force-sensitive touch screens could be fabricated.

4.3 Spin Coating

Spin coating is widely used for small-area uniform thin films of Ag NWs in the laboratory.[181-184] Although this method is simple, fast, and less costly, it is unsuitable for large-scale industrial production, due to the loss of a large amount of material during the rotation process and limited control over the film thickness. Parameters, such as spin speed, acceleration, coating time, and solution concentration, have a great influence on the performance of the fabricated thin film. Zhai *et al*. prepared a flexible plasmonic random laser device by spin coating a solution of polydimethylsiloxane doped with

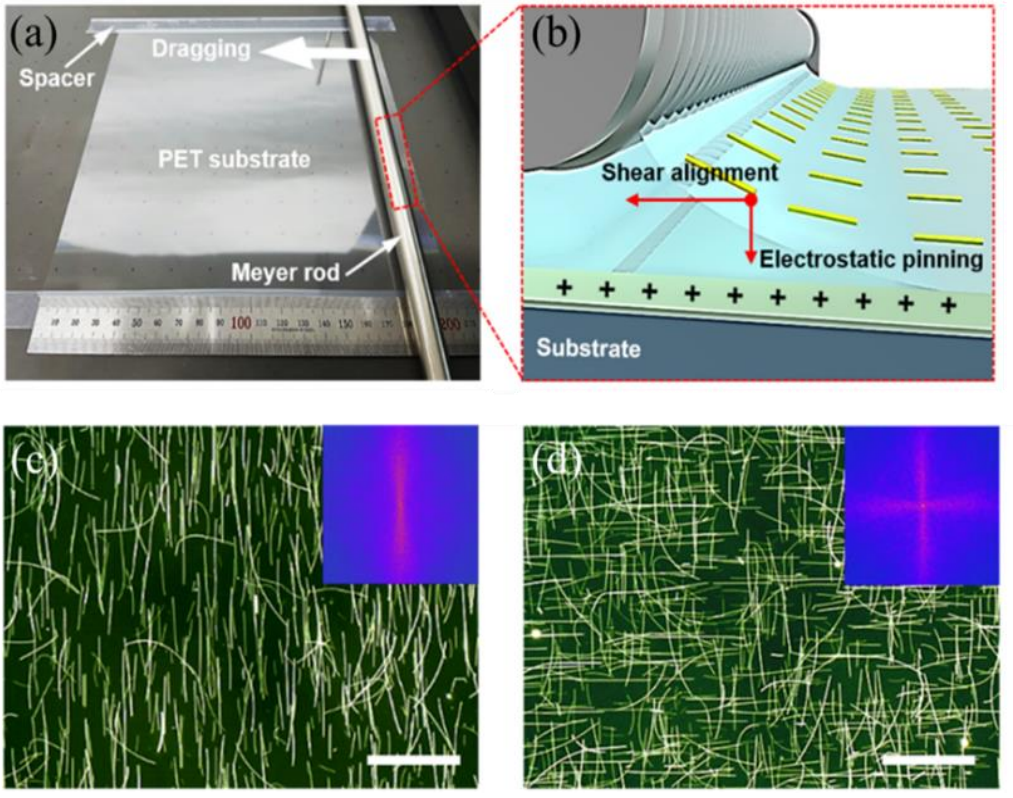

Fig. 14 Large-scale alignment of unidirectional and cross-aligned Ag NW arrays by Meyer rod coating. Reproduced with permission from [180], Copyright RSC Publishing (a) photograph of the experimental setup of the Meyer rod coating process on a 20 × 20 cm^2 PET substrate; (b) Schematic image showing the alignment mechanism of Ag NWs during the Meyer rod coating process. The combined effect of shear stress alignment and electrostatic pinning produces highly aligned and uniform Ag NW arrays; Dark-field optical microscope images of the (c)unidirectionally and (d) cross-aligned Ag NW arrays. Insets are the fast Fourier transform (FFT) analyses of the optical micrographs. The scale bars are 40 μm.

the rhodamine 6G organic dye and silver nanowires onto a silicone rubber slab.[185] Sun *et al*. fabricated a highly transparent and flexible conductive film through spin coating Ag NWs onto hydrophilic modified polydimethylsiloxane (PDMS).[186] The obtained films possess high transparency (90.86%) and low sheet resistance (3.22 Ω/sq). As shown in Figs. 15a-b, they also produced finely designed complex patterns on PDMS, making the Ag NWs only present in the circuits. In addition, spin coating can be used to apply two or more kinds of materials in layers. Li *et al*. successfully developed a transparent and stretchable NO sensor by spin-coating of Ag NWs and carbon nanotubes (CNTs) on a PDMS substrate (Figs. 15c-e).[187] The prepared CNTs/Ag NWs/PDMS film electrodes showed superior and stable sensing ability for NO in both static and stretched states.

4.4 Spray Coating

In spray coating, a continues spray of paint is generated at the spray nozzle, where pressurized air or gas (e.g., nitrogen or argon) breaks up the liquid paint into droplets and helps deposit the materials on the substrate. This method enables uniform and large-area deposition of Ag NW networks with high roll-to-roll compatibility and therefore is widely used in industry.[188] Almost any type of substrate can be coated via spray coating.[189] The quality of the spray-coated layer is affected by many parameters, such as the distance between nozzle and substrate, coating speed, air or gas pressure, size and shape of the nozzle, number of coated layers, substrate temperature, and density, viscosity and the surface tension of the solution sprayed.[190,191]

The spray coating method can also be used to obtain patterned nanowire films with the help of shadow masks.[192] However, it is also important to consider its drawbacks, because it will not only cause contamination of the processing equipment but also cause ink loss and lower edge resolution.[191] Kim *et al*. introduced a supersonic cold spraying technique, which achieves strong adhesion between the deposited materials and the fabric substrate without post-treatment.[193] The as-prepared rGO/Ag NW-decorated fabric is washable, wearable, stretchable, hydrophobic, and antibacterial, which can be used for multifunctional sensors and supercapacitors (Fig. 16a). Akter *et al*. reported a high-

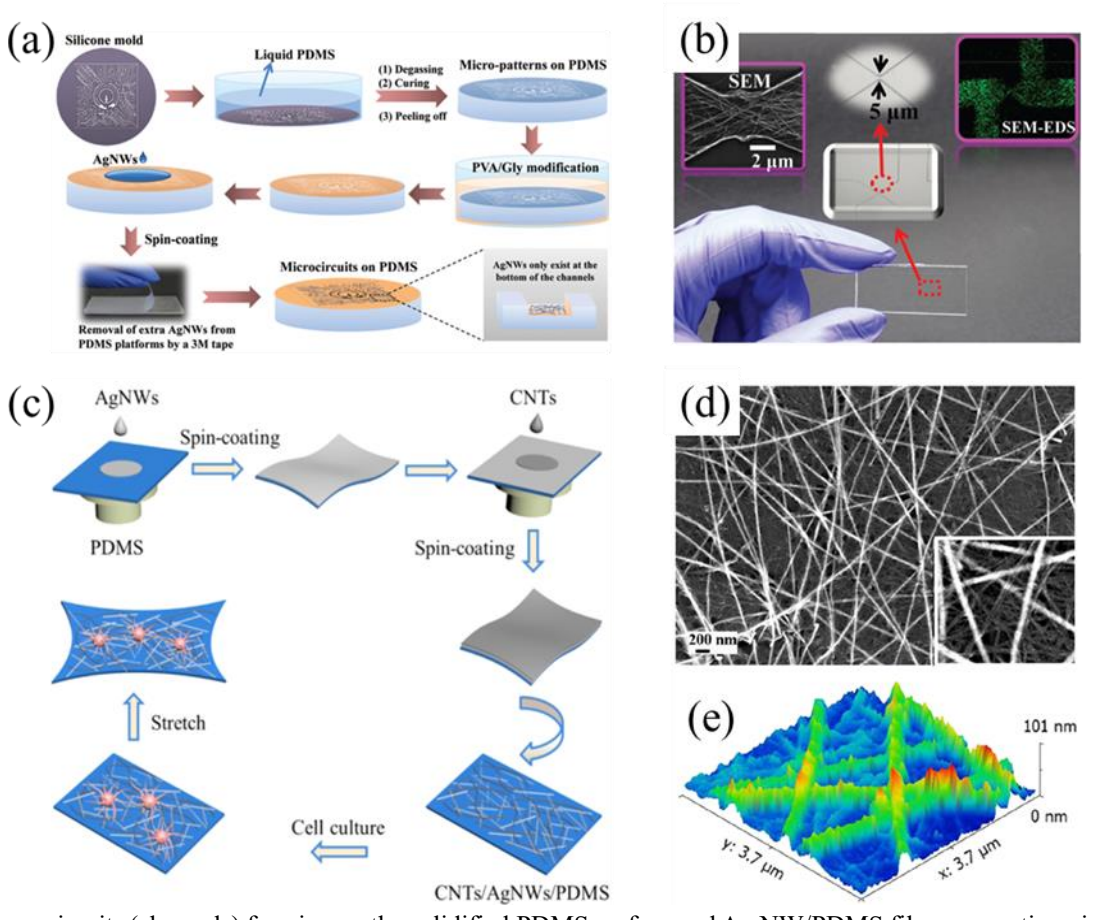

Fig. 15 (a) Concave circuits (channels) forming on the solidified PDMS surface and Ag NW/PDMS film preparation via spin coating Ag NW onto a PVA/Gly modified hydrophilic PDMS surface. Ag NWs that are not in the circuit channels are removed using a 3M tape; (b) Circuits with a width of 5 μm. The SEM and SEM-EDS mapping image in the inset indicates that the Ag NWs were successfully filled and evenly and continuously distributed through the entire circuit; Reproduced with the permission from [186], Copyright Royal Society of Chemistry (c) Preparation scheme of flexible CNTs/Ag NWs/PDMS films and the subsequent cell culture; (d) SEM image of CNTs/Ag NWs/PDMS; (e) AFM surface image of CNTs/Ag NWs/PDMS. Reproduced with permission from [187], Copyright 2022 Elsevier B.V.

performance stretchable and transparent conductor prepared by spray coating, in which the adhesion force between the Ag NW and substrate was effectively enhanced by modifying the PDMS substrate with dopamine.[194] A sandwich-like flame retardant nanocoating with super-hydrophobicity and supersensitive fire-warning response based on graphene-oxide (GO), Ag NWs, and fluoride polyvinyl butyral was successfully fabricated via spray-coating.[195] The preparation route of the sandwiched nanocoating is illustrated in Fig. 16b.

4.5 Screen Printing

Printing techniques include inkjet printing, gravure printing, screen printing, electro-hydrodynamic jet printing, and capillary printing,[132] among which screen printing is the most widely used technique in printed electronics due to its scalable capability, low cost, versatile pattern designs, and little waste.[196-199]

The screen-printing method uses a customized screen and printing ink to obtain the desired pattern by scratch printing. Patterned electrodes can be obtained directly by this method without any extra patterning process, such as laser ablation, shadow mask, or chemical etching. As reported by Ke *et al*., the Ag NWs conductive ink was directly printed onto the surface of a stretchable textile and paper by facile screen-printing technology to prepare stretchable electronics (Fig. 17b).[200] Screen printing can also be combined with another fabrication method. For example, Lin *et al*. combined screen printing with vacuum filtration for patterning Ag NWs network and achieved a 50 μm patterning resolution.[201] They transferred the patterned Ag NW films to the surface of PDMS and successfully made patterned stretchable transparent conductive films (TCFs).

Screen printing has a large wet film thickness defined by the thickness and the open area of the screen. In general, the

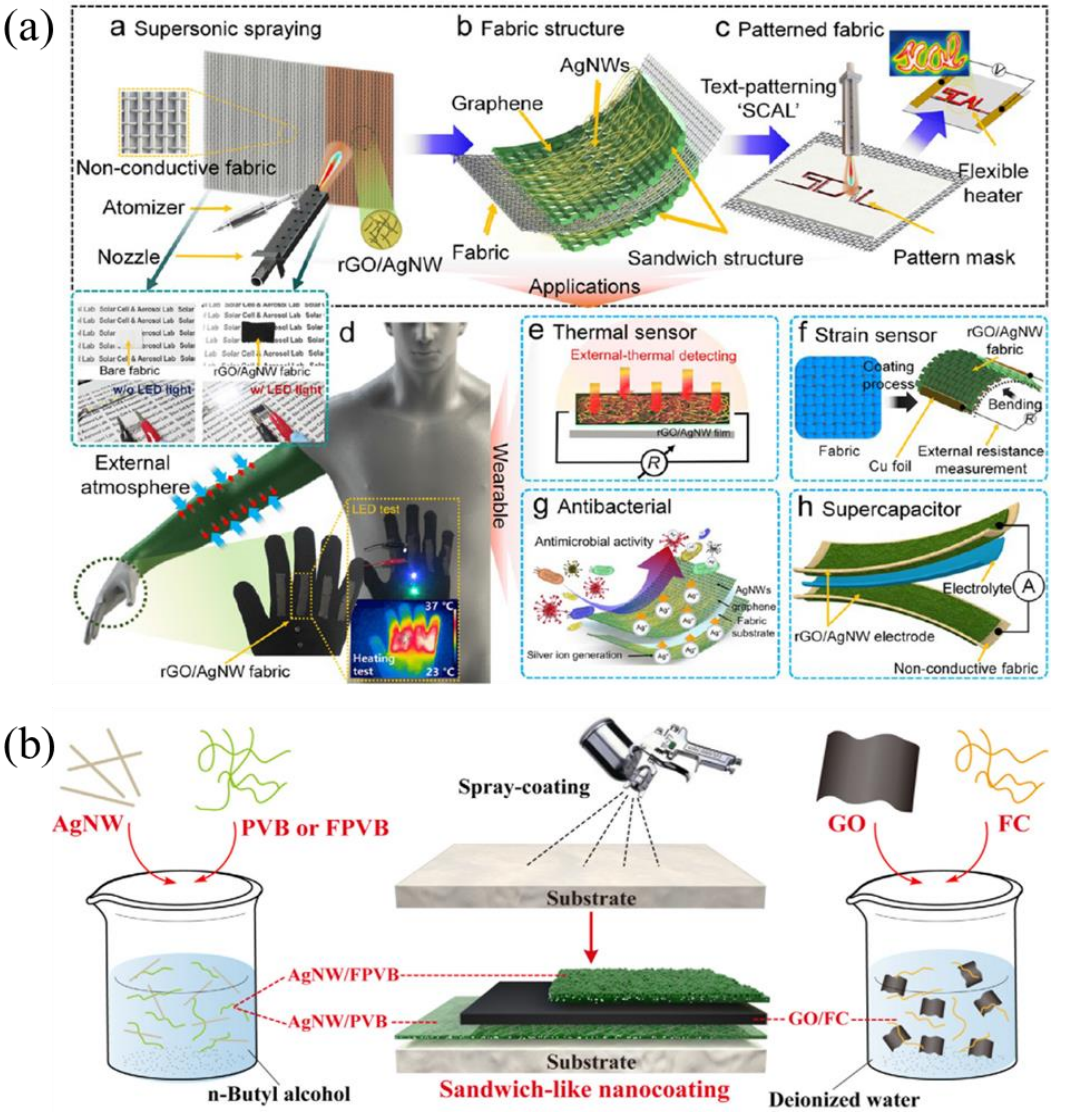

Fig. 16 (a) Schematic of the fabrication process and multifunctionality of the rGO/Ag NW fabric sensor; Reproduced with permission from [193], Copyright 2021 American Chemical Society (b) Preparation route of the sandwich-like flame retardant nanocoating. Reproduced with permission from [195], Copyright 2019 Elsevier B.V.

properties and printability of the conductive inks also highly influence the screen-printed conductive line characteristics.[202] The properties of the ink depend on the solid loading, particle dispersion, viscosity, rheological properties, particle-specific surface area, and density, *etc*. The inks used need to have high viscosity and low volatility, as low viscosity will cause the inks to pass directly through the screen opening and high volatility will result in the ink drying out on the screen and thus damaging the definition of the printed pattern.[203] Nevertheless, too high viscosity may lead to the formation of pores because the leveling of the ink after printing may not be completed.[202]

Liang *et al*. successfully printed uniform and sharp-edged patterns of Ag NWs both on flexible poly(ethylene terephthalate) (PET) and rigid glass substrates via the screen-printing method.[202] Ali *et al*. used a screen printing method to prepare flexible strain sensors by printing Ag NW/Ag flake composites on flexible thermoplastic polyurethane (TPU) substrates in straight or folded configurations (as shown in Fig. 17c).[204] Moreover, screen printing was used to prepare a class of microstrip patch antennas with Ag NWs embedded in the surface layer of an elastomeric substrate.[205]

4.6 Vacuum Filtration

During the vacuum filtration process, the Ag NWs network layer on the filter is prepared by filtering the Ag NW solution onto it. Then the Ag NW network layer is transferred to the target substrate (PDMS, PET, paper, etc.). The vacuum filtration method is actively used to fabricate the thin film structure of Ag NWs since the losses of Ag NWs during the

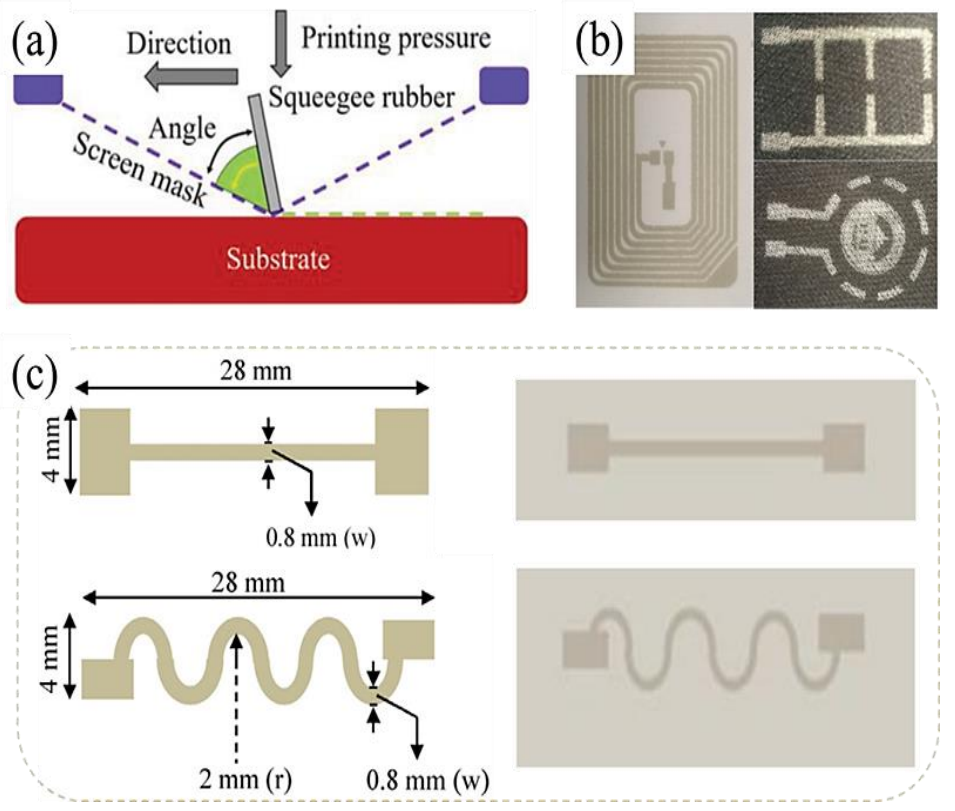

Fig. 17 (a) Schematic diagram of the process of screen-printing; Reproduced with permission from [198], Copyright 2019 WILEY-VCH Verlag GmbH & Co. KGaA, Weinheim, (b) Photographs of the screen-printed patterns on the textile and conventional paper; Reproduced with the permission from [200], (c) Schematics and photographs of screen printed straight and wavy line configuration for strain sensors on TPU substrate. Reproduced with permission from [204], Copyright 2018 Elsevier B.V.

fabrication process are much smaller than those of other processes.[206-209] The thickness of the films and the areal density of the Ag NW network can be easily controlled by tuning the amount and concentration of the solution to be filtered.[210]

Liu *et al*. fabricated two kinds of environmentally responsive composite films based on Ag NWs and silk nanofibrils (SNFs) using the vacuum filtration method.[211] By simply adjusting the distribution of Ag NWs in the SNF matrix, different sensory properties can be achieved. The Ag NW/SNF hybrid film exhibited unique humidity sensitivity, and the Ag NW/SNF layered film could be assembled into a pressure sensor. In an effective fabrication strategy developed by Shen *et al*., the Ag NW film was easily transferred from the membrane to a pre-cured flexible substrate after vacuum filtration to synthesize a flexible electrochromic supercapacitor Ag NW/WO_3 electrode.[212] Based on vacuum-assisted filtration and hot-pressing, Liang *et al*. fabricated multifunctional flexible EMI shielding Ag NWs/cellulose films.[213]

As shown in Fig. 18, a programmable mechanical cutter and vacuum filtration method was presented to pattern Ag NWs on a PDMS substrate for electrophysiological signal monitoring.[210] The resulting flexible and highly conductive (0.6 Ω/sq) Ag NW/PDMS dry electrodes recorded high-quality electrophysiological signals with a signal-to-noise ratio of 25.4 dB. In addition, the penetration of PDMS into the Ag NW network was enhanced by the vacuum pump device, which resulted in excellent adhesion between the PDMS and the Ag NW network and made it highly reliable for the long-term recording of electrophysiological signals.

Although the vacuum filtration technique is considered a simple approach to obtain an ultrathin film and uniformed Ag NW networks, it still suffers from incompatibility with large-area production due to the transfer areas being limited by the size of the membrane filter.

Every fabrication method has its advantages, and meanwhile, has its disadvantages. The comparison of these fabrication methods is summarized in Table 2.

5. Strategies to Reduce Contact Resistance

When Ag NWs network is used as conductors, a major problem is the high contact resistance of Ag NWs junctions, where both the in-plane and out-of-plane charge transport barriers are formed due to the nanoscale gaps between weakly bonded nanowires and the insulating layer of the residual PVP

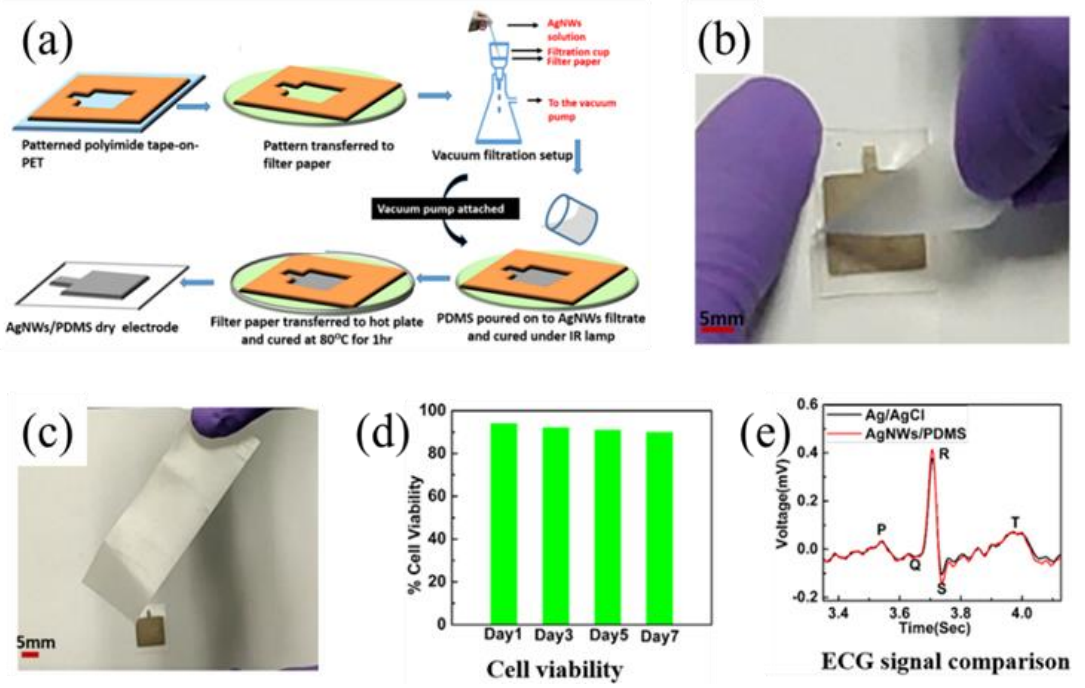

Fig. 18 (a) Schematic of the fabrication process of Ag NW/PDMS dry electrodes; (b, c) Scotch tape adhesion test of the patterned Ag NWs on the PDMS substrate; (d) Percentage cell viability by MTT assay for days 1, 3, 5, and 7; (e) Comparison of the magnified electrocardiogram signals of Ag/AgCl and Ag NW/PDMS electrodes. Reproduced with permission from [210], Copyright 2020 American Chemical Society

on the surface of Ag NWs. Several post-treatment strategies have been developed for welding the junction of the Ag NWs network.

Thermal annealing at high temperatures (≥150 °C) has been widely used to remove the residual PVP surfactant and weld the adjacent Ag NWs due to its simplicity and efficiency at a large scale.[132] However, direct thermal annealing will cause undesired fractures and oxidation of NWs and even damage the underlying flexible substrates. Based on this point, Song *et al*. proposed a nanoscale point reaction process that could effectively target the high-resistance contact points between NWs through current-assisted localized Joule heating and electromigration.[214] This method significantly improved the contact performance of NWs junction. The temperature of the adjacent device layers could be maintained close to room temperature, making this method particularly suitable for those devices containing thermally sensitive materials.

Chemical approach strategies are also used for Ag NWs welding. Lu *et al*. demonstrated a simple alcohol-based solution approach to confine the precursor at the junction region and induce a localized chemical reaction, through which the Ag NWs were welded together, and the sheet resistances and operational stabilities were improved.[215] This precursor solution was composed of $AgNO_3$, HNO_3, ascorbic acid, and ethanol. In addition, O_2 and HCl vapors,[216] H_2O_2 vapor,[217] ammonia-glucose mixed solution (Fig. 19a),[218] etc. are also used to weld Ag NWs. Nevertheless, additional chemicals were usually used in these strategies, which will result in increasing in surface roughness and decreasing in film transmittance inevitably.

Another effective method for enhancing Ag NWs junction is mechanical pressing. Tokuno *et al*. demonstrated that the electrical conductivity of Ag NW electrodes could be improved by mechanical pressing at 25 MPa for 5 s at room temperature and the surface roughness of the pressed Ag NW electrodes was one-third of that of the heat-treated electrode (Fig. 19c).[219] However, direct mechanical pressing will normally destroy the useful under-layers. This method might be used on some special occasions.

Capillarity can drive surface diffusion and induce a localized geometrical rearrangement that reduces spatial curvature.[220] Thus, at the nanoscale, the capillary force can be effective in achieving self-limiting cold welding of Ag NWs. By simply applying moisture on the Ag NW film and with the evaporation of water, the capillary force-induced welding could be achieved and thus the contact resistance was reduced (Fig. 19e).[221] Although this method provides a novel idea to optimize Ag NW conductivity, it is difficult for practical operation, for the hydrophobicity of the substrate, the volatilization rate, and other factors need to be considered well. Laser nano-welding has been used to reduce the contact resistance at the NWs junction for a transparent and flexible

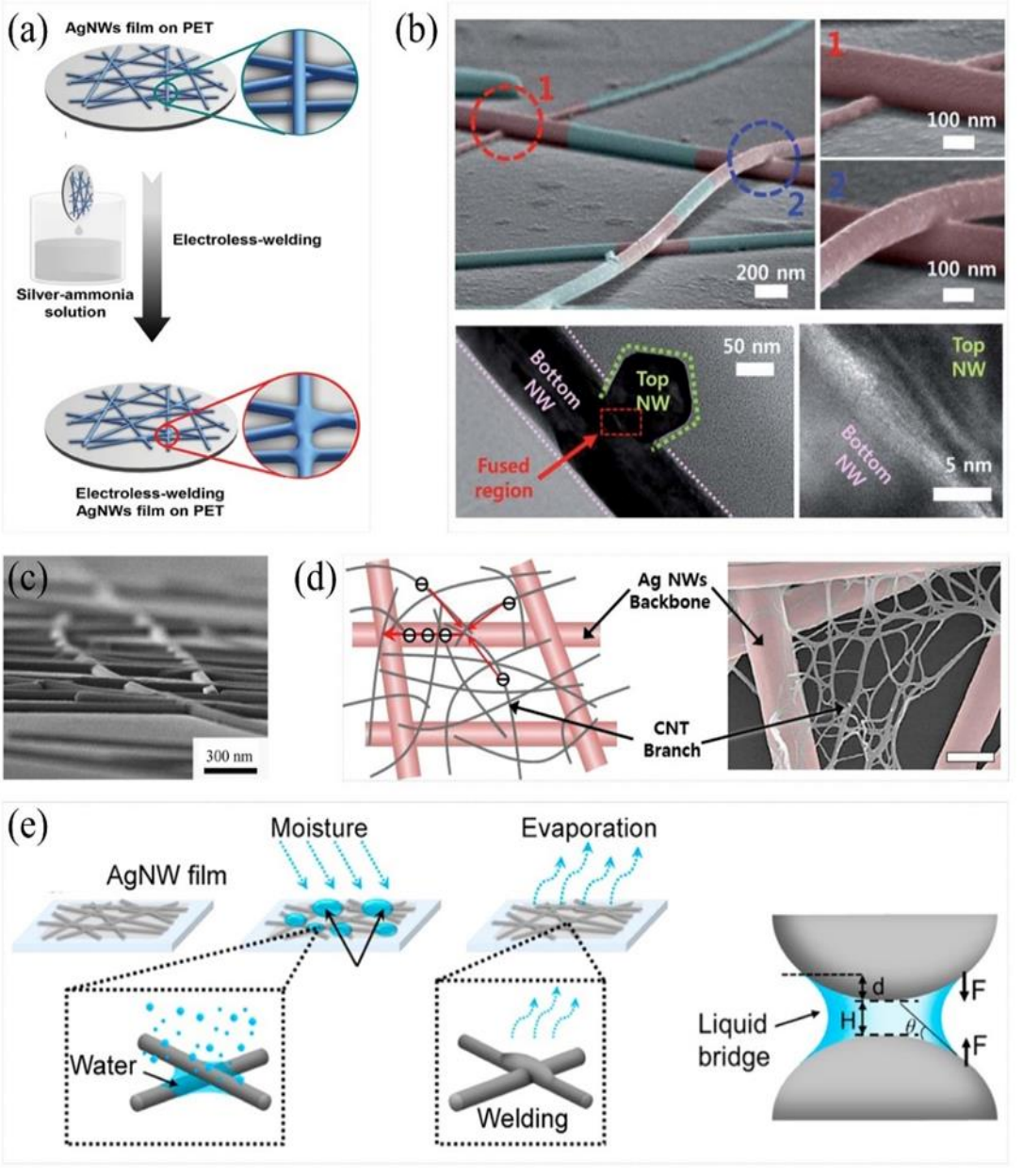

Fig. 19 (a) Electroless-welding of the Ag NWs film on PET using silver-ammonia solution; Reproduced with the permission from [218], Copyright 2016 WILEY-VCH Verlag GmbH & Co. KGaA, Weinheim, (b) Magnified SEM and HRTEM images of laser nano-welded spots between very long Ag NWs; Reproduced with the permission from [222], Copyright Royal Society of Chemistry (c) Off-angle cross-sectional view of FE-SEM image of tightly connected Ag NWs with smooth surfaces after being pressed at 25 MPa for 5 s; Reproduced with the permission from [219], Copyright 2011, Tsinghua University Press and Springer-Verlag Berlin Heidelberg, (d) Schematic diagram (left) and SEM image (right) of hierarchical multiscale Ag NW/CNT hybrid nanocomposite; Reproduced with the permission from [224], Copyright 2014 WILEY-VCH Verlag GmbH & Co. KGaA, Weinheim (e) Schematic of the moisture treatment process and assumed mechanism of capillary-force-induced cold welding of Ag NWs. Reproduced with permission from [221], Copyright 2017 American Chemical Society.

electrode (Fig. 19b).[222] The advantages of this strategy have been proven to be highly selective annealing with minimized thermal damage and ultrashort processing time (only a few seconds). This is because the laser is a monochromatic photon source, which maximizes the photon energy coupling into the NWs junction with much higher e-field enhancement, and also allows the photon energy and treatment temperature to be accurately controlled.[223]

The contact resistance of Ag NWs can also be reduced by nano-joining at the junctions with CNT. Mixing single-wall CNTs (d~1.2 nm, L~2-10 μm) into Ag NWs (d~150 nm, L~50-100 μm) network can enhance the conductivity through

providing local electron transport paths by filling the inter-nanowire space of the backbone electrode of Ag NW mesh (Fig 19d).[224] Meanwhile, the elastic single-wall CNTs may endow Ag NWs network with high stretchability and flexibility.

6. Devices and Applications

Ag NWs have emerged as an excellent alternative for transparent conductive materials due to their comprehensive properties, such as superior electrical conductivity and light transmission, remarkable flexibility, and stretchability. Other key advantages include the fact that it is simple to process and is rather affordable. All these advantages promote Ag NW to real-world applications. In this section, we aim to review the recent advances of devices and applications of Ag NW networks into the following categories: optoelectronic devices, including photovoltaic, light emitting devices and touch screens; electromagnetic applications, such as electromagnetic shielding, frequency selective surfaces, and transparent antennas; and other applications in transparent heaters, strain sensors and transistors for flexible electronics.

6.1 Optoelectronic Applications

6.1.1 Photovoltaic Devices

Transparent conductive electrodes (TCEs) are a critical component of photovoltaic devices, as they have a direct effect on photo conversion efficiency. To achieve low resistance and high-efficient photon absorption, high electrical conductivity, and light transmittance are the main properties that should be taken into account when choosing the electrode materials. While transparent metal oxides are the most developed TCEs employed for photovoltaic devices, there are still certain issues to resolve, such as complex processes and increased prices. More importantly, they have difficulties in compatible with flexible and stretchable devices.

By comparison, Ag NW networks are flexible and maintain their electrical characteristics during bending and folding, which are considered promising candidates for flexible organic photovoltaic devices (OPV) devices. Sun *et al*.[225] demonstrated a method for fabricating grid-like, smooth, and flexible Ag NW-based electrodes for OPV. The approach employs a water suspension of Ag NWs with poly(sodium 4-styrenesulfonate) (PSSNa) as the polyelectrolyte and is capable of producing flexible TCEs in a single step without the need for post-treatment. The fabricated flexible OPV devices performed comparably to those using commercial ITO glass electrodes (Fig. 20b). Power conversion efficiencies of 13.1% and 16.5% were observed for the flexible single-junction and tandem OPV devices, respectively.

Despite the excellent optoelectronic properties of Ag NW materials, there are a number of issues that need to be addressed prior to the use of Ag NWs in commercial optoelectronic applications. Some research efforts have been devoted to solving these problems, including reducing high roughness,[226] enhancing the adhesion to surfaces,[227] and improving resistance to environmental corrosion.[228]

In addition to the excellent optoelectronic properties (high conductivity and transparency), Ag NWs are introduced as the primary material to replace indium tin oxide for fabricating flexible organic solar cells because of their remarkable solution-processing ability, which can be compatible with low-cost roll-to-roll manufacturing in the ambient environment. Recent work demonstrated the reproducibility and efficiency of a semitransparent organic photovoltaic with modified Ag NW top electrodes.[229] Notably, there was no use of high-temperature thermal annealing. As a result of the outstanding compatibility and enhanced performance of the solution-processed top bimodal Ag NW electrodes with the underlying poly(3,4-ethylenedioxythiophene): poly(styrenesulfonate) (PEDOT:PSS) layer, the semitransparent OPV devices demonstrate an excellent power convention efficiency (PCE) of 7.49% with a high degree of transparency invisible region. Benatto *et al*.[230] reported the use of roll-to-roll printed Ag NW networks as front electrodes for fully roll-to-roll processed flexible ITO-free OPV modules, indicating the high-volume production of Ag NW-based OPV devices is promising.

More recently, Wang *et al*.[231] reported flexible polymer solar cells based on gravure-printed Ag NW electrodes and achieved a high PCE of 13.61%. They first obtained Ag NW inks that are suitable for the gravure printing process for fabricating TCEs (as illustrated in Fig. 20d). The benefits of the ease of large-area electrode fabrication and increased uniformity in gravure printing were demonstrated by comparing with the spin-coating technique. Due to the great homogeneity of the gravure-printed Ag NW electrode, the maximum PCE of 13.61% for 1 cm^2 polymer solar cells based on gravure-printed flexible TCEs is attained, which exhibited better performance than devices with electrodes prepared by spin coating (Fig. 20e). Xie *et al*.[232] fabricated flexible single-component organic solar cells (SCOSCs) based on a double-cable polymer on a transparent Ag NWs electrode on a plastic foil. Impressively, the obtained flexible SCOSCs exhibited a PCE of 7.21% and possessed superior mechanical robustness (>95% retention after 1000 bending cycles) and storage stability (>97% retention after 430 h in a nitrogen atmosphere). Wang *et al*.[233] developed an ultrathin flexible transparent composite electrode (~9 μm) via semi-embedding an Ag NW

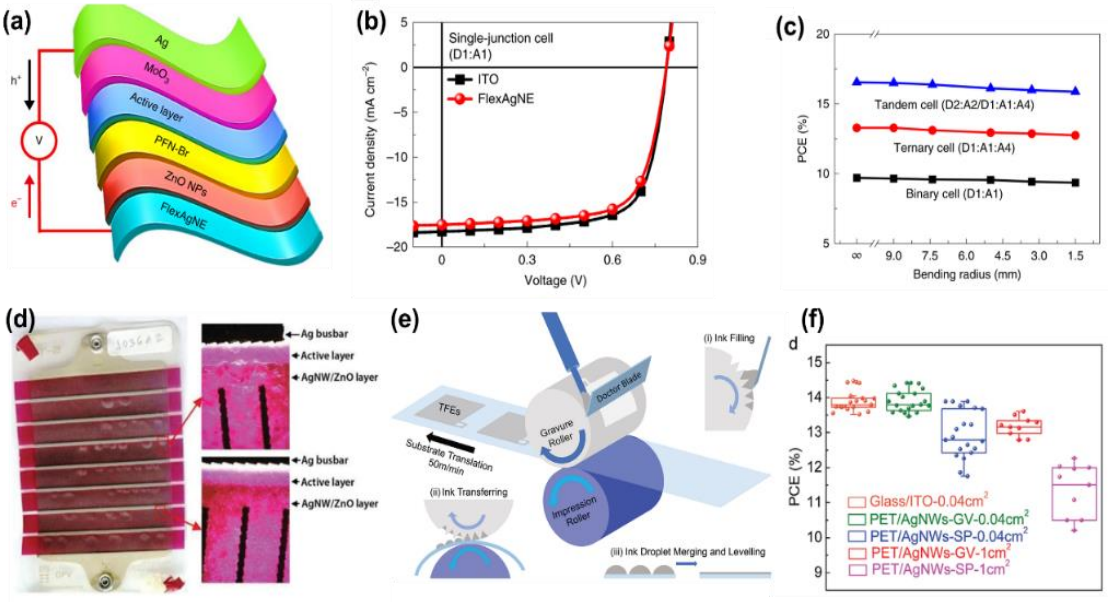

Fig. 20 OPV devices based on Ag NWs transparent electrodes. (a) The schematic architecture of the flexible OPV; (b) J–V curves of typical single-junction devices based on ITO and FlexAgNE; (c) PCEs for flexible OPV devices based on FlexAgNEs as a function of bending radius (9.0 mm, 7.5 mm, 5.0 mm, 3.5 mm, and 1.5 mm); Reproduced with the permission from [225], Copyright 2019, The Author(s), under exclusive license to Springer Nature Limited, (d) Microscope images of a sample with Ag NW front electrode and Ag-grid back electrode under ISOS-L-3 of a region with (right top) and without (right bottom) a bubble defect; Reproduced with the permission from [230], Copyright The Royal Society of Chemistry, (e) Schematic diagram of the high-speed gravure printing process for fabricating Ag NW electrodes; (f) PCE distribution diagram of the devices based on PET/Ag NWs-GV, PET/Ag NWs-SP, and glass/ITO electrodes. Reproduced with permission from [231], Copyright 2020 Wiley-VCH GmbH.

electrode in a colorless polyimide (cPI) substrate. Based on this electrode, an ultra-flexible OSC with a high PCE value of 14.37% and outstanding mechanical robustness was constructed, in which the PCE could still maintain above 96% of its initial value after 1000 bending cycles at a bending radius of 0.5 mm.

6.1.2 Light-emitting Devices

Similarly, TCEs are of great importance to various types of light-emitting devices, such as organic light-emitting diodes (OLED),[234,235] quantum dot emitting-diodes (QLED),[236] polymer light-emitting diodes (PLED).[172,237,238] Ag NW material seems also to be a promising alternative to commercial ITO electrodes owing to its excellent electrical conductivity, high optical transmittance, superior flexibility, and facile process.[41]

Generally, OLEDs have been constructed by sequentially depositing thin organic active layers and metallic layers over an anode. Leakage current may occur during the fabricating procedure due to the spikes on the anode. Reducing the roughness of the surface of cathode nanoelectrodes is the key to their application in high-performance OLED devices. To address this problem, Ok *et al*. demonstrated flexible and leakage-free OLED by employing an ultra-thin and smooth Ag NW-based transparent anode (Figs. 21a-c).[234] By embedding Ag NWs into a cPI, they obtained smooth and flexible TCEs with high optoelectric performance (a transmittance of >80%, and low *Rs* of 8 Ω/sq), and the fabricated devices exhibited a leakage-free and foldable character.

The fact that cannot be ignored is that the performance of Ag NW percolation networks is limited in thin-film device applications due to the reduced effective electrical area caused by their inherent dimple structure and percolation voids. To address this problem, Lee *et al*.[235] prepared a TCE based on a dual-scale Ag NW percolation network that significantly increased the effective electrical area by filling the enormous percolative gaps in a long/thick Ag NW network with short/thin Ag NWs, in which the long/thick Ag NW network acts as a backbone highway for carrier transport and the short/thin Ag NW network connects to long/thick Ag NWs across large percolation voids. As a result, the TCE exhibited outstanding optoelectric performance (high transmittance of 90% at 550 nm, and low *Rs* of 50 Ω/sq), and the fabricated OLED device with the dual-scale Ag NW percolation network achieved superior efficiencies (Fig. 21d). Ricciardulli *et al*.[238] proposed a synergic coupling strategy for the fabrication of TCEs based on hybrid Ag NW and exfoliated graphene. The electrodes demonstrated a low surface roughness, outstanding

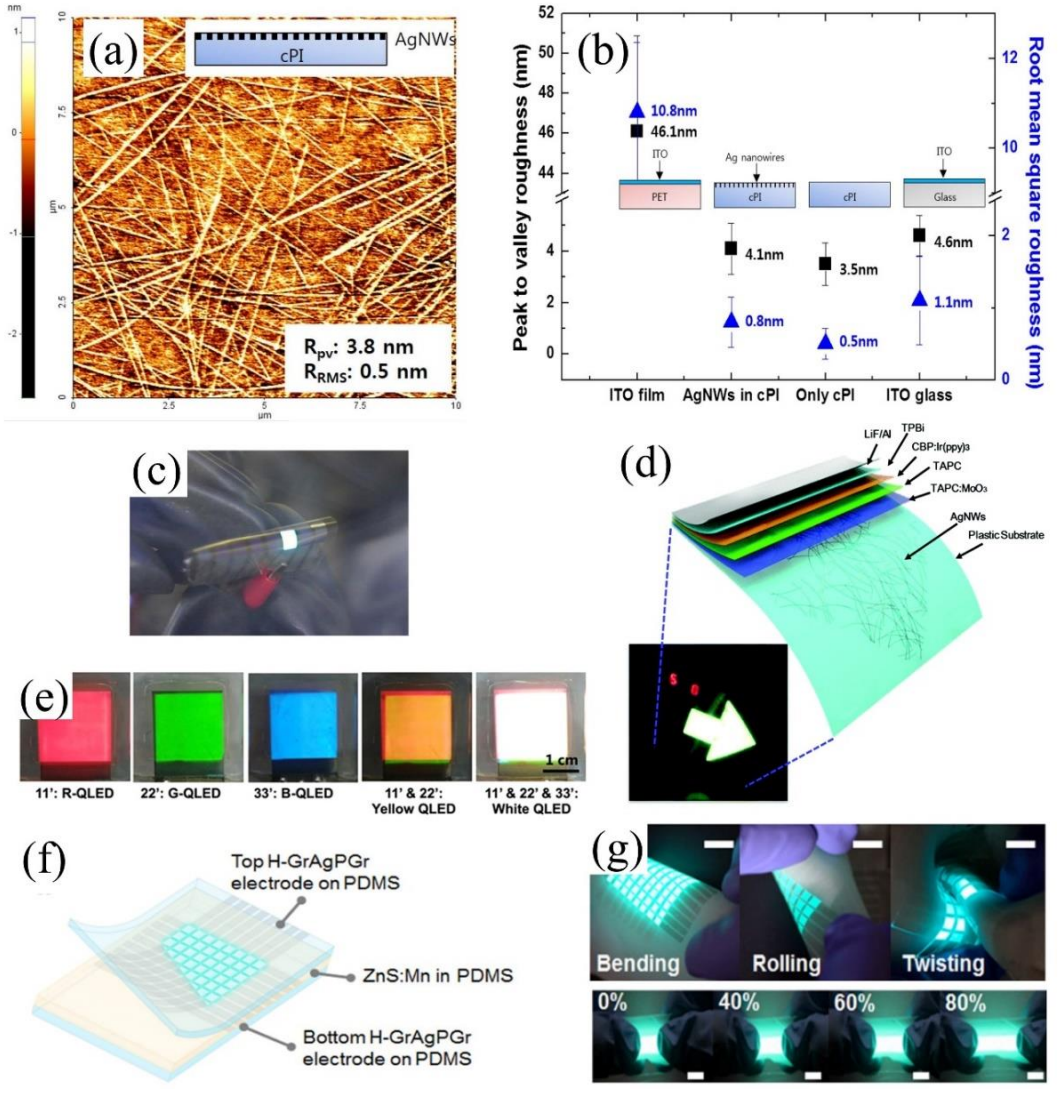

Fig. 21 High-performance Ag NW-based transparent electrodes used in light-emitting devices. (a) AFM of Ag NW-cPI composite electrode; (b) a diagram comparing the roughness of various samples; (c) Bending stability of the flexible OLEDs based on Ag NW-cPI composite electrodes; Reproduced with the permission from [234], Copyright 2015, The Author(s), (d) dual-scale Ag NW network transparent conductor for highly efficient and flexible organic light-emitting diodes; Reproduced with the permission from [235], Copyright The Royal Society of Chemistry (e) Schematic illustration of the stretchable electroluminescent device based on Ag NW electrodes luminescent photographs of the R/G/B QLED by driving three pairs of electrodes; Reproduced with the permission from [236], Copyright 2020 American Chemical Society (f) Luminescent photographs of the R/G/B QLED by driving three pairs of electrodes. g) bending, rolling, and twisting of the array. Reproduced with permission from [239], Copyright 2019 American Chemical Society.

optoelectric performance, and superior mechanical and chemical stabilities. By employing the TCE in a PLED, the device exhibited an external quantum efficiency of 4.4%, which is comparable to their commercial ITO counterparts.

By sandwiching an insulating resin layer between two conductive Ag NW layers, a novel Ag NWs/resin/Ag NWs sandwich-structured electrode with low R_s on both sides and good transparency was produced by Sun *et al*. The prepared electrode was used to fabricate a large-area transparent red/green/blue QLED (Fig. 21e), presenting an external quantum efficiency of 11.42% and a transmittance of 72.5%.[236]

At present, some of the reported light-emitting devices based on Ag NW TCEs have been comparable to ITO electrode devices in terms of lighting performance. Although it possesses the additional advantages of flexibility and stretchability, how to achieve uniform electroluminescence and stable light emission during folding and stretching is still a challenge. Shin *et al*. proposed a fabrication scheme for flexible TCEs, in which two-dimensional graphene layers and

Ag NWs embedded PEDOT: PSS film was combined together.[239] The developed hybrid electrode overcomes the limitations of Ag NWs and ionic conductor-based electrodes, thus achieving uniform emission under stretching and folding (as shown in Fig. 21g).

6.1.3 Touch Screens

Although the research of using Ag NWs in touch screens has been less studied than in solar cells and heaters *etc*., it is also a very promising application area with the advantages of high light transmission, high conductivity, large size, low cost, and high flexibility.[240] Nowadays, researchers pay attention to large-area and good-performance Ag NWs touch screens.[189,241]

For example, to improve the bond strength between the Ag NW electrode layers and the polymer substrates, thus enhancing the durability of flexible touch screen panels (f-TSPs). Yu *et al*.[242] introduced strong Ag–S bonding and developed tough and strong electrode-substrate bonded Ag NWs/thiol-modified nano fibrillated cellulose (NFC-HS) transparent conductive electrodes. Its structure was illustrated in Fig. 22a and the bonding strength between Ag NW networks and substrates was evaluated through bending and peeling test cycles (Figs. 22c-d). After 500 cycles of bending around an arm (Fig. 22b), the as-prepared f-TSP device can still exhibit high sensitivity without significant loss of electrical performance. Cho *et al*.[180] fabricated a kind of flexible, transparent, and force-sensitive touch screens using cross-aligned Ag NW electrodes (Fig. 22e), which exhibited excellent electrical conductivity as well as optical transmittance over a large area of the film (R_s of 21.0 Ω/sq at 95.0% of optical transmittance with large-area >20×20 cm^2). The force-sensitive touch screens are capable of accurately monitoring dynamic writing, tracing and drawing underneath pictures and sensing handwriting patterns with locally varying writing forces.

6.2 Electromagnetic Applications

6.2.1 EMI Shielding

Electromagnetic interference (EMI) shielding is an effective approach of attenuate electromagnetic waves to avoid interference and damage to sensitive devices caused by electromagnetic radiation, thus playing an important role in the reliability of electronics in complex electromagnetic environments. One-dimensional silver nanostructured materials have also attracted considerable interest in electromagnetic applications. In this section, we mainly focus on the ability of Ag NW conductive film to attenuate electromagnetic waves. The shielding effect can be caused by

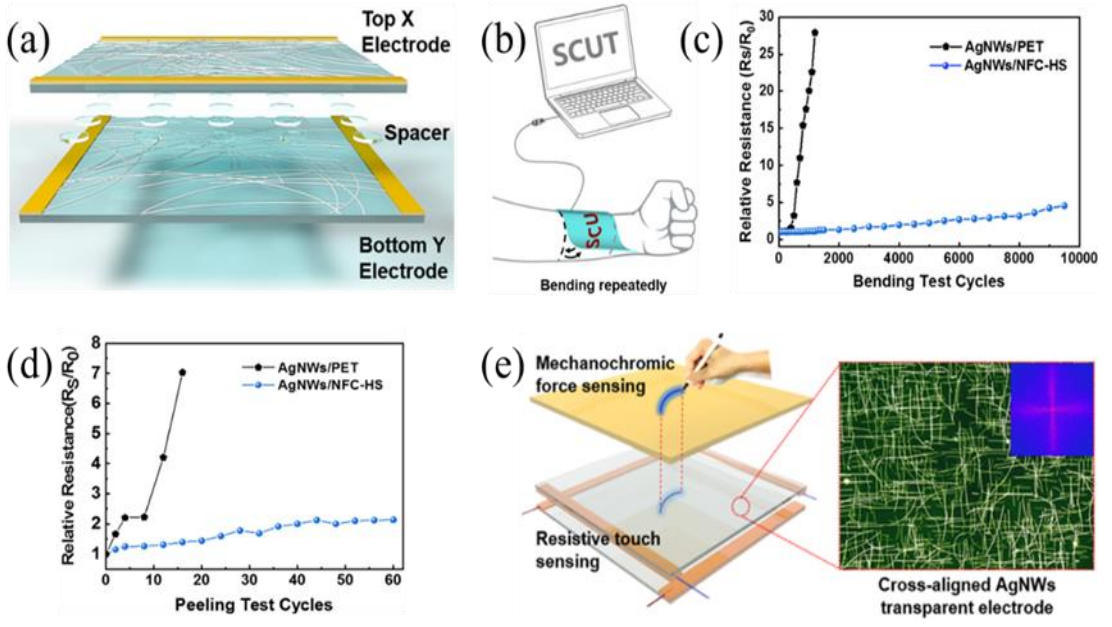

Fig. 22 High-performance touch screens based on Ag NWs. (a) Schematic illustration of the structure of f-TSP device using Ag NWs/NFC-HSas it's top and bottom TCEs; (b) Schematic illustration of the durability test for the f-TSPs. The plot of relative resistance vs. (c) bending test cycles, (d) peeling test cycles of Ag NWs/PET and Ag NWs/NFC-HS for evaluating the bonding strength between Ag NW networks and substrates Reproduced with permission from [242], Copyright 2021 Elsevier Ltd, (e) Schematic illustration of the device structure of a force-sensitive touchscreen showing simultaneous force and touch sensing in response to dynamic writings. The Ag NW arrays are cross-aligned. Inset is the fast Fourier transform (FFT) analysis of the optical micrographs, indicating the direction and uniformity of the aligned Ag NW structures. The scale bar is 40 μm. Reproduced with permission from [180], Copyright 2017 American Chemical Society.

electromagnetic waves being reflected at the surface of shielding materials, by electromagnetic waves being absorbed, or by multiple reflection losses occurring within the shielding material itself. Metals are frequently used as EMI shielding materials due to their superior electrical conductivity. However, their application is constrained by the drawbacks of high density and difficult processing. As an emerging conductive material with light weight and easy processing characteristics, Ag NWs networks have great potential to be used in EMI shielding applications.

Typically, Ag NW networks are prepared as composite films together with other functional materials to increase the conductivity, permeability, and stability, thus obtaining better electromagnetic shielding performance and environmental stability. An example was performed by Wang *et al*., who introduced ferroferric oxide into an Ag NWs film to prepare the shielding films.[243] They demonstrated a robust composite EMI shielding film with shielding effectiveness (SE) of 24.9 dB at 8.2 GHz and 90% optical transparency. The introduced ferroferric oxide improves electromagnetic radiation absorption and reflection due to its high permeability and increased conductivity. Qin *et al*.[244] recently fabricated transparent, stable, and uniform Ag NW–PEDOT: PSS composite film an EMI shielding material. They investigated the shielding performance of the prepared film and achieved a SE of 30.5 dB in the tested frequency of 1-12 GHz while reaming a high optical transmittance of 91%. More interestingly, the composite shielding film exhibited outstanding SE exceeding 50 dB at the excitation power density of 40 W cm^{-2} (Fig. 23b), indicating the tremendous potential of Ag NW for shielding high-power microwaves.

Additionally, Ag NWs are employed in composite electromagnetic shielding materials with layered structures.[245-249] The overall performance can be improved by developing a layered architecture comprising multiple thin films towards high electromagnetic shielding performance. Ma *et al*.[250] recently reported a layered hybrid EMI shielding film constructed by multi-walled carbon nanotubes (MWCNTs) and Ag NWs. The EMI SE was greater than 45 dB over the ultra-wide frequencies of 4-40 GHz and reached a maximum of 72 dB at 10 GHz. For the shielding film with a layered structure of Ag NWs and MWCNTs, the high conductivity of the Ag NWs results in ohmic loss, while the numerous defects in the MWCNTs result in polarization loss. This configuration enhanced impedance matching across the MWCNT top layer and multiple reflected absorption over the macroscopic interface between the MWCNT and Ag NW layers, hence improving the overall EMI shielding performance.

Ag NWs could be incorporated into other conductive networks to achieve enhanced conductivity for high-performance EMI shielding composite films. For example, Zeng *et al*. prepared ultralight biopolymer aerogels with biomimetic lamellar, honeycomb-like, and random micrometer-sized pores combining renewable cellulose nanofibers with Ag NWs in an ice-templated freeze-casting process.[251] Owing to the introduction of Ag NWs, porous scaffolds were extremely conductive, with tunable densities, strength, and flexibility, showing an outstanding EMI shielding performance (>70 dB in the density of 6.2 $mg \cdot cm^{-3}$). Yang *et al*.[252] reported that Ag NWs with a high aspect ratio could be embedded in MXene Sediment-based hydrogels to increase the intrinsic conductivity of cell walls (Fig. 23j), thus enhancing the EMI-shielding performance by more than 20 dB in X-band.

Electromagnetic protecting materials for optoelectronic systems must not only perform well in terms of electromagnetic shielding but also meet certain light transmission standards in order to ensure that the signal transmission of the optoelectronic system is not affected. As a conductive material with excellent light transmission properties, Ag NW-based conductive film finds its applications in transparent EMI shielding to reduce the risk of complex electromagnetic environments for optoelectronic systems. In recent years, researchers have carried out a series of research work on Ag NW-based composite films to further improve the comprehensive performance of Ag NW transparent electromagnetic shielding films.[243,244,253-257]

For Ag NW materials, transparent conductive films with effective electromagnetic shielding performance can usually be obtained by simple solution-based preparation methods. Wang *et al*.[258] reported flexible transparent Ag NWs EMI shielding films with a sandwich structure. They used a straightforward rod-coating approach to fabricate the shielding film in which the Ag NW networks are covered by the biodegradable gelatin-based substrate. The results showed a SE of 37.74 dB at the X-band and a light transmission of 72.0% (Figs. 23d-e). In a recent work by Chen *et al*., the authors suggested a multiscale structure optimization strategy for fabricating transparent and conductive Ag NW films with good EMI shielding performance and high light transmittance using a scalable spray-coating technique.[256] In their work, Ag NW networks were decorated by a $Ti_3C_2T_x$ MXene coating, thus significantly enhancing the connection of Ag NWs. As a result, the layered structural design on a macroscopic scale resulted in an outstanding EMI SE of 49.2 dB and an 83% light transmittance (Fig. 23f). Jinwook Jung *et al*.[46] demonstrated a highly stretchable and transparent electromagnetic

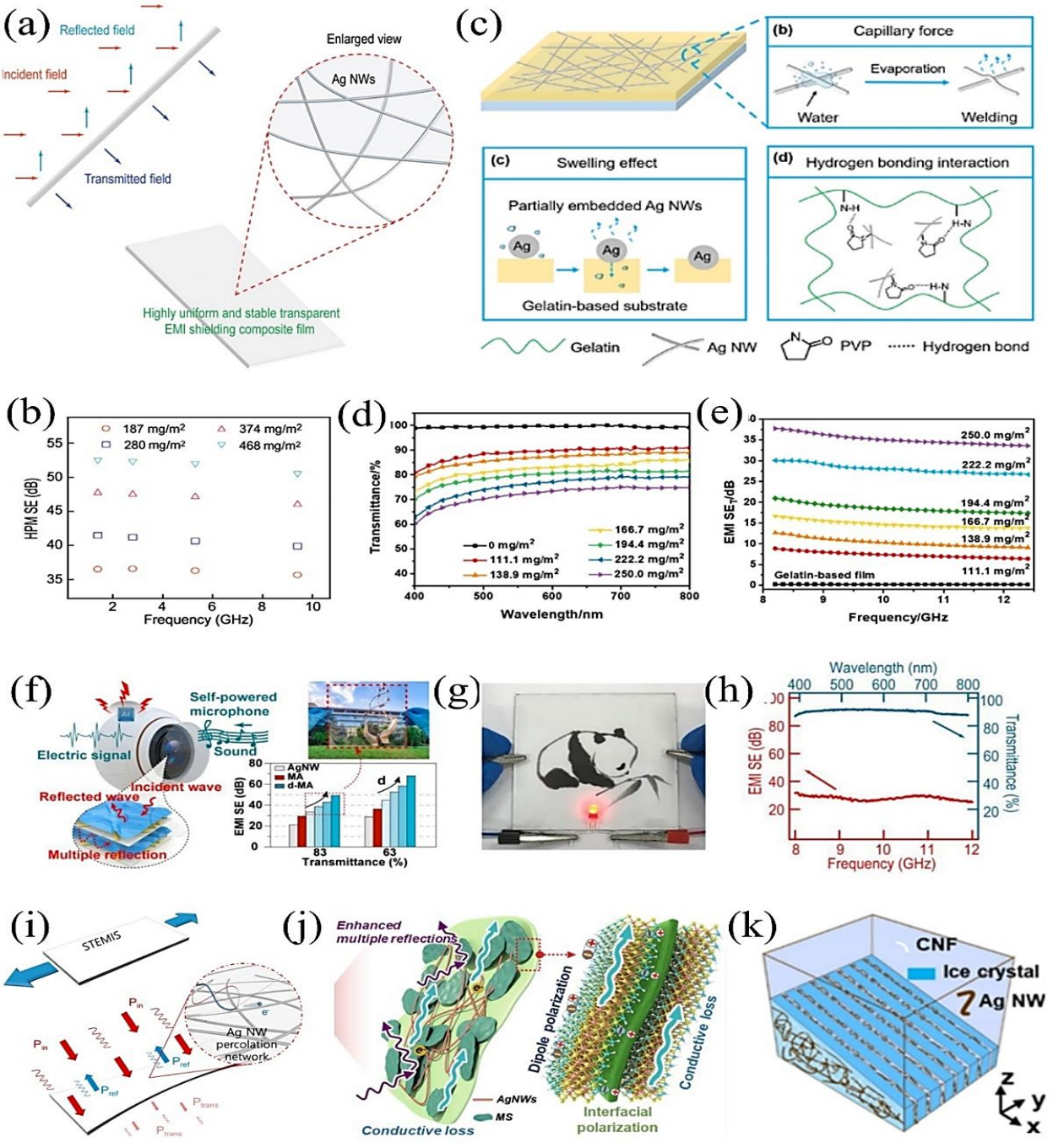

Fig. 23 Ag NWs materials used in transparent shielding applications. (a) Schematic showing the transparent EM shielding film composed of Ags NW and PEDOT: PSS; (b) High-power microwave SE of the composite film; Reproduced with the permission from [244], Copyright 2020 Wiley-VCH GmbH, (c) Schematic illustration of the strong adhesion between Ag NWs and gelatin-based layers. and capillary force induced welding of Ag NWs, swelling effect of the gelatin-based substrate, the hydrogen bonding interaction between Ag NWs and gelatin-based layers; (d) transparent and (e) Total EMI SE of gelatin-based film and G/Ag NW/G films; Reproduced with the permission from [258], Copyright 2021 Elsevier Inc. (f) Flexible, Transparent and Conductive $Ti_3C_2T_x$ MXene Ag NWs Films with Smart Acoustic Sensitivity for High-Performance Electromagnetic Interference Shielding; Reproduced with the permission from [256], Copyright 2020 American Chemical Society (g) Image and (h) performance of stable transparent electromagnetic interference shielding film is realized based on Ag NWs by integrating a polymer layer; Reproduced with the permission from [47], Copyright RSC Publication, (i) Stretchable and transparent electromagnetic wave shielding film; Reproduced with the permission from [46], Copyright 2017 American Chemical Society, (j) The EMI shielding mechanism of the hydrogels with biomimetic ordered porous structure; Reproduced with the permission from [252], Copyright 2022 American Chemical Society, (k) Schematic illustrations of the growth of the ice crystals in bidirectional freezing approaches for the CNF/Ag NW dispersion. Reproduced with permission from [251], Copyright 2020 American Chemical Society.

interference shielding (STEMIS) layer for wearable electronics (Fig. 23i). The stretchable and transparent EMI shielding sheet shields electromagnetic waves well even under extreme tensile strain, expanding the application area in soft or non-planar surfaces such as biological systems and human skin.

Since there is a trade-off between conductivity and light transmittance of Ag NWs transparent conductive films, a fair balance between the two is required in transparent shielding applications. To ensure high-quality signal transmission in the optoelectronic system, an extremely transparency characteristic is a necessity.

Excellent flexibility and environmental stability are also essential for transparent EMI shielding films from the perspective of practical applications. A number of research works have demonstrated the way to increase the flexibility and stability of Ag NW transparent electromagnetic shielding films by means of designing layered structures and constructing protective coating layers.[245-247,253,255,259,260] Using the liquid-to-vapor pressure-assisted wet sintering method, Kim *et al*. fabricated a transparent acrylic polymer-coated/reduced graphene oxide/Ag NWs EMI shielding film. The multilayer film demonstrated excellent flexibility and humidity resistance, as well as excellent transparent shielding performance. Due to the high contact angle of the acrylic coating layer, the multilayer shielding film demonstrated excellent temperature and humidity resistance, with no change in the SE after 500 hours at 85°Cand 85% relative humidity.[253] Zhu *et al*. demonstrated the improved stability of the Ag NW/PDDA composite films. With the assistance of the covering layer, a significantly improved stability aging 35 days at 25 °C/65% RH was achieved. Additionally, the EMI SE of the composite films was 28 dB on average at 91.3% transmittance and gradually increased to 31.3 dB while maintaining an optical transmittance of 86.8% (Fig. 23h).[47] And more recently, the authors fabricated highly transparent flexible EMI shielding films using Ag NWs and polymethyl methacrylate (PMMA). In this study, purified Ag NWs with consistent size and shape were used to construct the sandwich structure of the PET/Ag NW/PMMA flexible transparent conductive films with low surface roughness was obtained by Mayer-rod coating the Ag NWs and spin-coating the PMMA polymer on a PET substrate. The prepared films exhibited an acceptable EMI SE of 21.3 dB and high optical transmittance of 95.6%.[259]

The facile and various preparation method of electromagnetic shielding films based on Ag NWs is a non-negligible advantage that has been demonstrated in many kinds of literature.[245, 253,256,261-263] In the research work by Fang *et al*., Ag NW-based composite films were prepared via a simple and novel casting process and demonstrated effective electromagnetic shielding ability.[245] Lee *et al*.[261] used an efficient and straightforward dip-coating procedure to fabricate Ag NW-coated cellulose papers with a hierarchical structure, providing an effective way to form highly conductive Ag NW networks for EMI shielding films.

High-performance transparent electromagnetic shielding films can be achieved by optimizing Ag NWs network property and layered structure design strategies. Due to the conductive mechanism of Ag NWs, the carriers in Ag NWs exhibit strong scattering characteristics, resulting in much less conductivity than the bulk material, it is difficult to achieve low sheet resistance while ensuring a high light transmission of the film, thus exhibiting a more general transparent electromagnetic shielding performance. In addition, Ag NWs are easily corroded by oxidation, leading to a decrease in conductivity and serious stability problems. These are some of the problems that currently exist and are to be solved with further research.

6.2.2 Ag NW-based Transparent Frequency Selective Surfaces

Apart from being utilized as EMI shielding films, Ag NW networks can also be applied in other electromagnetic applications to manipulate the propagation of electromagnetic waves, including frequency selective surfaces (FSS), antennas, and so on. Due to their flexible, transparent nature, highly conductive Ag NWs can be used in place of conventional conductive metallic materials in certain electromagnetic applications, endowing them with new features like flexibility, stretchability, and reconfiguration. Moreover, the adoption of Ag NW networks would significantly reduce the usage of metals, which is favorable to lightweight devices and low-cost manufacturing.

FSS is an array structure composed of resonant cells arranged periodically in a two-dimensional plane, which can exhibit frequency-selective characteristics of electromagnetic waves.[264,265] It is one of the hot spots in the field of electromagnetic research. Research have proved that Ag NW networks are promising in the construction of flexible and transparent FSS. Wang *et al*.[266] designed an optically transparent FSS for GSM shielding by screen printing a transparent Ag NW-based ink on a flexible polymer substrate. Dual-band reflectance performance was achieved, as well as high optical transparency and good flexibility (as shown in Fig. 24). Another transparent FSS was demonstrated by Song *et al*.[267] who deposited patterned Ag NW film on a glass substrate, demonstrating -15 dB of a stop-band notch in the

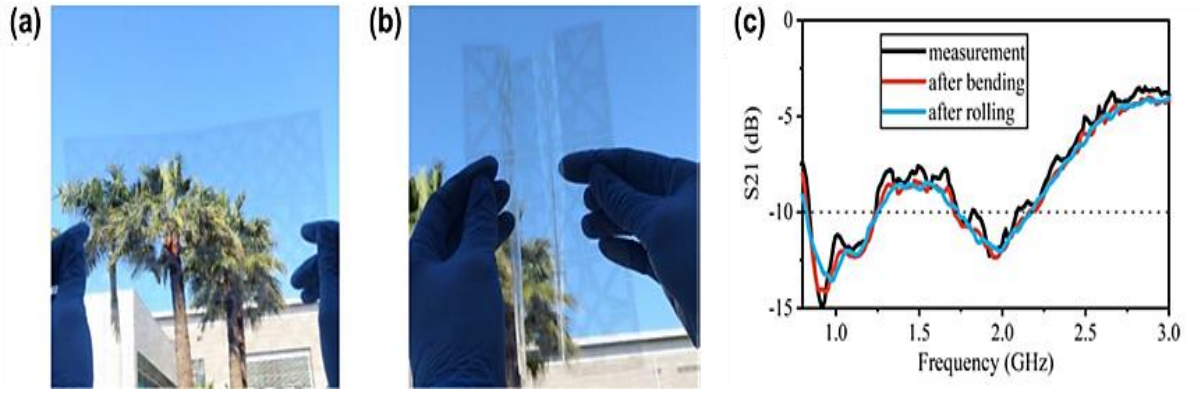

Fig. 24 Optically transparent FSS based on Ag NWs for GSM shielding. (a) Digital photograph of the printed Ag NW-based FSS; (b) FSS under bending condition; (c) Measured transmission response of the transparent FSS after bending or rolling. Reproduced with the Permission from [266], Copyright 2021, IEEE.

Ku-band and optically transparency in the visible spectrum range.

By optimizing the Ag NWs ink preparation method and screen-printing process parameters, Li *et al*. achieved a balance of the electrical conductivity, transparency, flexibility, and stretching properties of Ag NWs materials. When exposed to 1000 bending cycles with a bending radius of 28mm and 1000 stretch-release cycles with 10% strain, the screen-printed transparent patterns exhibit excellent electrical stability and mechanical repeatability, making them suitable for fabricating flexible, transparent microwave absorbers. The constructed FSS absorbers exhibit no noticeable decrease in absorption performance after bending and stretching test cycles,[268] demonstrating the promising prospect of Ag NWs materials for flexible and stretchable FSS.

6.2.3 Flexible and Transparent Antennas

The flexible transparent antenna has the characteristics of easy integration and high concealability and has broad application prospects in the field of wearable electronics and wireless communications. Studies have also focused on the potential of Ag NW materials in wireless communications, and a number of papers have demonstrated the use of Ag NWs to construct flexible and stretchable antennas.[205,269-272] The superior mechanical property endows Ag NW-based antennas with outstanding conformal ability, allowing it easy to be integrated into numerous wearable devices and functional systems for signal monitoring, detection, and navigation. In addition, Ag NWs are compatible with printing electronics due to their solution-processing ability. By patterning Ag NWs using additive manufacturing techniques like inkjet printing, fabrication costs can be greatly reduced and flexibility may be improved.

For instance, a stretchable, flexible antenna made of Ag NW and polydimethylsiloxane (PDMS) was fabricated by the screen-printing method. Highly conductive Ag NWs are proven to give promising results for radio frequency sensing when combined with mechanically flexible and resilient PDMS.[270] According to the measurement results, there is a shift of resonant frequency to the left as the force applied increases (Fig. 25a), indicating its potential application in wireless communications. Likewise, microstrip patch antennas that can be stretched, mechanically adjustable, and reversibly deformed are demonstrated by Song *et al*. (Fig. 25b).[205] The radiating element of the antenna is fabricated by screen printing highly conductive Ag NW material onto an elastomeric substrate. The antenna's resonance frequency may be changed by varying the tensile strain applied to it, endowing it with additional reconfigurable characteristics. Kim *et al*.[271] reported a facile compressing and transferring method to construct reversibly stretchable, optically transparent radio-frequency antennas based on wavy Ag NW networks. It exhibited an interesting result that the antennas formed from the wavy NW networks obtained improved performance when strained compared with the antennas formed from the straight NW networks. And recently, Li *et al*. have developed a transparent Ag NW-based triangular monopole antenna for 5G applications with the assistance of inkjet printing technology.[272] Extremely high radiation efficiency (55%), large bandwidth (26 GHz), and high gain (1.45 dBi) are achieved by the Ag NW antenna. Moreover, the Ag NW antenna has achieved transparency levels of over 90% (Figs. 25d-e).

As discussed above, Ag NW-based materials exhibit the potential for electromagnetic functional materials and devices, especially for those being applied in the flexible and transparent application scenario. To develop various high-performance electromagnetic functional materials and devices, more attention should be paid to the fundamental electromagnetic properties and behavior of Ag NW materials,

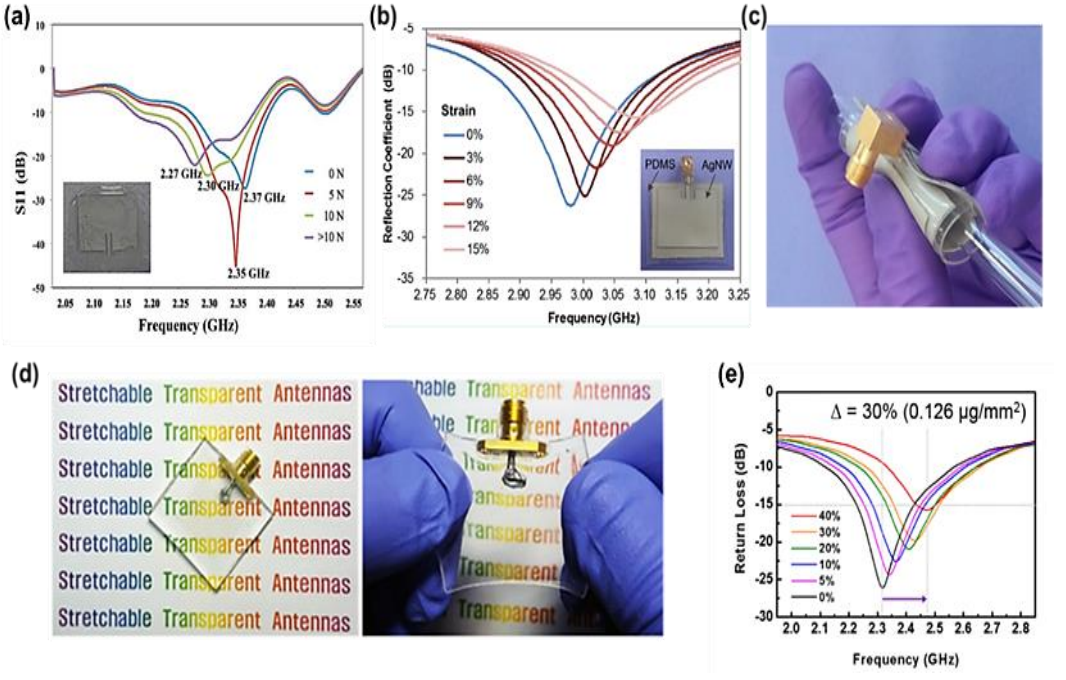

Fig. 25 Flexible and stretchable transparent antennas based on Ag NWs. (a) The resonant frequency of the stretchable RF antenna. Inset: the antenna prototype; Reproduced with the Permission from [270], Copyright 2013, IEEE, (b) Frequency response of reflection coefficient for the Ag NW/PDMS microstrip patch antenna under tensile strains from 0% to 15%. Inset: Photographs of a stretchable microstrip patch antenna composed of Ag NW/PDMS flexible conductor; (c) The antenna is rolled; Reproduced with the Permission from [205], Copyright 2014 American Chemical Society (d) Photographs of the stretchable, transparent antenna formed using wavy Ag NWs; (e) Return loss (RL) as a function of strain for the Ag-NW-based antennas. Reproduced with permission from [271], Copyright 2016 American Chemical Society

such as conductivity and dielectric losses. It is also necessary to conduct in-depth investigations of Ag NWs for guiding the development and design of functional materials and devices by accurate electromagnetic calculation and analysis methods.

6.3 Flexible, Stretchable, and Wearable Electronics

6.3.1 Strain Sensors

Ag NWs materials possess excellent mechanical compliance properties due to their large length-to-diameter aspect ratio.[202] Thus it is considered a promising class of stretchable conductors which can exhibit distinct electrical changes in reaction to mechanical deformation. The superior electromechanical performance makes Ag NWs ideal for constructing devices in strain-sensing applications.[273-278] A significant advantage of Ag NWs materials over other stretchable conductors used in the construction of pressure sensors is their printability, which makes improvements in design flexibility and cost control. Cai *et al*.[273] developed Ag NWs-based stretchable conductors capable of sustaining a constant conductance under area strains of up to 156% via a direct printing method. They obtained uniform and well-defined Ag NWs patterns by optimizing printing parameters and constructed capacitive pressure sensor arrays (Figs. 26a-b) for cost-effective wearable electronics.

In another work, Ke *et al*.[275] prepared all-printed flexible straight-line sensors by screen printing a conductive ink containing Ag NWs onto a PET substrate. The authors conducted a comprehensive investigation into the sensing performance of the sensor (see Figs. 26c-h). This printed flexible sensor exhibits a comparable fluctuation in the resistance of the Ag NWs layer with respect to bending angles, which can be used in intelligent and tamper-evident packaging. With the use of Ag NWs, it is also possible to fabricate multifunctional sensors, which can meet the complexity of various practical applications and are becoming a growing trend. For instance, using Ag NWs as electrodes (conductors) and Ecoflex as a dielectric, Yao, *et al*.[199] developed highly stretchable multifunctional sensors that can detect strain (up to 50%), pressure (up to ~1.2 MPa), finger touch with high sensitivity, a fast response time (~40 ms), and good pressure mapping function. They demonstrated these sensors for several wearable applications including monitoring thumb movement, sensing the strain of the knee joint in patellar reflex, and other human motions. When the interconnected Ag NWs were assembled into nano-fibrillated cellulose (NFC) aerogel through unidirectional freeze-drying, an ultralight and

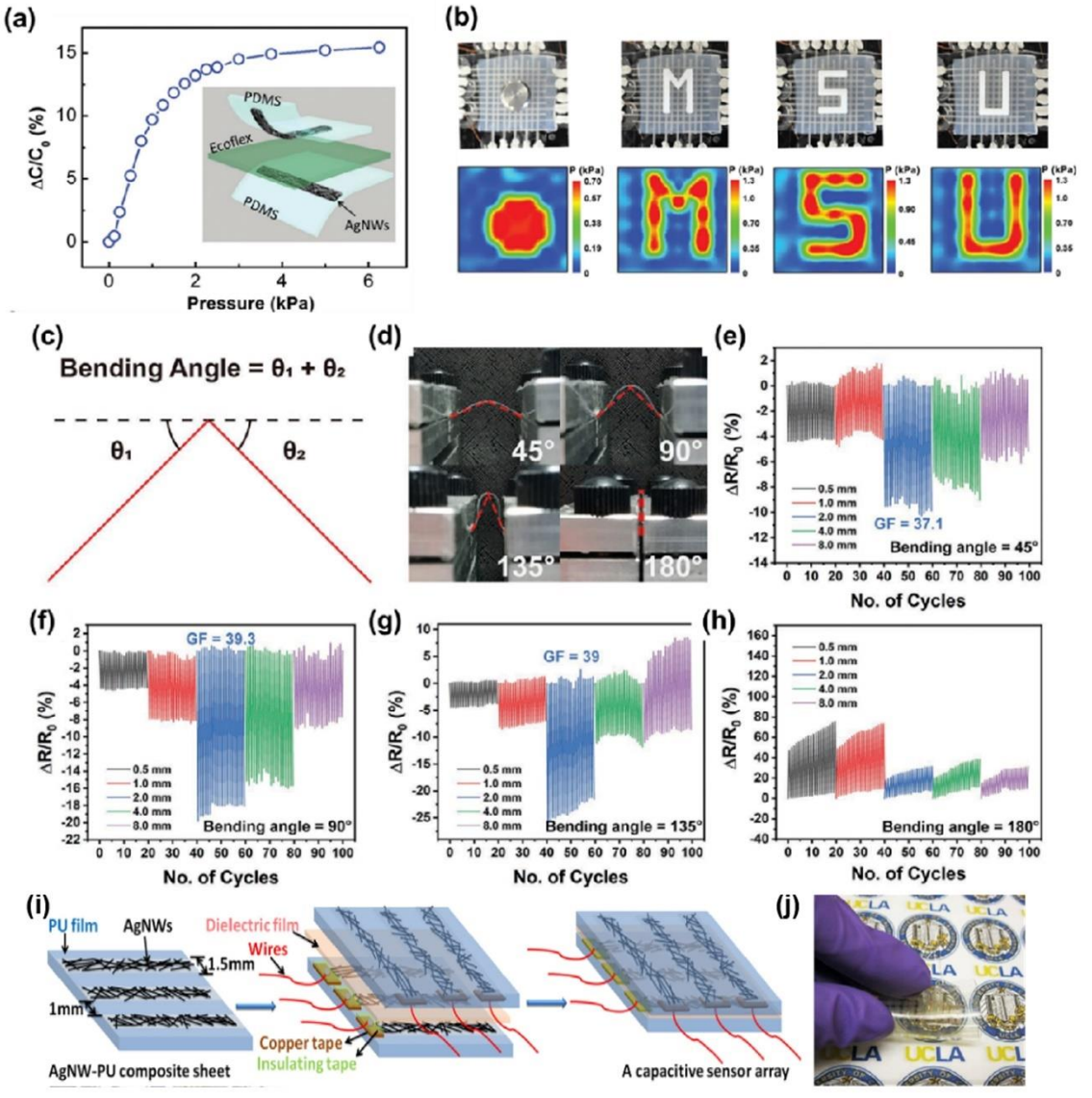

Fig. 26 Ag NWs-based stretchable electrodes applied in strain sensing devices. (a) Capacitance changes as a function of applied pressure for a single pixel. Inset: Schematic representation of the pressure sensor; (b) Photographs of various objects being placed on the sensor array to demonstrate the pressure mapping capacity; Reproduced with the permission from [273], Copyright 2017 WILEY-VCH Verlag GmbH & Co. KGaA, Weinheim (c) Calculation diagram of bending angle; (d) Photographs of flexible sensors being tested at 45°, 90°, 135°, and 180° angles; (e–h) Sensing performance of strain sensors with different linewidths (0.5, 1, 2, 4, and 8 mm) at different angles; Reproduced with the permission from [275], Copyright 2020 WILEY-VCH Verlag GmbH & Co. KGaA, Weinheim, (i) The schematic illustration of the fabrication of a transparent capacitive array comprising an acrylic elastomer layer as the dielectric spacer between two transparent AgNW-PU composite electrodes; (j) Photograph of the sensor array bent at 180°. Reproduced with permission from [280], Copyright AIP Publishing.

conductive Ag NWs/NFC aerogel with ordered pore orientation can be yielded.[279] The derived multifunctional strain sensor showed desirable sensing performance, ultralow density (less than 13.58 mg/cm^3), and exceptional stability and durability (over 10,000 cycles). Significantly, it can simultaneously offer real-time monitoring of subtle deformations and electrophysiological signals.

Ag NWs can also be used as transparent electrodes for capacitive sensors owing to the advantages of high stretchability, high conductivity, high transparency, and low-cost large-area fabrication. Hu *et al.*[280] prepared a high-performance transparent electrode by embedding an Ag NW network in elastomeric PU (Fig. 24i). The composite electrodes retained high surface conductance at tensile strains up to 60% and could be repeatedly stretched with negligible electrical conductivity loss. High-performance stretchy transparent capacitors were fabricated by sandwiching an acrylic elastomer layer between two Ag NW-PU composites

electrodes, and stretchable sensor arrays with 10 x10 pixels were made by patterning composite electrodes into an X-Y addressable passive matrix.

6.3.2 Transistors, Soft Robotics, and Other Wearable Electronics

Transistors are fundamental and critical components in the design of modern sophisticated electronic systems. The development of flexible and stretchable electronics presents basic challenges in terms of producing novel electronic materials that are mechanically compliant and solution-processable for stretchable thin-film transistors. Ag NWs materials expand the material choices for source and drain electrodes in flexible transistor devices.[281-283] Simultaneously, due to its printable processing, it enables the construction of fully printable flexible electronic systems, thus printed electronics utilize it extensively. [202,273-275,284,285] Liang *et al*. reported transparent and stretchable Ag NWs-based transistors. Fig. 27e shows the device in a stretched state along the channel direction. The devices can be stretched up to a maximum of 50% strain and subjected to 500 cycles of repetitive stretching to 20% strain without deteriorating their electrical properties significantly.[283] They also demonstrated high-resolution printed patterns of Ag NWs with a continuous and dense network/mesh structure as stretchable electrodes for flexible and wearable thin-film transistor (TFT) arrays (see Figs. 27a-d),[202] demonstrating the possibility for constructing a fully printed flexible electronic system as well.

Apart from those applications with a single function, Ag NWs also have promising potential to fabricate multifunctional flexible nanocomposites for next-generation wearable and portable electronic devices for electronic skin and artificial intelligence, etc. The main issue is to endow the nanocomposites with multiple functions while maintaining their intrinsic flexible and porous features. However, the types of multifunctional wearable electronic devices are limited, research in this area is still relatively small, and the manufacturing of the devices is often complex and difficult to achieve mass production.

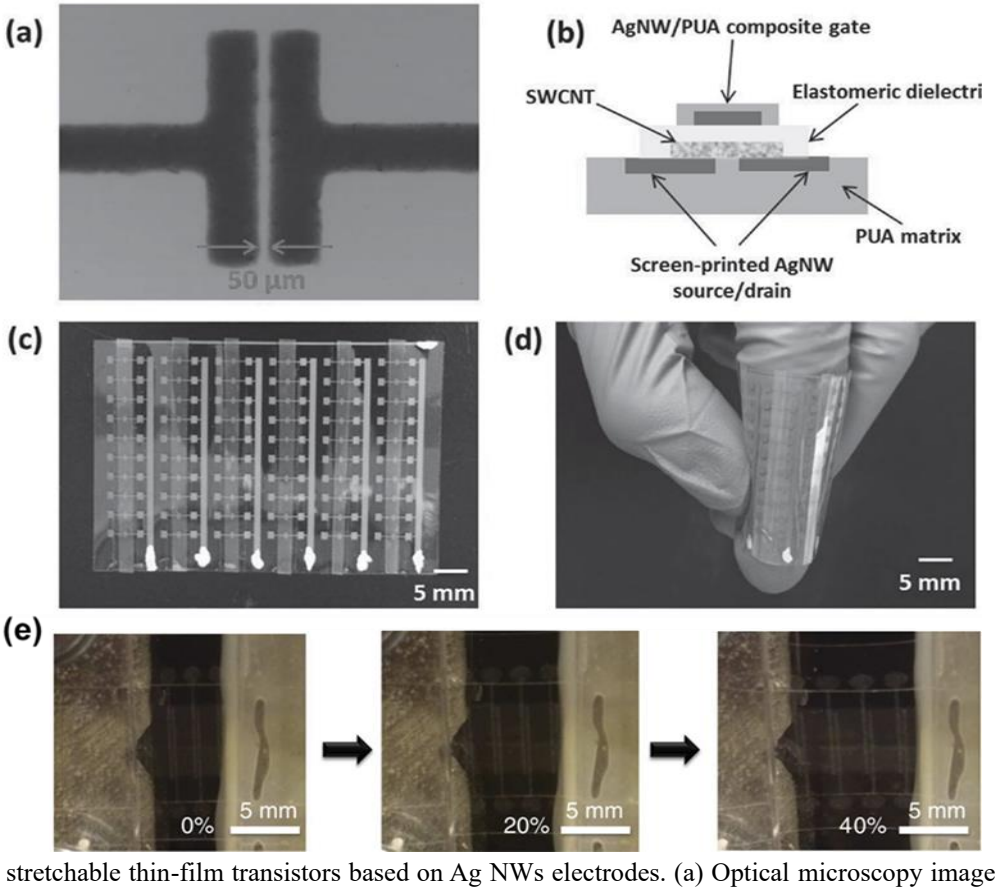

Fig. 27 Flexible and stretchable thin-film transistors based on Ag NWs electrodes. (a) Optical microscopy image of screen-printed Ag NWs source/drain electrodes; (b) Schematic illustration of the configuration of a fully printed TFT based on screen-printed Ag NWs source/drain electrodes; (c) Optical image of a fully printed stretchable 10 × 6 TFT array; (d) Optical image of TFT array contorted around a finger; Reproduced with the permission from [202], Copyright 2016 WILEY-VCH Verlag GmbH & Co. KGaA, Weinheim, (e) Magnified photographs of a device at specified strains applied along the channel length direction. Reproduced with permission from [283], Copyright 2015, The Author(s).

Ma *et al*.[286] fabricated multifunctional wearable Ag NWs/leather nanocomposites with hierarchical structures (Ag NWs penetrate the micro nanoporous structures in the corium side of leather) via a facile vacuum-assisted filtration process. The resulting flexible and mechanically strong device exhibited extremely low R_s of 0.8 Ω/sq, superior visual Joule heating temperatures up to 108°C at a low supplied voltage of 2.0 V, excellent EMI SE of ~55 dB, and excellent piezo resistive sensing ability in human motion detection (Fig. 28a). Based on the textile-laminated patterns prepared by integrating Ag NWs and textiles through a laser scribing patterning and a heat press lamination process, Yao *et al*.[287] further designed and fabricated an integrated patch that incorporates four dry electrophysiological electrodes, a capacitive strain sensor, and a wireless heater as shown in Fig. 28b. Sun *et al*.[288] developed a multifunctional electronic smart band-aid that gives new functionality to traditional band-aids by simply screen-printing a network of Ag NWs and PTFE/PDMS layer on top of them (Fig. 28c). This smart band-aid can be easily stretched, bent, or twisted. It can be used not only for wound protection but also for self-powered motion sensing and human-machine interaction. Moreover, there is still some research exploring Ag NW/wrap yarn composite for a wearable strain sensor and heater,[289] Silk textiles with biomimetic leaf-like MXene/Ag NWs nanostructures for EMI shielding, humidity monitoring, and self-derived hydrophobicity[290] and so on.

In the coming era of wearable devices, a new research focus is expected to be placed on imperceptible soft robotics comprised primarily of optically transparent imperceptible components, such as actuators and sensors. Studies have shown that Ag NWs is an ideal material that combines mechanical compliance with optical properties and is highly promising in constructing these hardware components for soft robotics.[291,292] S.H. Ko *et al*.[293] demonstrated an application of Ag NWs in color-shifting soft actuators. The electrothermally powered soft actuators contain a built-in transparent Ag NWs percolation network heater, allowing for instant temperature viewing via color change and simple actuation direction programming. Besides, the S.H. Ko group combined a thermochromic liquid crystal layer with vertically stacked, patterned Ag NWs heaters in a multilayer structure to circumvent the limits of the standard lateral pixelated approach by superimposing the heater-induced temperature profiles (Fig. 28d).[294] In addition, as a novel concept of imperceptible soft robotics, camouflage skin aims to enable transparent systems to adapt to natural environments or humans for covert operation, which can be achieved using Ag NWs.[294]

Some studies are now focusing on the fabrication of patterned Ag NWs film for achieving highly transparent electrodes, which is of great importance to E-skin and other flexible and stretchable electronics. Won *et al*.[52] reported a novel kirigami approach to fabricate patterned highly conductive and transparent electrodes for E-skin applications. The kirigami engineered patterns can be designed to intentionally limit strain or grant ultra stretchability depending on applications over the range of 0 to over 400% tensile strain with strain-invariant electrical properties and show outstanding strain reversibility even after 10 000 cycles of stretching while exhibiting high optical transparency (>80%). Ultra-stretchable transparent kirigami electrodes were applied in heaters for personal temperature management and conformal transparent kirigami electrophysiology sensor for continuous health monitoring, demonstrating the versatility in flexible and stretchable applications. Similarly, Han *et al*.[295] used 2D ice-templating to assemble Ag NWs into a large-area conductive pattern by regulating ice crystal growth and Ag NW interaction during directed freezing, which is another novel approach for patterned Ag NWs-based electrodes. The ice-templated Ag NWs-based electrode possesses good optical transparency (91%) and low sheet resistance ($20\Omega \cdot sq^{-1}$). The potential applications of ice-templated Ag NW-based electrodes in both electronic skin sensors and touch screens were also demonstrated.

Challenges taking on these Ag NW-based flexible and stretchable devices lie in how to sustain their electrical performance under severe strains and deformations. With the development of material preparation technology and the improvement of device design, it can be expected that Ag NWs will become a promising conductive material in flexible and stretchable electronics.

6.4 Other Applications

It cannot be ignored that the excellent mechanical properties of Ag NW materials make them promising for flexible and stretchable electronics. One can notice that Ag NWs have been studied and used to varying degrees in other devices, including transparent heaters,[296-298] flexible sensors,[274,275,277,278,299] flexible thin-film transistors, and other wearable electronics applications.[281-283] In this section, we focus on these Ag NWs-based devices out of numerous optoelectronics and electromagnetic applications.

6.4.1 Transparent Heaters

Transparent heaters are devices that use the Joule effect to convert electrical energy into heat and have attracted considerable interest from both the scientific and industrial

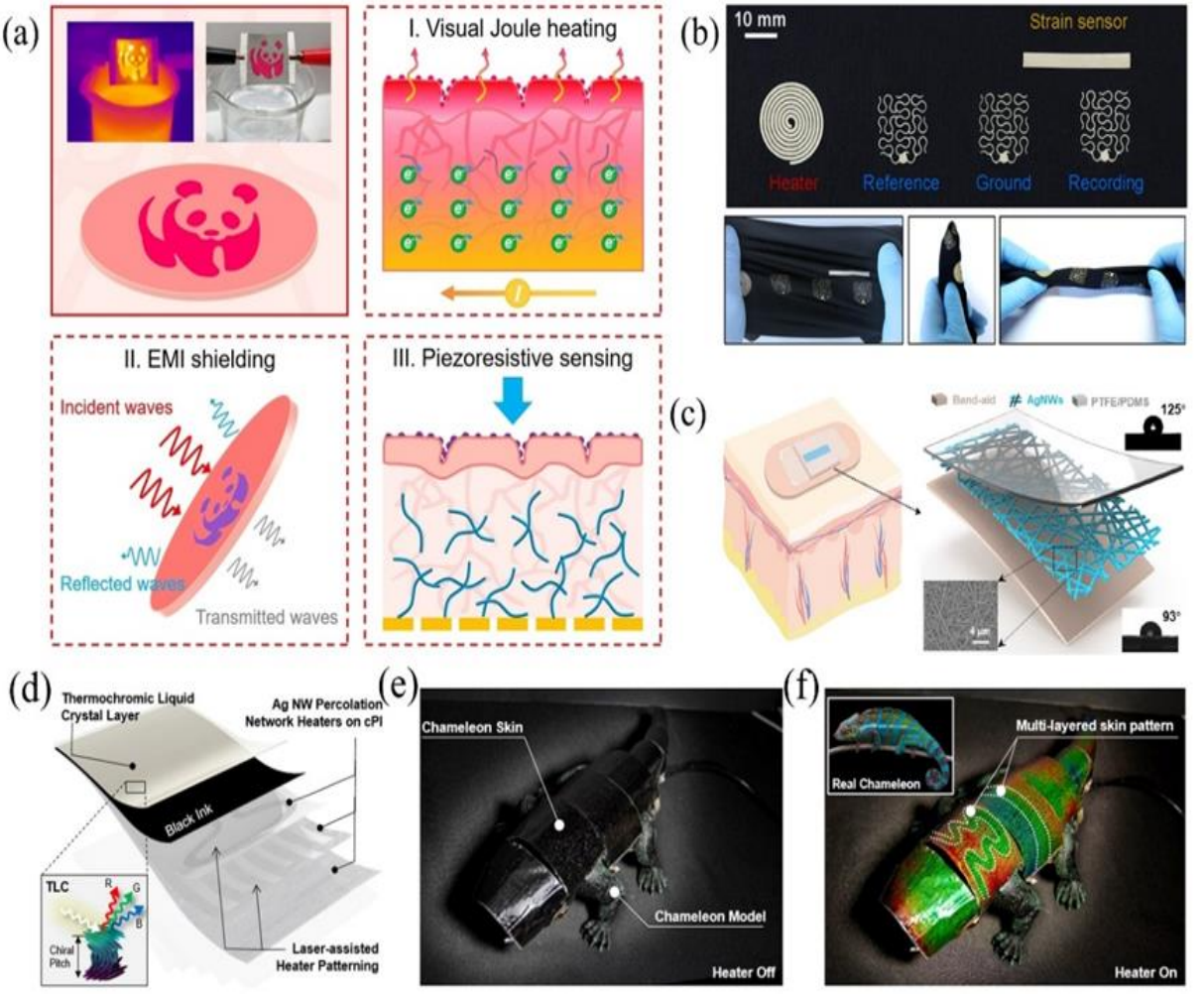

Fig. 28 Ag NW-based multifunctional wearable electronic devices. (a) Multifunctional wearable Ag NW/leather nanocomposites with integrated capabilities of Joule heating, EMI shielding and piezo resistive sensing; Reproduced with the permission from [287], Copyright 2019 American Chemical Society, (b) Integrated textile patch consisting of four dry electrodes, a capacitive strain sensor, and a wireless heater for sports applications. The patch can be stretched, folded, and twisted; Reproduced with the permission from [287], Copyright 2019 American Chemical Society (c) Application scenario of the smart band-aid attached to the epidermis and schematic illustration of the structure of the smart band-aid; Reproduced with the permission from [288], Copyright 2021 Elsevier Ltd, (d) Configuration of the multi-layered ATACS: TLC is coated on the black ink layer. Ag NWs percolation network heaters were stacked on cPI films and patterned by the UV laser ablation process; (e) The chameleon model with 7 of the multi-layered highly flexible ATACS patches; (f) Demonstration of the multi-layered ATACT patches on the chameleon model. Inset is a real chameleon with full coloring. Reproduced with permission from [294], Copyright 2021 The Author(s).

communities.[300] Their main functional structure is a transparent conductive layer, which is dominated by transparent conductive oxides for decades. With the emergence of various nanomaterials in recent years, the construction of transparent heaters has also begun to undergo developments, the most notable of which are transparent heaters based on Ag NWs conductive film. According to recent advances,[296-298,300-304] Ag NWs-based transparent heaters have shown superior overall performance due to their outstanding conductivity, light transmission, and mechanical qualities.

The primary requirements for heating devices are low power consumption and rapid thermal response. He *et al*. verified the practicability of Ag NWs-based transparent heaters with fast response under low voltages. They fabricated the Ag NWs-polyimide composite via a facile solution process and generated a temperature of 58°C at a low voltage of 3.5 V within 20 s, indicating the promising application in heating devices that require low power consumption and fast response (Fig. 29b).[301] Some multi-component or multilayer hybrid film design strategies are equally effective in enhancing the performance of Ag NWs transparent heaters. For example,

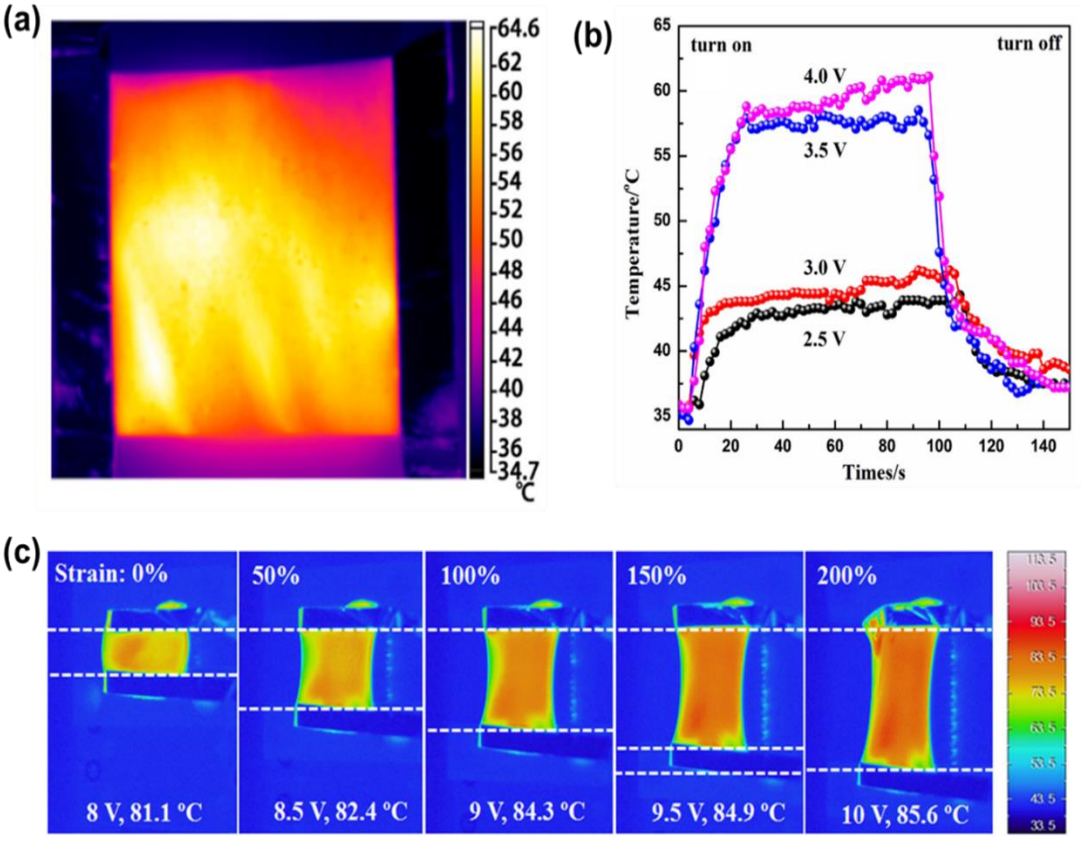

Fig. 29 Ag NWs-based transparent heaters. (a) Infrared thermal images of the composite films with the transmittance of 53%; (b) Evolution of generated temperature of the composite films with a transmittance of 53% at various voltages from 2.5 to 4 V; Reproduced with permission from [301], Copyright 2021 The Author(s). (c) IR thermometer images of the stretchable film heaters with a pristine Ag NW and b 75:1 SWCNT-Ag NW composite electrodes prepared on VHB substrates at each strain. Reproduced with permission from [297], Copyright 2018, Springer Science Business Media, LLC.

SWCNT- Ag NWs composite film exhibited enhanced electrical and thermal stability, because CNT helps construct network bridges for scaling up an electrode area, resulting in a transparent stretchable film heater with enhanced electrical stability.[297] The future of Ag NWs transparent electric heaters will develop towards higher thermal efficiency and stability.

6.4.2 Energy devices

Energy devices with high efficiency and sustainability have recently emerged as an important research topic both in industrial and academic fields. The flexibility, stretchability, and lightweight properties of Ag NW make it an excellent candidate as a platform for energy devices such as supercapacitors and fuel cells.[305-312]

Ag NWs can also be integrated into flexible and stretchable energy-storage devices as electrodes, and the most prevalent type is utilized in supercapacitors.[313-316] Ag NWs with long wires are especially promising for providing transparent conductive networks with low sheet resistance, high transparency, and exceptional mechanical flexibility, all of which contribute significantly to the development of high-performance and flexible supercapacitors. Li *et al*.[315] obtained uniform Ag NWs and prepared flexible all-solid-state supercapacitors. The device demonstrates remarkable mechanical flexibility and cyclic stability, with only a modest decrease in areal capacitance after multiple bending charge-discharge cycles.

Despite these advantages, it is still a key technical problem to improve the electrochemical stability of Ag NW-based electrodes when used in supercapacitors. In this regard, Lee *et al*.[308] introduced a highly stretchable and transparent supercapacitor using an electrochemically stable Ag−Au core−shell nanowire percolation network electrode (Fig. 30a). The Ag-Au core-shell nanowire can be obtained by a simple solution process, exhibiting superior electrical conductivity and excellent chemical and electrochemical stabilities compared to pristine Ag nanowire. Similarly, Moon *et al*.[305] presented a stretchable and transparent supercapacitor using Ag/Au/Polypyrrole core-shell nanowire networks as electrodes by decorating the surface of Ag NWs with a gold coating. The core-shell nanowire networks can provide higher redox potential than the electro-polymerizable monomer and

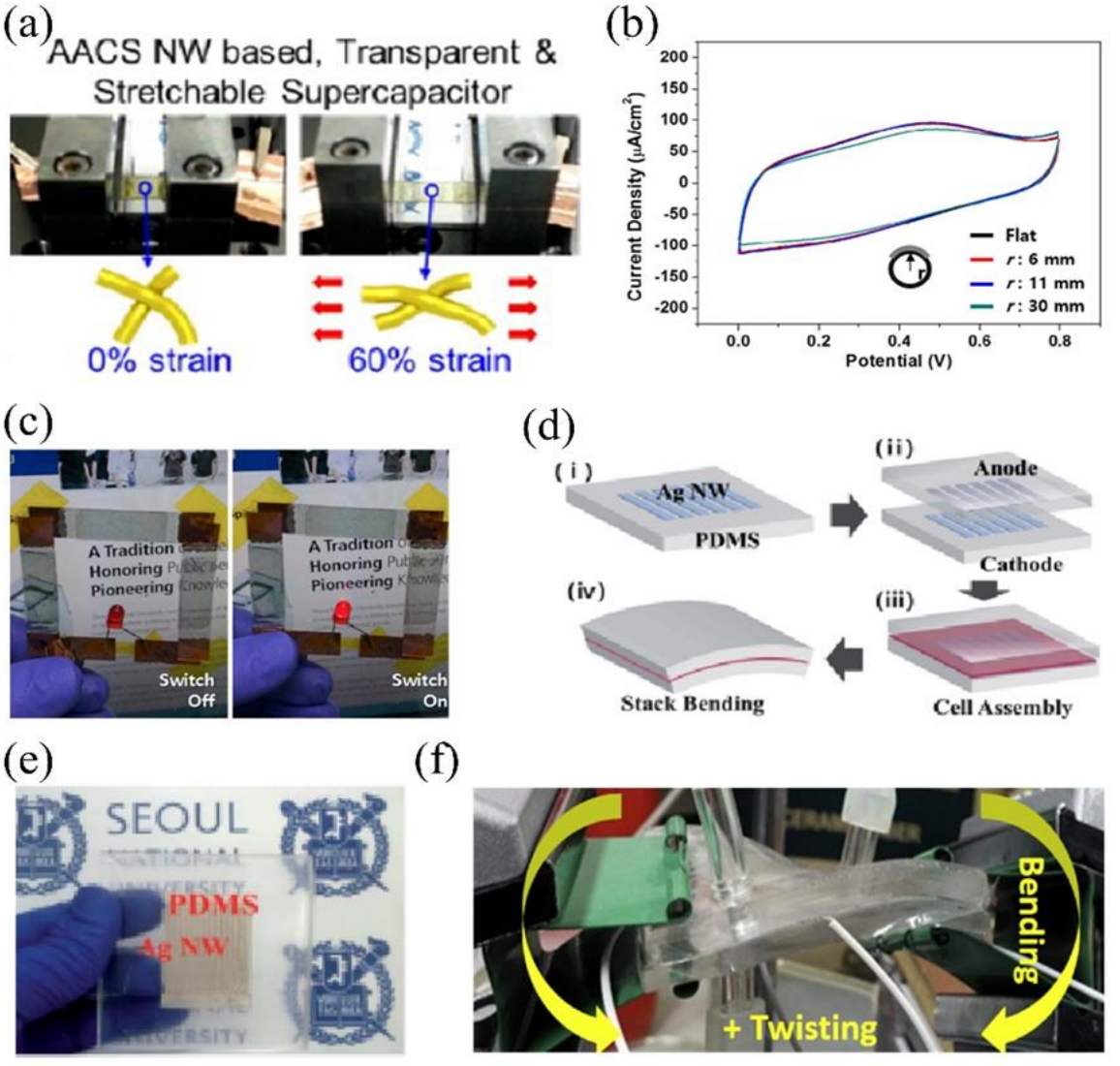

Fig. 30 (a) Shell nanowire-based supercapacitor still possesses fine optical transmittance and outstanding mechanical stability up to 60% strain; Reproduced with the permission from [308], Copyright Royal Society of Chemistry (b) Bending stability test: CV curves of the supercapacitor based on Ag/Au/PPy (3-cycle) at a scan rate of 500mV/s at an indicated bending radii; (c) Demonstration of a series-connected TFS supercapacitor to power a commercial LED; Reproduced with the permission from [305], Copyright 2017, The Author(s) (d) Schematic of the process for fabricating the bendable fuel cell: (i) shows the p Ag NW percolation network electrode patterns on the flow channel patterned PDMS, and then, (ii) an anode/cathode PDMS pad is fabricated, (iii) the bendable/flexible fuel cell stack is assembled and (iv) the fuel cell performance is tested under a bent condition; (e) images of anode PDMS pad with flow channel; Reproduced with the permission from [301] (f) Picture of the bendable fuel cell subject to mixed bending and twisting load. Reproduced with permission from [310], Copyright 2017 Tomsk Polytechnic University.

demonstrate outstanding mechanical stability under bending and stretching. These works provide optimized strategies for achieving high-performance flexible, stretchable, and transparent supercapacitors in energy storage applications.

The electrical conductivity of Ag NW percolation networks also needed high enough for constructing a current-collecting layer in fuel cells. And the optical transparency, flexibility, and stretchability of Ag NW percolation networks endow the Ag NW-based fuel cells with multiple features. For example, Chang *et al.*[306] reported a bendable polymer electrolyte fuel cell that uses an Ag nanowire layer for current collecting (Fig. 30d), achieving a power density of 71 mW in the reactive area of 9 cm^2. The device is not only bendable but also exhibits an enhanced performance in the bent state due to the reduced resistance caused by the compression force. The authors further verified the performance enhancement in bendable Ag NW-based fuel cells in an asymmetric configuration,[309] and explored performance variation under

mixed bending and twisting conditions.[310] Zeng *et al*.[307] synthesized high-performance supportless Ag NW catalyst and fabricated anion exchange membrane fuel cells. The device achieved a maximum power density of 164 $mW \cdot cm^{-2}$, indicating that supportless Ag NW is a promising alternative to carbon-supported electrocatalysts in fuel cells.

Since Ag NWs can be widely used in photovoltaics, supercapacitors, fuel cells, and light-emitting devices, which covers a wide range of energy generation, storage, and consumption, Ag NWs-based materials have been developed into a promising candidate for constructing flexible, stretchable and transparent platform toward self-sustainable energy devices.

6.4.3 Air Filters

It is worth noting that the Ag NWs network is also promising for constructing compact and transparent air filters due to their outstanding antimicrobial property.[317,318] In 2017, Jeong *et al*.[317] demonstrated an environmental application of an air filter using a hierarchical Ag NWs percolation network for particulate matter (PM) collection (Figs. 31a-b). The transparent, reusable, and active PM (TRAP) filter was fabricated on a nylon mesh filter by simple vacuum filtration and exhibited high efficiency (>99.99%). The TRAP filter uses both long-range electrostatic force and short-range van der Waals forces when low voltage is applied on the Ag NW network, making it easier to collect particulate matter. Jeong's study showed the tremendous potential of Ag NWs in developing highly efficient air filters. In a recent study carried out by Park *et al*.,[318] Ag NWs were electrospray onto the surface of polyacrylonitrile (PAN) fibers to construct a fibrous air filter medium. Due to the introduction of Ag NWs, the overall filtration efficiency of the nanofiber web was increased, as shown in Figs. 31c-d. Unlike conventional polymeric filter systems, Ag NW-based air filters have advantages in terms of efficiency, sustainability, multifunction, and cost. The application of Ag NWs in air filters is of great importance in light of the increasing environmental concerns.

7. Summary and Outlooks

Thanks to the efforts of many research groups, a rich variety of progress of Ag NWs and Ag NWs-based multifunctional devices have been achieved. Ag NWs have shown great potential for many kinds of blossoming engineered applications. However, there are still some challenges or limitations that need to be addressed.

(a) The dependence of the optoelectronic performance on the dimensions, size distribution, and aspect ratio of Ag NWs has been figured out through the experiments. One preferable

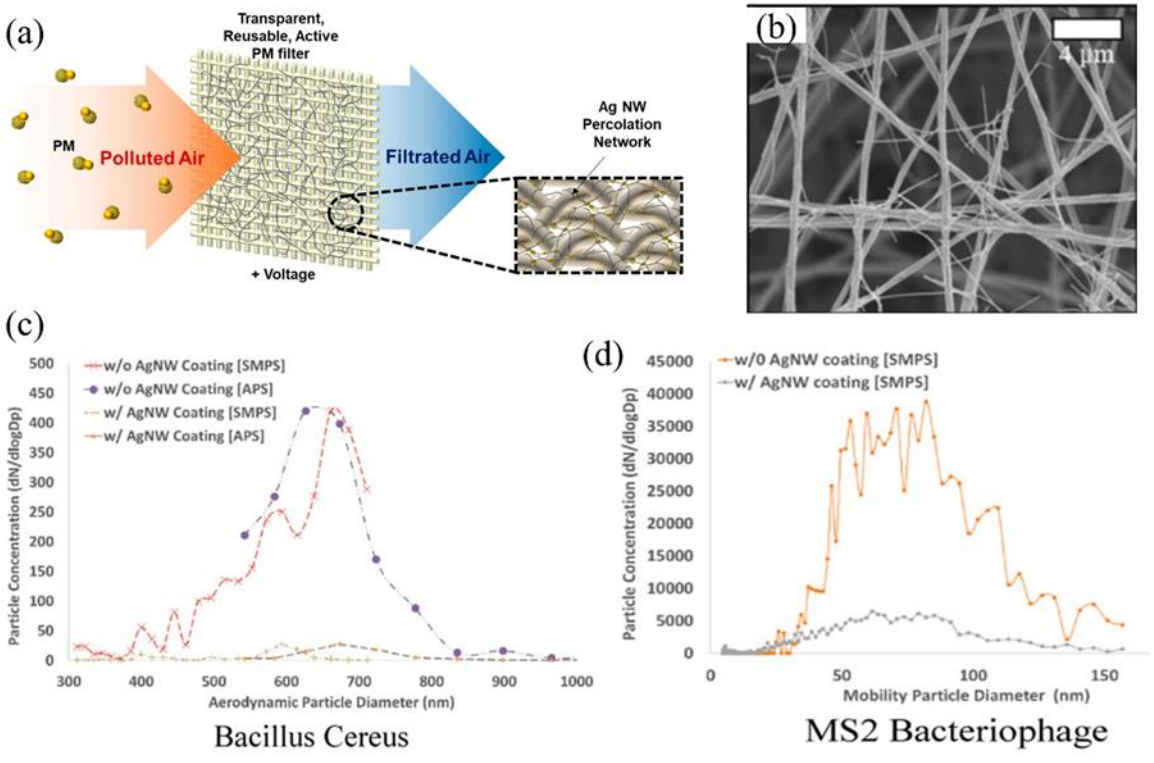

Fig. 31 (a) A schematic explanation for the mechanism of PM removal by air filter; (b) FESEM image of Ag coated fiber web; Reproduced with the permission from [317], Copyright 2017 American Chemical Society (c) Bacillus cereus and (d) MS2 bacteriophage particle size distributions downstream of the fiber web before and after the Ag NW coating. Reproduced with permission from [318], Copyright 2021 Elsevier B.V.

green chemistry synthesis route for uniform Ag NWs with high yield, and easy-to-be industrialized fabrication method still need to be pursued.

(b) The trade-off between electrical conductivity and optical transparency has attracted great concerns. However, the effect of light scattering on the performance of flexible optoelectronic devices cannot be ignored. Though more and more researchers have found the importance of the haze factor on the efficiency of optoelectronic devices recently, the quantitative index is still lacking to take all these factors into account to measure the overall optoelectronic performance.[16]

(c) The mechanism of synthesis of Ag NWs is complicated, and the investigation and understanding of the synthesis process are crucial and essential for tuning the properties of Ag NWs. With the development of advanced microstructure characterization techniques, some in-situ characterization, such as in-situ TEM, or in-situ synchrotron, could be used to detect the synthesis mechanism of Ag NWs thoroughly and elaborately. Our group carried out some experiments by using in-situ TEM under the cooperation of partners, and some interesting results have been obtained. And also, it is expected that the synthesis mechanism of Ag NWs could be reported by other advanced techniques.

(d) The purification and disperse of Ag NWs are other issues that need to be addressed furthers. During the growth of Ag NWs, the formation of nanoparticles is unavoidable, and thus the complete removal of particles is important. The centrifugation speed, centrifugation time, and the selection of solvent all affect the purification products. Meanwhile, since the dispersions or solutions are usually used to fabricate films, the Ag NWs must be homogenously dispersed in order to yield uniform films, and the gradual settlement of Ag NWs can influence the homogeneity. The disperse technique should be improved elaborately.[113]

(e) It is worth noting that, although Ag NWs-based transparent conductive films have surpassed traditional electronic materials in many properties, it is still challenging to replace traditional electronic materials. The high cost of raw materials and the electromigration issue of Ag NWs hinder their practical application.[319] Comparatively, copper is only 6% less conductive than silver, but is 1000 times more abundant and 100 times cheaper than silver.[320] Cu NWs can also easily form transparent networks just like Ag NWs and transparent Cu NW conductors have been demonstrated for various applications.[321-324] Thus, Cu NWs film is considered to be a potential candidate, on the premise of solving the easy oxidation problem.

This review attempts to summarize the efforts and achievements of Ag NWs networks, and we highlight the progress of Ag NWs from synthesis, growth mechanism, and device fabrications to prospective engineered applications. We believe that with the development of preparation of Ag NWs and manufacturing technology, Ag NWs-based devices will be further developed, and the commercialization of the Ag NWs will be blossoming.

Acknowledgments

This work was supported by the National Natural Science Foundation of China (Nos. 51971028, 61974021) and the Zhishan Scholar Program of Southeast University.

Conflict of Interest

There is no conflict of interest.

Supporting Information

Not applicable.

References

[1] J. Tian, Z. Zhao, A. Kumar, R. I. Boughton, H. Liu, Recent progress in design, synthesis, and applications of one-dimensional TiO2 nanostructured surface heterostructures: a review, *Chemical Society Reviews*, 2014, **43**, 6920-6937, doi: 10.1039/c4cs00180j.

[2] L. Kong, W. Chen, Carbon nanotube and graphene-based bioinspired electrochemical actuators, *Advanced Materials*, 2014, **26**, 1025-1043, doi: 10.1002/adma.201303432.

[3] X. Lu, W. Zhang, C. Wang, T.-C. Wen, Y. Wei, One-dimensional conducting polymer nanocomposites: synthesis, properties and applications, *Progress in Polymer Science*, 2011, **36**, 671-712, doi: 10.1016/j.progpolymsci.2010.07.010.

[4] D. Huo, M. J. Kim, Z. Lyu, Y. Shi, B. J. Wiley, Y. Xia, One-dimensional metal nanostructures: from colloidal syntheses to applications, *Chemical Reviews*, 2019, **119**, 8972-9073, doi: 10.1021/acs.chemrev.8b00745.

[5] Y. Xia, P. Yang, Y. Sun, Y. Wu, B. Mayers, B. Gates, Y. Yin, F. Kim, H. Yan, One-dimensional nanostructures: synthesis, Characterization, and Applications, *Advanced Materials*, 2003, **15**, 15196064, doi: 10.1002/ADMA.200390087.

[6] G. Zhou, L. Xu, G. Hu, L. Mai, Y. Cui, Nanowires for electrochemical energy storage, *Chemical Reviews*, 2019, **119**, 11042-11109, doi: 10.1021/acs.chemrev.9b00326.

[7] L. Hu, D. S. Hecht, G. Grüner, Carbon nanotube thin films: fabrication, properties, and applications, *Chemical Reviews*, 2010, **110**, 5790-5844, doi: 10.1021/cr9002962.

[8] S. Park, M. Vosguerichian, Z. Bao, A review of fabrication and applications of carbon nanotube film-based flexible electronics, *Nanoscale*, 2013, **5**, 1727, doi: 10.1039/c3nr33560g.

[9] T. Sattar, Current review on synthesis, composites and

multifunctional properties of graphene, *Topics in Current Chemistry*, 2019, **377**, 10, doi: 10.1007/s41061-019-0235-6.

[10] H. Y. Mao, S. Laurent, W. Chen, O. Akhavan, M. Imani, A. A. Ashkarran, M. Mahmoudi, Graphene: promises, facts, opportunities, and challenges in nanomedicine, *Chemical Reviews*, 2013, **113**, 3407-3424, doi: 10.1021/cr300335p.

[11] A. Kausar, Overview on conducting polymer in energy storage and energy conversion system, *Journal of Macromolecular Science, Part A*, 2017, **54**, 640-653, doi: 10.1080/10601325.2017.1317210.

[12] Q. Wang, Y. Yu, J. Liu, Preparations, characteristics and applications of the functional liquid metal materials, *Advanced Engineering Materials*, 2018, **20**, 1700781, doi: 10.1002/adem.201700781.

[13] X. Wang, J. Liu, Recent advancements in liquid metal flexible printed electronics: properties, technologies, and applications, *Micromachines*, 2016, **7**, 206, doi: 10.3390/mi7120206.

[14] S. Huang, Y. Liu, F. Yang, Y. Wang, T. Yu, D. Ma, Metal nanowires for transparent conductive electrodes in flexible chromatic devices: a review, *Environmental Chemistry Letters*, 2022, **20**, 3005-3037, doi: 10.1007/s10311-022-01471-4.

[15] S. Huang, Y. Liu, Y. Zhao, Z. Ren, C. F. Guo, Flexible electronics: stretchable electrodes and their future, *Advanced Functional Materials*, 2019, **29**, 1805924, doi: 10.1002/adfm.201805924.

[16] Y. Zhu, Y. Deng, P. Yi, L. Peng, X. Lai, Z. Lin, Flexible transparent electrodes based on silver nanowires: material synthesis, fabrication, performance, and applications, *Advanced Materials Technologies*, 2019, **4**, 1900413, doi: 10.1002/admt.201900413.

[17] L. Hu, H. S. Kim, J.-Y. Lee, P. Peumans, Y. Cui, Scalable coating and properties of transparent, flexible, silver nanowire electrodes, *ACS Nano*, 2010, **4**, 2955-2963, doi: 10.1021/nn1005232.

[18] M. C. Vasudev, K. D. Anderson, T. J. Bunning, V. V. Tsukruk, R. R. Naik, Exploration of plasma-enhanced chemical vapor deposition as a method for thin-film fabrication with biological applications, *ACS Applied Materials & Interfaces*, 2013, **5**, 3983-3994, doi: 10.1021/am302989x.

[19] Qinghui Zhang, Pornnipa Vichchulada, M. D. Lay, Length, Bundle, and Density gradients in spin cast single-walled carbon nanotube networks, *The Journal of Physical Chemistry C*, 2010, **114**, 16292-16297, doi: 10.1021/jp105884e.

[20] S. L. Hellstrom, H. W. Lee, Z. Bao, Polymer-assisted direct deposition of uniform carbon nanotube bundle networks for high performance transparent electrodes, *ACS Nano*, 2009, **3**, 1423-1430, doi: 10.1021/nn9002456.

[21] L. Yang, T. Zhang, H. Zhou, S. C. Price, B. J. Wiley, W. You, Solution-processed flexible polymer solar cells with silver nanowire electrodes, *ACS Applied Materials & Interfaces*, 2011, **3**, 4075-4084, doi: 10.1021/am2009585.

[22] C. Yang, H. Gu, W. Lin, M. M. Yuen, C. P. Wong, M. Xiong, B. Gao, Silver nanowires: from scalable synthesis to recyclable foldable electronics, *Advanced Materials*, 2011, **23**, 3052-3056, doi: 10.1002/adma.201100530.

[23] J. Kwon, Y. D. Suh, J. Lee, P. Lee, S. Han, S. Hong, J. Yeo, H. Lee, S. H. Ko, Recent progress in silver nanowire based flexible/wearable optoelectronics, *Journal of Materials Chemistry C*, 2018, **6**, 7445-7461, doi: 10.1039/c8tc01024b.

[24] M. Hu, J. Gao, Y. Dong, K. Li, G. Shan, S. Yang, R. K.-Y. Li, Flexible transparent PES/silver nanowires/PET sandwich-structured film for high-efficiency electromagnetic interference shielding, *Langmuir*, 2012, **28**, 7101-7106, doi: 10.1021/la300720y.

[25] Y.-H. Yu, C.-C M. Ma, C.-C. Teng, Y.-L. Huang, S.-H. Lee, I. Wang, M.-H. Wei, Electrical, morphological, and electromagnetic interference shielding properties of silver nanowires and nanoparticles conductive composites, *Materials Chemistry and Physics*, 2012, **136**, 334-340, doi: 10.1016/j.matchemphys.2012.05.024.

[26] M. Amjadi, A. Pichitpajongkit, S. Lee, S. Ryu, I. Park, Highly stretchable and sensitive strain sensor based on silver nanowire-elastomer nanocomposite, *ACS Nano*, 2014, **8**, 5154-5163, doi: 10.1021/nn501204t.

[27] C. Jiang, Q. Li, S. Fan, Q. Guo, S. Bi, X. Wang, X. Cao, Y. Liu, J. Song, Hyaline and stretchable haptic interfaces based on serpentine-shaped silver nanofiber networks, *Nano Energy*, 2020, **73**, 104782, doi: 10.1016/j.nanoen.2020.104782.[LinkOut]

[28] S. Choi, J. Park, W. Hyun, J. Kim, J. Kim, Y. B. Lee, C. Song, H. J. Hwang, J. H. Kim, T. Hyeon, D.-H. Kim, Stretchable heater using ligand-exchanged silver nanowire nanocomposite for wearable articular thermotherapy, *ACS Nano*, 2015, **9**, 6626-6633, doi: 10.1021/acsnano.5b02790.

[29] T. Kim, Y. W. Kim, H. S. Lee, H. Kim, W. S. Yang, K. S. Suh, Silver nanowires: uniformly interconnected silver-nanowire networks for transparent film heaters (adv. funct. mater. 10/2013), *Advanced Functional Materials*, 2013, **23**, 1225, doi: 10.1002/adfm.201370048.

[30] S. Hong, H. Lee, J. Lee, J. Kwon, S. Han, Y. D. Suh, H. Cho, J. Shin, J. Yeo, S. H. Ko, Highly stretchable and transparent metal nanowire heater for wearable electronics applications, *Advanced Materials*, 2015, **27**, 4744-4751, doi: 10.1002/adma.201500917.

[31] B. Wiley, Y. Sun, B. Mayers, Y. Xia, Shape-controlled synthesis of metal nanostructures: the case of silver, *Chemistry - A European Journal*, 2005, **11**, 454-463, doi: 10.1002/chem.200400927.

[32] M. Rycenga, C. M. Cobley, J. Zeng, W. Li, C. H. Moran, Q.

Zhang, D. Qin, Y. Xia, Controlling the synthesis and assembly of silver nanostructures for plasmonic applications, *Chemical Reviews*, 2011, **111**, 3669-3712, doi: 10.1021/cr100275d.

[33] B. Wiley, Y. Sun, J. Chen, H. Cang, Z.-Y. Li, X. Li, Y. Xia, Shape-controlled synthesis of silver and gold nanostructures, *MRS Bulletin*, 2005, **30**, 356-361, doi: 10.1557/mrs2005.98.

[34] J. Chen, B. J. Wiley, Y. Xia, One-dimensional nanostructures of metals: large-scale synthesis and some potential applications, *Langmuir*, 2007, **23**, 4120-4129, doi: 10.1021/la063193y.

[35] Y. Sun, Y. Yin, B. T. Mayers, T. Herricks, Y. Xia, Uniform silver nanowires synthesis by reducing $AgNO_3$ with ethylene glycol in the presence of seeds and poly(vinyl pyrrolidone), *Chemistry of Materials*, 2002, **14**, 4736-4745, doi: 10.1021/cm020587b.

[36] S. Behrens, J. Wu, W. Habicht, E. Unger, Silver nanoparticle and nanowire formation by microtubule templates, *Chemistry of Materials*, 2004, **16**, 3085-3090, doi: 10.1021/cm049462s.

[37] Y. Wu, T. Livneh, Y. X. Zhang, G. Cheng, J. Wang, J. Tang, M. Moskovits, G. D. Stucky, Templated synthesis of highly ordered mesostructured nanowires and nanowire arrays, Nano Letters, 2004, **4**, 2337-2342, doi: 10.1021/nl048653r.

[38] F. M. Reicha, A. Sarhan, M. I. Abdel-Hamid, I. M. El-Sherbiny, Preparation of silver nanoparticles in the presence of chitosan by electrochemical method, *Carbohydrate Polymers*, 2012, **89**, 236-244, doi: 10.1016/j.carbpol.2012.03.002.

[39] T. Kim, A. Canlier, G. H. Kim, J. Choi, M. Park, S. M. Han, Electrostatic spray deposition of highly transparent silver nanowire electrode on flexible substrate, *ACS Applied Materials & Interfaces*, 2013, **5**, 788-794, doi: 10.1021/am3023543.

[40] X. Zhang, S. Tang, Z. Wu, Y. Chen, Z. Li, Z. Wang, J. Zhou, Centrifugal spinning enables the formation of silver microfibers with nanostructures, *Nanomaterials*, 2022, **12**, 2145, doi: 10.3390/nano12132145.

[41] W. He, C. Ye, Flexible Transparent Conductive Films on the Basis of Ag Nanowires: Design and Applications: A Review, *Journal of Materials Science & Technology*, 2015, **31**, 581-588, doi: 10.1016/j.jmst.2014.11.020.

[42] Y. Ahn, Y. Jeong, Y. Lee, Improved thermal oxidation stability of solution-processable silver nanowire transparent electrode by reduced graphene oxide, *ACS Applied Materials & Interfaces*, 2012, **4**, 6410-6414, doi: 10.1021/am301913w.

[43] D. Y. Choi, H. W. Kang, H. J. Sung, S. S. Kim, Annealing-free, flexible silver nanowire-polymer composite electrodes via a continuous two-step spray-coating method, *Nanoscale*, 2013, **5**, 977-983, doi: 10.1039/c2nr32221h.

[44] C.H. Liu, X. Yu, Silver nanowire-based transparent, flexible, and conductive thin film, *Nanoscale Research Letters*, 2011, **6**, 75, doi: 10.1186/1556-276X-6-75.

[45] J. Wang, J. Jiu, T. Araki, M. Nogi, T. Sugahara, S. Nagao, H. Koga, P. He, K. Suganuma, Silver nanowire electrodes: conductivity improvement without post-treatment and application in capacitive pressure sensors, *Nano-Micro Letters*, 2015, **7**, 51-58, doi: 10.1007/s40820-014-0018-0.

[46] J. Jung, H. Lee, I. Ha, H. Cho, K. K. Kim, J. Kwon, P. Won, S. Hong, S. H. Ko, Highly stretchable and transparent electromagnetic interference shielding film based on silver nanowire percolation network for wearable electronics applications, *ACS Applied Materials & Interfaces*, 2017, **9**, 44609-44616, doi: 10.1021/acsami.7b14626.

[47] X. Zhu, J. Xu, F. Qin, Z. Yan, A. Guo, C. Kan, Highly efficient and stable transparent electromagnetic interference shielding films based on silver nanowires, *Nanoscale*, 2020, **12**, 14589-14597, doi: 10.1039/d0nr03790g.

[48] Z. Zhang, W. Li, X. Wang, W. Liu, K. Chen, W. Gan, Low effective content of reduced graphene oxide/silver nanowire hybrids in epoxy composites with enhanced conductive properties, *Journal of Materials Science: Materials in Electronics*, 2019, **30**, 7384-7392, doi: 10.1007/s10854-019-01050-4.

[49] H. Hosseinzadeh Khaligh, K. Liew, Y. Han, N. M. Abukhdeir, I. A. Goldthorpe, Silver nanowire transparent electrodes for liquid crystal-based smart windows, *Solar Energy Materials and Solar Cells*, 2015, **132**, 337-341, doi: 10.1016/j.solmat.2014.09.006.

[50] L. Veeramuthu, B.-Y. Chen, C.-Y. Tsai, F.-C. Liang, M. Venkatesan, D.-H. Jiang, C.-W. Chen, X. Cai, C.-C. Kuo, Novel stretchable thermochromic transparent heaters designed for smart window defroster applications by spray coating silver nanowire, *RSC Advances*, 2019, **9**, 35786-35796, doi: 10.1039/c9ra06508c.

[51] P.-C. Hsu, X. Liu, C. Liu, X. Xie, H. R. Lee, A. J. Welch, T. Zhao, Y. Cui, Personal thermal management by metallic nanowire-coated textile, *Nano Letters*, 2015, **15**, 365-371, doi: 10.1021/nl5036572.

[52] P. Won, J. J. Park, T. Lee, I. Ha, S. Han, M. Choi, J. Lee, S. Hong, K.-J. Cho, S. H. Ko, Stretchable and transparent kirigami conductor of nanowire percolation network for electronic skin applications, *Nano Letters*, 2019, **19**, 6087-6096, doi: 10.1021/acs.nanolett.9b02014.

[53] M. R. Jones, K. D. Osberg, R. J. MacFarlane, M. R. Langille, C. A. Mirkin, Templated techniques for the synthesis and assembly of plasmonic nanostructures, *Chemical Reviews*, 2011, **111**, 3736-3827, doi: 10.1021/cr1004452.

[54] W. Xu, L. Zhang, J. Zhang, X. Hu, L. Sun, A comparison of surface enhanced Raman scattering property between silver electrodes and periodical silver nanowire arrays, *Applied Surface Science*, 2009, **255**, 6612-6614, doi: 10.1016/j.apsusc.2009.02.053.

[55] S. J. Lee, A. R. Morrill, M. Moskovits, Hot spots in silver nanowire bundles for surface-enhanced Raman spectroscopy, *Journal of the American Chemical Society*, 2006, **128**, 2200-2201,

doi: 10.1021/ja0578350.
[56] A. P. Li, F. Müller, A. Birner, K. Nielsch, U. Gösele, Hexagonal pore arrays with a 50-420 nm interpore distance formed by self-organization in anodic alumina, *Journal of Applied Physics*, 1998, **84**, 6023-6026, doi: 10.1063/1.368911.
[57] Y. Du, L. Shi, T. He, X. Sun, Y. Mo, SERS enhancement dependence on the diameter and aspect ratio of silver-nanowire array fabricated by anodic aluminium oxide template, *Applied Surface Science*, 2008, **255**, 1901-1905, doi: 10.1016/j.apsusc.2008.06.140.
[58] S. Vilayurganapathy, M. I. Nandasiri, A. G. Joly, P. Z. El-Khoury, T. Varga, G. Coffey, B. Schwenzer, A. Pandey, A. Kayani, W. P. Hess, S. Thevuthasan, Silver nanorod arrays for photocathode applications, *Applied Physics Letters*, 2013, **103**, 161112, doi: 10.1063/1.4825262.
[59] C. Zhang, C. Li, X. Si, Z. He, J. Qi, J. Feng, J. Cao, Single-crystalline silver nanowire arrays directly synthesized onto substrates by template-assisted chemical wetting, *Materialia*, 2020, **9**, 100529, doi: 10.1016/j.mtla.2019.100529.
[60] Z.-J. Wang, Y. Xie, C. J. Liu, Synthesis and characterization of noble metal (pd, pt, au, ag) nanostructured materials confined in the channels of mesoporous SBA-15, *The Journal of Physical Chemistry C*, 2008, **112**, 19818-19824, 10.1021/jp805538j.
[61] K.-J. Kim, E.-S. Lee, Y.-U. Kwon, Syntheses of micrometer-long Pt and Ag nanowires through SBA-15 templating, *Journal of Nanoparticle Research*, 2012, **14**, 1270, doi: 10.1007/s11051-012-1270-1.
[62] P. M. Ajayan, S. Lijima, Capillarity-induced filling of carbon nanotubes, *Nature*, 1993, **361**, 333-334, doi: 10.1038/361333a0.
[63] D. Ugarte, A. Châtelain, W. A. de Heer, Nanocapillarity and chemistry in carbon nanotubes, *Science*, 1996, **274**, 1897-1899, doi: 10.1126/science.274.5294.1897.
[64] E. Borowiak-Palen, M. H. Ruemmeli, T. Gemming, T. Pichler, R. J. Kalenczuk, S. P. Silva, Silver filled single-wall carbon nanotubes—synthesis, structural and electronic properties, *Nanotechnology*, 2006, **17**, 2415-2419, doi: 10.1088/0957-4484/17/9/058.
[65] E. Braun, Y. Eichen, U. Sivan, G. Ben-Yoseph, DNA-templated assembly and electrode attachment of a conducting silver wire, *Nature*, 1998, **391**, 775-778, doi: 10.1038/35826.
[66] S. M. D. Watson, A. R. Pike, J. Pate, A. Houlton, B. R. Horrocks, DNA-templated nanowires: morphology and electrical conductivity, *Nanoscale*, 2014, **6**, 4027-4037, doi: 10.1039/c3nr06767j.
[67] K. Ijiro, H. Mitomo, Metal nanoarchitecture fabrication using DNA as a biotemplate, *Polymer Journal*, 2017, **49**, 815-824, doi: 10.1038/pj.2017.63.
[68] N. R. Jana, L. Gearheart, C. J. Murphy, Wet chemical synthesis of silver nanorods and nanowires of controllable aspect ratio, *Chemical Communications*, 2001, 617-618, doi: 10.1039/b100521i.
[69] C. J. Murphy, N. R. Jana, Controlling the aspect ratio of inorganic nanorods and nanowires, *Advanced Materials*, 2002, **14**, 80-82, doi: 10.1002/1521-4095(20020104)14: 180: aid-adma80>3.0.co;2-#.
[70] D. M. Eisele, H. V. Berlepsch, C. Böttcher, K. J. Stevenson, D. A. Vanden Bout, S. Kirstein, J. P. Rabe, Photoinitiated growth of sub-7 nm silver nanowires within a chemically active organic nanotubular template, *Journal of the American Chemical Society*, 2010, **132**, 2104-2105, doi: 10.1021/ja907373h.
[71] B. H. Hong, S. C. Bae, C.-W. Lee, S. Jeong, K. S. Kim, Ultrathin single-crystalline silver nanowire arrays formed in an ambient solution phase, *Science*, 2001, **294**, 348-351, doi: 10.1126/science.1062126.
[72] T. Y. Kim, W. J. Kim, S. H. Hong, J. E. Kim, K. S. Suh, Ionic-Liquid-Assisted Formation of Silver Nanowires, *Angewandte Chemie International Edition*, 2009, **48**, 3806-3809, doi: 10.1002/anie.200806379.
[73] C. Wang, M. Chen, G. Zhu, Z. Lin, A novel soft-template technique to synthesize metal Ag nanowire, *Journal of Colloid and Interface Science*, 2001, **243**, 362-364, doi: 10.1006/jcis.2001.7776.
[74] C. Y. Liu, Y. S. Zhang, C. K. Kao, J. H. Liu, Fabrication of silver nanowires via a β-cyclodextrin-derived soft template, *Express Polymer Letters*, 2018, **12**, 591-599, doi: 10.3144/expresspolymlett.2018.50.
[75] S. Berchmans, R. G. Nirmal, G. Prabaharan, S. Madhu, V. Yegnaraman, Templated synthesis of silver nanowires based on the layer-by-layer assembly of silver with dithiodipropionic acid molecules as spacers, *Journal of Colloid and Interface Science*, 2006, **303**, 604-610, doi: 10.1016/j.jcis.2006.07.060.
[76] M. Reches, E. Gazit, Casting metal nanowires within discrete self-assembled peptide nanotubes, *Science*, 2003, **300**, 625-627, doi: 10.1126/science.1082387.
[77] K. T. Nam, Y. J. Lee, E. M. Krauland, S. T. Kottmann, A. M. Belcher, Peptide-mediated reduction of silver ions on engineered biological scaffolds, *ACS Nano*, 2008, **2**, 1480-1486, doi: 10.1021/nn800018n.
[78] S. Behrens, J. Wu, W. Habicht, E. Unger, Silver nanoparticle and nanowire formation by microtubule templates, *Chemistry of Materials*, 2004, **16**, 3085-3090, doi: 10.1021/cm049462s.
[79] Z. Wang, J. Liu, X. Chen, J. Wan, Y. Qian, A simple hydrothermal route to large-scale synthesis of uniform silver nanowires, *Chemistry - A European Journal*, 2005, **11**, 160-163, doi: 10.1002/chem.200400705.
[80] B. Bari, J. Lee, T. Jang, P. Won, S. H. Ko, K. Alamgir, M. Arshad, L. J. Guo, Simple hydrothermal synthesis of very-long and thin silver nanowires and their application in high quality

transparent electrodes, *Journal of Materials Chemistry A*, 2016, **4**, 11365-11371, doi: 10.1039/c6ta03308c.

[81] Y. Zhang, J. Guo, D. Xu, Y. Sun, F. Yan, One-pot synthesis and purification of ultralong silver nanowires for flexible transparent conductive electrodes, *ACS Applied Materials & Interfaces*, 2017, **9**, 25465-25473, doi: 10.1021/acsami.7b07146.

[82] Y. Li, X. Yuan, H. Yang, Y. Chao, S. Guo, C. Wang, One-step synthesis of silver nanowires with ultra-long length and thin diameter to make flexible transparent conductive films, *Materials*, 2019, **12**, 401, doi: 10.3390/ma12030401.

[83] M. Ćwik, D. Buczyńska, K. Sulowska, E. Rożniecka, S. Mackowski, J. Niedziółka-Jönsson, Optical properties of submillimeter silver nanowires synthesized using the hydrothermal method, *Materials*, 2019, **12**, 721, doi: 10.3390/ma12050721.

[84] B. Liu, H. Yan, S. Chen, Y. Guan, G. Wu, R. Jin, L. Li, Stable and controllable synthesis of silver nanowires for transparent conducting film, *Nanoscale Research Letters*, 2017, **12**, 212, doi: 10.1186/s11671-017-1963-6.

[85] D. Sharma, D. A. Rakshana, R. M. Balakrishnan, P. E. JagadeeshBabu, One step synthesis of silver nanowires using fructose as a reducing agent and its antibacterial and antioxidant analysis, *Materials Research Express*, 2019, **6**, 075050, doi: 10.1088/2053-1591/ab170a.

[86] J. Xu, J. Hu, C. Peng, H. Liu, Y. Hu, A simple approach to the synthesis of silver nanowires by hydrothermal process in the presence of gemini surfactant, *Journal of Colloid and Interface Science*, 2006, **298**, 689-693, doi: 10.1016/j.jcis.2005.12.047.

[87] M. F. Meléndrez, C. Medina, F. Solis-Pomar, P. Flores, M. Paulraj, E. Pérez-Tijerina, Quality and high yield synthesis of Ag nanowires by microwave-assisted hydrothermal method, *Nanoscale Research Letters*, 2015, **10**, 48, doi: 10.1186/s11671-015-0774-x.

[88] M.-R. Azani, A. Hassanpour, N. Plaia, M. Meshkat-Mamalek, Movement-reactor oven and wire mesh filter for large-scale solvothermal preparation and purification of silver nanowires with high uniformity in length and diameter for the fabrication of low and high haze transparent conductive films, *Nanoscale Advances*, 2019, **1**, 2732-2739, doi: 10.1039/c9na00189a.

[89] E.-J. Lee, M.-H. Chang, Y.-S. Kim, J.-Y. Kim, High-pressure polyol synthesis of ultrathin silver nanowires: electrical and optical properties, *APL Materials*, 2013, **1**, 042118, doi: 10.1063/1.4826154.

[90] H.-W. Jang, Y.-H. Kim, K.-W. Lee, Y.-M. Kim, J.-Y. Kim, Research Update: synthesis of sub-15-nm diameter silver nanowires through a water-based hydrothermal method: fabrication of low-haze 2D conductive films, *APL Materials*, 2017, **5**, 080701, doi: 10.1063/1.4985764.

[91] M.-R. Azani, A. Hassanpour, Synthesis of silver nanowires with controllable diameter and simple tool to evaluate their diameter, concentration and yield, *ChemistrySelect*, 2019, **4**, 2716-2720, doi: 10.1002/slct.201900298.

[92] H. Jia, Z.-L. Yi, X.-H. Huang, F.-Y. Su, Q.-Q. Kong, X. Yang, Z. Wang, L.-J. Xie, Q.-G. Guo, C.-M. Chen, A one-step graphene induction strategy enables in situ controllable growth of silver nanowires for electromagnetic interference shielding, *Carbon*, 2021, **183**, 809-819, doi: 10.1016/j.carbon.2021.07.067.

[93] F. Fiévet, S. Ammar-Merah, R. Brayner, F. Chau, M. Giraud, F. Mammeri, J. Peron, J.-Y. Piquemal, L. Sicard, G. Viau, The polyol process: a unique method for easy access to metal nanoparticles with tailored sizes, shapes and compositions, *Chemical Society Reviews*, 2018, **47**, 5187-5233, doi: 10.1039/c7cs00777a.

[94] Y. Sun, B. Gates, B. Mayers, Y. Xia, Crystalline silver nanowires by soft solution processing, *Nano Letters*, 2002, **2**, 165-168, doi: 10.1021/nl010093y.

[95] Y. G. Sun, Y. N. Xia, Large-Scale synthesis of uniform silver nanowires through a soft, Self-Seeding, *Polyol Process*, *Advanced Materials*, 2002, **14**, 833-837, doi: 10.1002/1521-4095(20020605)14:11<833::Aid-Adma833>3.0.Co;2-K.

[96] S. M. Bergin, Y.-H. Chen, A. R. Rathmell, P. Charbonneau, Z.-Y. Li, B. J. Wiley, The effect of nanowire length and diameter on the properties of transparent, conducting nanowire films, *Nanoscale*, 2012, **4**, 1996, doi: 10.1039/c2nr30126a.

[97] D. Jia, Y. Zhao, W. Wei, C. Chen, G. Lei, M. Wan, J. Tao, S. Li, S. Ji, C. Ye, Synthesis of very thin Ag nanowires with fewer particles by suppressing secondary seeding, *CrystEngComm*, 2017, **19**, 148-153, doi: 10.1039/c6ce02075e.

[98] B. Li, S. Ye, I. E. Stewart, S. Alvarez, B. J. Wiley, Synthesis and purification of silver nanowires to make conducting films with a transmittance of 99%, *Nano Letters*, 2015, **15**, 6722-6726, doi: 10.1021/acs.nanolett.5b02582.

[99] Z. Niu, F. Cui, E. Kuttner, C. Xie, H. Chen, Y. Sun, A. Dehestani, K. Schierle-Arndt, P. Yang, Synthesis of silver nanowires with reduced diameters using benzoin-derived radicals to make transparent conductors with high transparency and low haze, *Nano Letters*, 2018, **18**, 5329-5334, doi: 10.1021/acs.nanolett.8b02479.

[100] P. Lee, J. Lee, H. Lee, J. Yeo, S. Hong, K. H. Nam, D. Lee, S. S. Lee, S. H. Ko, Highly stretchable and highly conductive metal electrode by very long metal nanowire percolation network, *Advanced Materials*, 2012, **24**, 3326-3332, doi: 10.1002/adma.201200359.

[101] J. H. Lee, P. Lee, D. Lee, S. S. Lee, S. H. Ko, Large-scale synthesis and characterization of very long silver nanowires via successive multistep growth, *Crystal Growth & Design*, 2012, **12**, 5598-5605, doi: 10.1021/cg301119d.

[102] M. B. Gebeyehu, Y.-H. Chang, A. K. Abay, S.-Y. Chang, J.-

Y. Lee, C.-M. Wu, T.-C. Chiang, R.-I. Murakami, Fabrication and characterization of continuous silver nanofiber/polyvinylpyrrolidone (AgNF/PVP) core-shell nanofibers using the coaxial electrospinning process, *RSC Advances*, 2016, **6**, 54162-54168, doi: 10.1039/c6ra05869h.

[103] J. Xue, T. Wu, Y. Dai, Y. Xia, Electrospinning and electrospun nanofibers: methods, materials, and applications, *Chemical Reviews*, 2019, **119**, 5298-5415, doi: 10.1021/acs.chemrev.8b00593.

[104] T.-M. Huang, F. Pang, I.-F. Hsieh, M. Cakmak, Control of radial structural gradient in PAN/silver nanofibers using solvent vapor treatment, *Synthetic Metals*, 2016, **221**, 309-318, doi: 10.1016/j.synthmet.2016.09.009.

[105] Y. Liu, C. Du, X. Lv, Z. Jia, S. Sun, J. Yu, Synthesis of silver nanofiber transparent electrodes by silver mirror reaction with electrospun nanofiber template, *Composite Interfaces*, 2021, **28**, 683-692, doi: 10.1080/09276440.2020.1812947.

[106] H.-T. Chen, H.-L. Lin, C. Kuo, I.-G. Chen, UV-induced synthesis of silver nanofiber networks as transparent electrodes, *Journal of Materials Chemistry C*, 2016, **4**, 7675-7682, doi: 10.1039/c6tc01858k.

[107] J. Jang, B. G. Hyun, S. Ji, E. Cho, B. W. An, W. H. Cheong, J.-U. Park, Rapid production of large-area, transparent and stretchable electrodes using metal nanofibers as wirelessly operated wearable heaters, *NPG Asia Materials*, 2017, **9**, e432, doi: 10.1038/am.2017.172.

[108] H. Wu, L. Hu, M. W. Rowell, D. Kong, J. J. Cha, J. R. McDonough, J. Zhu, Y. Yang, M. D. McGehee, Y. Cui, Electrospun metal nanofiber webs as high-performance transparent electrode, *Nano Letters*, 2010, **10**, 4242-4248, doi: 10.1021/nl102725k.

[109] A. Khalil, B. Singh Lalia, R. Hashaikeh, M. Khraisheh, Electrospun metallic nanowires: synthesis, characterization, and applications, *Journal of Applied Physics*, 2013, **114**, 171301, doi: 10.1063/1.4822482.

[110] Y. Sun, B. Mayers, T. Herricks, Y. Xia, Polyol synthesis of uniform silver nanowires: a plausible growth mechanism and the supporting evidence, *Nano Letters*, 2003, **3**, 955-960, doi: 10.1021/nl034312m.

[111] Y. Xia, Y. Xiong, B. Lim, S. Skrabalak, Shape-controlled synthesis of metal nanocrystals: simple chemistry meets complex physics? *Angewandte Chemie International Edition*, 2009, **48**, 60-103, doi: 10.1002/anie.200802248.

[112] V. K. LaMer, R. H. Dinegar, Theory, production and mechanism of formation of monodispersed hydrosols, Journal of the American Chemical Society, 1950, **72**, 4847–4854, doi: 10.1021/ja01167a001

[113] P. Zhang, I. Wyman, J. Hu, S. Lin, Z. Zhong, Y. Tu, Z. Huang, Y. Wei, Silver nanowires: synthesis technologies, growth mechanism and multifunctional applications, *Materials Science and Engineering: B*, 2017, **223**, 1-23, doi: 10.1016/j.mseb.2017.05.002.

[114] B. Blin, F. Fievet, D. Beaupere, M. Figlarz, Double oxidation of glycol ethylene in a new process of powder metallurgy elaboration, *New Journal of Chemistry*, 1989, **13**, 67–72.

[115] S. E. Skrabalak, B. J. Wiley, M. Kim, E. V. Formo, Y. Xia, On the polyol synthesis of silver nanostructures: glycolaldehyde as a reducing agent, *Nano Letters*, 2008, **8**, 2077-2081, doi: 10.1021/nl800910d.

[116] H. J. Kim, Y. Roh, B. Hong, Selective alignment of gold nanowires synthesized with DNA as template by surface-patterning technique, *IEEE Transactions on Nanotechnology*, 2010, **9**, 254-257, doi: 10.1109/tnano.2009.2025130.

[117] L. D. Marks, Experimental studies of small particle structures, *Reports on Progress in Physics*, 1994, **57**, 603-649, doi: 10.1088/0034-4885/57/6/002.

[118] Y. Gao, P. Jiang, L. Song, J. X. Wang, L. F. Liu, D. F. Liu, Y. J. Xiang, Z. X. Zhang, X. W. Zhao, X. Y. Dou, S. D. Luo, W. Y. Zhou, S. S. Xie, Studies on silver nanodecahedrons synthesized by PVP-assisted N, N-dimethylformamide (DMF) reduction, *Journal of Crystal Growth*, 2006, **289**, 376-380, doi: 10.1016/j.jcrysgro.2005.11.123.

[119] C. Özmetin, M. Çopur, A. Yartasi, M. M. Kocakerim, Kinetic investigation of reaction between metallic silver and nitric acid solutions, *Chemical Engineering & Technology*, 2000, **23**, 707-711, doi: 10.1002/1521-4125(200008)23: 8707: aid-ceat707>3.0.co;2-l.

[120] B. Wiley, T. Herricks, Y. Sun, Y. Xia, Polyol synthesis of silver nanoparticles: use of chloride and oxygen to promote the formation of single-crystal, truncated cubes and tetrahedrons, *Nano Letters*, 2004, **4**, 1733-1739, doi: 10.1021/nl048912c.

[121] R. Long, S. Zhou, B. J. Wiley, Y. Xiong, Oxidative etching for controlled synthesis of metal nanocrystals: atomic addition and subtraction, *Chemical Society Reviews*, 2014, **43**, 6288, doi: 10.1039/c4cs00136b.

[122] B. Wiley, Y. Sun, Y. Xia, Polyol synthesis of silver nanostructures: control of product morphology with Fe(II) or Fe(III) species, *Langmuir*, 2005, **21**, 8077-8080, doi: 10.1021/la050887i.

[123] K. E. Korte, S. E. Skrabalak, Y. Xia, Rapid synthesis of silver nanowires through a CuCl- or $CuCl_2$-mediated polyol process, *Journal of Material Chemistry*, 2008, **18**, 437-441, doi: 10.1039/b714072j.

[124] K. M. Koczkur, S. Mourdikoudis, L. Polavarapu, S. E. Skrabalak, Polyvinylpyrrolidone (PVP) in nanoparticle synthesis, *Dalton Transactions*, 2015, **44**, 17883-17905, doi: 10.1039/c5dt02964c.

[125] X. Xia, J. Zeng, L. K. Oetjen, Q. Li, Y. Xia, Quantitative analysis of the role played by poly(vinylpyrrolidone) in seed-mediated growth of Ag nanocrystals, *Journal of the American Chemical Society*, 2012, **134**, 1793-1801, doi: 10.1021/ja210047e.
[126] J. Zeng, Y. Zheng, M. Rycenga, J. Tao, Z.-Y. Li, Q. Zhang, Y. Zhu, Y. Xia, Controlling the shapes of silver nanocrystals with different capping agents, *Journal of the American Chemical Society*, 2010, **132**, 8552-8553, doi: 10.1021/ja103655f.
[127] T. Balankura, X. Qi, Y. Zhou, K. A. Fichthorn, Predicting kinetic nanocrystal shapes through multi-scale theory and simulation: Polyvinylpyrrolidone-mediated growth of Ag nanocrystals, *The Journal of Chemical Physics*, 2016, **145**, 144106, doi: 10.1063/1.4964297.
[128] Y. Gao, P. Jiang, L. Song, L. Liu, X. Yan, Z. Zhou, D. Liu, J. Wang, H. Yuan, Z. Zhang, X. Zhao, X. Dou, W. Zhou, G. Wang, S. Xie, Growth mechanism of silver nanowires synthesized by polyvinylpyrrolidone-assisted polyol reduction, *Journal of Physics D: Applied Physics*, 2005, **38**, 1061-1067, doi: 10.1088/0022-3727/38/7/015.
[129] P. Jiang, S.-Y. Li, S.-S. Xie, Y. Gao, L. Song, Machinable long PVP-stabilized silver nanowires, *Chemistry - A European Journal*, 2004, **10**, 4817-4821, doi: 10.1002/chem.200400318.
[130] J.-Y. Lin, Y.-L. Hsueh, J.-J. Huang, J.-R. Wu, Effect of silver nitrate concentration of silver nanowires synthesized using a polyol method and their application as transparent conductive films, *Thin Solid Films*, 2015, **584**, 243-247, doi: 10.1016/j.tsf.2015.02.067.
[131] C. C. Jia, P. Yang, A. Y. Zhang, *Mater. Chem. Phys.*, 2014, **143**, 794-800, doi: 10.1016/j.matchemphys.2013.10.015.
[132] A. Kumar, M. O. Shaikh, C.-H. Chuang, Silver nanowire synthesis and strategies for fabricating transparent conducting electrodes, *Nanomaterials*, 2021, **11**, 693, doi: 10.3390/nano11030693.
[133] S. Hemmati, M. T. Harris, D. P. Barkey, Polyol silver nanowire synthesis and the outlook for a green process, *Journal of Nanomaterials*, 2020, **2020**, 1-25, doi: 10.1155/2020/9341983.
[134] Y.-J. Song, M. Wang, X.-Y. Zhang, J.-Y. Wu, T. Zhang, Investigation on the role of the molecular weight of polyvinyl pyrrolidone in the shape control of high-yield silver nanospheres and nanowires, *Nanoscale Research Letters*, 2014, **9**, 17, doi: 10.1186/1556-276x-9-17.
[135] S. Fahad, H. Yu, L. Wang, Y. Wang, T. Lin, B. U. Amin, K.-U.-R. Naveed, R. U. Khan, S. Mehmood, F. Haq, Y. Xing, M. Usman, Synthesis of AgNWs using high molecular weight PVP As a capping agent and their application in conductive thin films, *Journal of Electronic Materials*, 2021, **50**, 2789-2799, doi: 10.1007/s11664-021-08770-6.
[136] K. Sheng Lau, S. X. Chin, S. Tee Tan, F. S. Lim, W. Sea Chang, C. Chin Yap, M. H. H. Jumali, S. Zakaria, S. W. Chook, C. H. Chia, Silver nanowires as flexible transparent electrode: role of PVP chain length, *Journal of Alloys and Compounds*, 2019, **803**, 165-171, doi: 10.1016/j.jallcom.2019.06.258.
[137] S. F. Li, H. Y. Zhang, Effect of polyvinylpyrrolidone on the preparation of silver nanowires, *Advanced Materials Research*, 2014, **881-883**, 940-943, doi: 10.4028/www.scientific.net/AMR.881-883.940.
[138] Y. Xiong, I. Washio, J. Chen, H. Cai, Z.-Y. Li, Y. Xia, Poly(vinyl pyrrolidone): a dual functional reductant and stabilizer for the facile synthesis of noble metal nanoplates in aqueous solutions, *Langmuir*, 2006, **22**, 8563-8570, doi: 10.1021/la061323x.
[139] S. Jharimune, R. Pfukwa, Z. Chen, J. Anderson, B. Klumperman, R. M. Rioux, Chemical identity of poly(N-vinylpyrrolidone) end groups impact shape evolution during the synthesis of Ag nanostructures, *Journal of the American Chemical Society*, 2021, **143**, 184-195, doi: 10.1021/jacs.0c08528.
[140] J. Hwang, Y. Shim, S.-M. Yoon, S. H. Lee, S.-H. Park, Influence of polyvinylpyrrolidone (PVP) capping layer on silver nanowire networks: theoretical and experimental studies, *RSC Advances*, 2016, **6**, 30972-30977, doi: 10.1039/c5ra28003f.
[141] J.-Y. Tseng, L. Lee, Y.-C. Huang, J.-H. Chang, T.-Y. Su, Y.-C. Shih, H.-W. Lin, Y.-L. Chueh, Pressure welding of silver nanowires networks at room temperature as transparent electrodes for efficient organic light-emitting diodes, *Small*, 2018, **14**, 1800541, doi: 10.1002/smll.201800541.
[142] Y. Ge, X. Duan, M. Zhang, L. Mei, J. Hu, W. Hu, X. Duan, Direct room temperature welding and chemical protection of silver nanowire thin films for high performance transparent conductors, *Journal of the American Chemical Society*, 2018, **140**, 193-199, doi: 10.1021/jacs.7b07851.
[143] X. Zhang, B. Liu, C. Hu, S. Chen, X. Liu, J. Liu, F. Chen, J. Chen, F. Xie, A facile method in removal of PVP ligands from silver nanowires for high performance and reusable SERS substrate, *Spectrochimica Acta Part A: Molecular and Biomolecular Spectroscopy*, 2020, **228**, 117733, doi: 10.1016/j.saa.2019.117733.
[144] Y. Ge, J. Liu, X. Liu, J. Hu, X. Duan, X. Duan, Rapid electrochemical cleaning silver nanowire thin films for high-performance transparent conductors, *Journal of the American Chemical Society*, 2019, **141**, 12251-12257, doi: 10.1021/jacs.9b02497.
[145] M. Han, Y. Ge, J. Liu, Z. Cao, M. Li, X. Duan, J. Hu, Mixed polyvinyl pyrrolidone hydrogel-mediated synthesis of high-quality Ag nanowires for high-performance transparent conductors, *Journal of Materials Chemistry A*, 2020, **8**, 21062-21069, doi: 10.1039/d0ta07273g.
[146] A. A. Ashkarran, M. Derakhshi, The effect of FeCl3 in the

shape control polyol synthesis of silver nanospheres and nanowires, *Journal of Cluster Science*, 2015, **26**, 1901-1910, doi: 10.1007/s10876-015-0887-5.

[147] J. Ma, M. Zhan, Rapid production of silver nanowires based on high concentration of $AgNO_3$ precursor and use of $FeCl_3$ as reaction promoter, *RSC Advances*, 2014, **4**, 21060, doi: 10.1039/c4ra00711e.

[148] S. Wang, Y. Tian, S. Ding, Y. Huang, Rapid synthesis of long silver nanowires by controlling concentration of Cu^{2+} ions, *Materials Letters*, 2016, **172**, 175-178, doi: 10.1016/j.matlet.2016.02.124.

[149] F. Fievet, J. P. Lagier, M. Figlarz, Preparing monodisperse metal powders in micrometer and submicrometer sizes by the polyol process, *MRS Bulletin*, 1989, **14**, 29-34, doi: 10.1557/s0883769400060930.

[150] M. Tsuji, K. Matsumoto, P. Jiang, R. Matsuo, X.-L. Tang, K. S. N. Kamarudin, Roles of Pt seeds and chloride anions in the preparation of silver nanorods and nanowires by microwave-polyol method, *Colloids and Surfaces A: Physicochemical and Engineering Aspects*, 2008, **316**, 266-277, doi: 10.1016/j.colsurfa.2007.09.014.

[151] S. Coskun, B. Aksoy, H. E. Unalan, Polyol synthesis of silver nanowires: an extensive parametric study, *Crystal Growth & Design*, 2011, **11**, 4963-4969, doi: 10.1021/cg200874g.

[152] R. R. da Silva, M. Yang, S.-I. Choi, M. Chi, M. Luo, C. Zhang, Z.-Y. Li, P. H. C. Camargo, S. J. L. Ribeiro, Y. Xia, Facile synthesis of sub-20 nm silver nanowires through a bromide-mediated polyol method, *ACS Nano*, 2016, **10**, 7892-7900, doi: 10.1021/acsnano.6b03806.

[153] W. M. Schuette, W. E. Buhro, Silver chloride as a heterogeneous nucleant for the growth of silver nanowires, *ACS Nano*, 2013, **7**, 3844-3853, doi: 10.1021/nn400414h.

[154] Y.-H. Chang, Y.-C. Lu, K.-S. Chou, Diameter control of silver nanowires by chloride ions and its application as transparent conductive coating, *Chemistry Letters*, 2011, **40**, 1352-1353, doi: 10.1246/cl.2011.1352.

[155] P. Zhang, Y. Wei, M. Ou, Z. Huang, S. Lin, Y. Tu, J. Hu, Behind the role of bromide ions in the synthesis of ultrathin silver nanowires, *Materials Letters*, 2018, **213**, 23-26, doi: 10.1016/j.matlet.2017.10.128.

[156] X. Zhu, A. Guo, J. Xu, C. Kan, The synthesis of silver nanowires with tunable diameters using halide ions for flexible transparent conductive films, *CrystEngComm*, 2020, **22**, 8421-8429, doi: 10.1039/d0ce01435d.

[157] Y. Rui, W. Zhao, D. Zhu, H. Wang, G. Song, M. Swihart, N. Wan, D. Gu, X. Tang, Y. Yang, T. Zhang, Understanding the effects of NaCl, NaBr and their mixtures on silver nanowire nucleation and growth in terms of the distribution of electron traps in silver halide crystals, *Nanomaterials*, 2018, **8**, 161, doi: 10.3390/nano8030161.

[158] S. Hemmati, D. P. Barkey, Parametric study, sensitivity analysis, and optimization of polyol synthesis of silver nanowires, *ECS Journal of Solid State Science and Technology*, 2017, **6**, 132-137, doi: 10.1149/2.0141704jss.

[159] M. B. Gebeyehu, T. F. Chala, S.-Y. Chang, C.-M. Wu, J.-Y. Lee, Synthesis and highly effective purification of silver nanowires to enhance transmittance at low sheet resistance with simple polyol and scalable selective precipitation method, *RSC Advances*, 2017, **7**, 16139-16148, doi: 10.1039/c7ra00238f.

[160] H. Ding, Y. Zhang, G. Yang, S. Zhang, L. Yu, P. Zhang, Large scale preparation of silver nanowires with different diameters by a one-pot method and their application in transparent conducting films, *RSC Advances*, 2016, **6**, 8096-8102, doi: 10.1039/c5ra25474d.

[161] W. M. Schuette, W. E. Buhro, Polyol synthesis of silver nanowires by heterogeneous nucleation; mechanistic aspects influencing nanowire diameter and length, *Chemistry of Materials*, 2014, **26**, 6410-6417, doi: 10.1021/cm502827b.

[162] Y. Liu, Y. Chen, R. Shi, L. Cao, Z. Wang, T. Sun, J. Lin, J. Liu, W. Huang, High-yield and rapid synthesis of ultrathin silver nanowires for low-haze transparent conductors, *RSC Advances*, 2017, **7**, 4891-4895, doi: 10.1039/c6ra27760h.

[163] J. Jiu, T. Araki, J. Wang, M. Nogi, T. Sugahara, S. Nagao, H. Koga, K. Suganuma, E. Nakazawa, M. Hara, H. Uchida, K. Shinozaki, Facile synthesis of very-long silver nanowires for transparent electrodes, *Journal of Material Chemistry A*, 2014, **2**, 6326-6330, doi: 10.1039/c4ta00502c.

[164] T. Araki, J. Jiu, M. Nogi, H. Koga, S. Nagao, T. Sugahara, K. Suganuma, Low haze transparent electrodes and highly conducting air dried films with ultra-long silver nanowires synthesized by one-step polyol method, *Nano Research*, 2014, **7**, 236-245, doi: 10.1007/s12274-013-0391-x.

[165] A. Amirjani, P. Marashi, D. H. Fatmehsari, The effect of agitation state on polyol synthesis of silver nanowire, *International Nano Letters*, 2016, **6**, 41-44, doi: 10.1007/s40089-015-0164-5.

[166] L. Zhang, T. Song, L. Shi, N. Wen, Z. Wu, C. Sun, D. Jiang, Z. Guo, Recent progress for silver nanowires conducting film for flexible electronics, *Journal of Nanostructure in Chemistry*, 2021, **11**, 323-341, doi: 10.1007/s40097-021-00436-3.

[167] H. Sohn, C. Park, J.-M. Oh, S. W. Kang, M.-J. Kim, Silver nanowire networks: mechano-electric properties and applications, *Materials*, 2019, **12**, 2526, doi: 10.3390/ma12162526.

[168] W. Xi, R. Ma, H. Wang, Z. Gao, W. Zhang, Y. Zhao, Ultrathin Ag nanowires electrode for electrochemical syngas production from carbon dioxide, *ACS Sustainable Chemistry & Engineering*, 2018, **6**, 7687-7694, doi: 10.1021/acssuschemeng.8b00527.

[169] X. Guo, X. Liu, J. Luo, Z. Gan, Z. Meng, N. Zhang, Silver nanowire/polyimide composite transparent electrodes for reliable flexible polymer solar cells operating at high and ultra-low temperature, *RSC Advances*, 2015, **5**, 24953-24959, doi: 10.1039/c5ra00403a.

[170] M. J. Saw, B. Ghosh, M. T. Nguyen, K. Jirasattayaporn, S. Kheawhom, N. Shirahata, T. Yonezawa, High aspect ratio and post-processing free silver nanowires as top electrodes for inverted-structured photodiodes, *ACS Omega*, 2019, **4**, 13303-13308, doi: 10.1021/acsomega.9b01479.

[171] D. Jiang, Y. Wang, B. Li, C. Sun, Z. Wu, H. Yan, L. Xing, S. Qi, Y. Li, H. Liu, W. Xie, X. Wang, T. Ding, Z. Guo, Flexible sandwich structural strain sensor based on silver nanowires decorated with self-healing substrate, *Macromolecular Materials* and Engineering, 2019, **304**, 1900074, doi: 10.1002/mame.201900074.

[172] Z. Yu, Q. Zhang, L. Li, Q. Chen, X. Niu, J. Liu, Q. Pei, Highly flexible silver nanowire electrodes for shape-memory polymer light-emitting diodes, Advanced Materials, 2011, **23**, 664-668, doi: 10.1002/adma.201003398.

[173] A. Kaliyaraj Selva Kumar, Y. Zhang, D. Li, R. G. Compton, A mini-review: how reliable is the drop casting technique? *Electrochemistry Communications*, 2020, **121**, 106867, doi: 10.1016/j.elecom.2020.106867.

[174] D. G. Lee, D. Lee, J. S. Yoo, S. Lee, H. S. Jung, Effective passivation of Ag nanowire-based flexible transparent conducting electrode by TiO_2 nanoshell, *Nano Convergence*, 2016, **3**, 20, doi: 10.1186/s40580-016-0080-z.

[175] F. Chen, P. Wan, H. Xu, X. Sun, Flexible transparent supercapacitors based on hierarchical nanocomposite films, ACS *Applied Materials & Interfaces*, 2017, **9**, 17865-17871, doi: 10.1021/acsami.7b02460.

[176] Y.-T. Kwon, J. W. Moon, Y.-M. Choi, S. Kim, S. H. Ryu, Y.-H. Choa, Novel concept for fabricating a flexible transparent electrode using the simple and scalable self-assembly of Ag nanowires, *The Journal of Physical Chemistry C*, 2017, **121**, 5740-5746, doi: 10.1021/acs.jpcc.7b00148.

[177] D. Chen, J. Liang, C. Liu, G. Saldanha, F. Zhao, K. Tong, J. Liu, Q. Pei, Thermally stable silver nanowire-polyimide transparent electrode based on atomic layer deposition of zinc oxide on silver nanowires, Advanced Functional Materials, 2015, **25**, 7512-7520, doi: 10.1002/adfm.201503236.

[178] J. Lee, P. Lee, H. B. Lee, S. Hong, I. Lee, J. Yeo, S. S. Lee, T.-S. Kim, D. Lee, S. H. Ko, Room-temperature nanosoldering of a very long metal nanowire network by conducting-polymer-assisted joining for a flexible touch-panel application, *Advanced Functional Materials*, 2013, **23**, 4171-4176, doi: 10.1002/adfm.201203802.

[179] H. Kang, I. Kang, J. Han, J. B. Kim, D. Y. Lee, S. M. Cho, J. H. Cho, Flexible and mechanically robust organic light-emitting diodes based on photopatternable silver nanowire electrodes, *The Journal of Physical Chemistry C*, 2016, **120**, 22012-22018, doi: 10.1021/acs.jpcc.6b06599.

[180] S. Cho, S. Kang, A. Pandya, R. Shanker, Z. Khan, Y. Lee, J. Park, S. L. Craig, H. Ko, Large-area cross-aligned silver nanowire electrodes for flexible, transparent, and force-sensitive mechanochromic touch screens, *ACS Nano*, 2017, **11**, 4346-4357, doi: 10.1021/acsnano.7b01714.

[181] S. Bai, X. Guo, T. Chen, Y. Zhang, H. Yang, Solution process fabrication of silver nanowire composite transparent conductive films with tunable work function, *Thin Solid Films*, 2020, **709**, 138096, doi: 10.1016/j.tsf.2020.138096.

[182] L. Zhang, F. Jiang, B. Wu, C. Lv, M. Wu, A one-step synthesis of ultra-long silver nanowires with ultra-high aspect ratio above 2000 and its application in flexible transparent conductive electrodes, *Nanotechnology*, 2021, **32**, 105710, doi: 10.1088/1361-6528/abce7a.

[183] H. Yang, T. Chen, H. Wang, S. Bai, X. Guo, One-pot rapid synthesis of high aspect ratio silver nanowires for transparent conductive electrodes, *Materials Research Bulletin*, 2018, **102**, 79-85, doi: 10.1016/j.materresbull.2018.02.010.

[184] W. Lee, K. David Kihm, W. Lee, P. Won, S. Han, G. Lim, K. R. Pyun, S. H. Ko, Boosted thermal conductance of polycrystalline graphene by spin-coated silver nanowires, *International Journal of Heat and Mass Transfer*, 2019, **134**, 547-553, doi: 10.1016/j.ijheatmasstransfer.2019.01.052.

[185] T. Zhai, J. Chen, L. Chen, J. Wang, L. Wang, D. Liu, S. Li, H. Liu, X. Zhang, A plasmonic random laser tunable through stretching silver nanowires embedded in a flexible substrate, *Nanoscale*, 2015, **7**, 2235-2240, doi: 10.1039/c4nr06632d.

[186] J. Sun, W. Zhou, H. Yang, X. Zhen, L. Ma, D. Williams, X. Sun, M.-F. Lang, Highly transparent and flexible circuits through patterning silver nanowires into microfluidic channels, *Chemical Communications*, 2018, **54**, 4923-4926, doi: 10.1039/c8cc01438h.

[187] J. Li, M. Su, M. Jiang, L. Tian, C. Zhu, X. Cao, Q. Jiang, X. Huo, C. Yu, Stretchable conductive film based on silver nanowires and carbon nanotubes for real-time inducing and monitoring of cell-released NO, *Sensors and Actuators B: Chemical*, 2022, **366**, 131983, doi: 10.1016/j.snb.2022.131983.

[188] S. Lin, H. Wang, X. Zhang, D. Wang, D. Zu, J. Song, Z. Liu, Y. Huang, K. Huang, N. Tao, Z. Li, X. Bai, B. Li, M. Lei, Z. Yu, H. Wu, Direct spray-coating of highly robust and transparent Ag nanowires for energy saving windows, *Nano Energy*, 2019, **62**, 111-116, doi: 10.1016/j.nanoen.2019.04.071.

[189] A. R. Madaria, A. Kumar, C. Zhou, Large scale, highly conductive and patterned transparent films of silver nanowires on arbitrary substrates and their application in touch screens,

Nanotechnology, 2011, **22**, 245201, doi: 10.1088/0957-4484/22/24/245201.

[190] V. Scardaci, R. Coull, P. E. Lyons, D. Rickard, J. N. Coleman, Spray deposition of highly transparent, low-resistance networks of silver nanowires over large areas, *Small*, 2011, **7**, 2621-2628, doi: 10.1002/smll.201100647.

[191] R. R. Søndergaard, M. Hösel, F. C. Krebs, Roll-to-Roll fabrication of large area functional organic materials, Journal of *Polymer Science Part B: Polymer Physics*, 2013, **51**, 16-34, doi: 10.1002/polb.23192.

[192] Y. Wang, J. Wang, S. Cao, D. Kong, A stretchable and breathable form of epidermal device based on elastomeric nanofibre textiles and silver nanowires, *Journal of Materials Chemistry C*, 2019, **7**, 9748-9755, doi: 10.1039/c9tc02584g.

[193] T. Kim, C. Park, E. P. Samuel, S. An, A. Aldalbahi, F. Alotaibi, A. L. Yarin, S. S. Yoon, Supersonically sprayed washable, wearable, stretchable, hydrophobic, and antibacterial rGO/AgNW fabric for multifunctional sensors and supercapacitors, *ACS Applied Materials & Interfaces*, 2021, **13**, 10013-10025, doi: 10.1021/acsami.0c21372.

[194] T. Akter, W. S. Kim, Reversibly stretchable transparent conductive coatings of spray-deposited silver nanowires, *ACS Applied Materials & Interfaces*, 2012, **4**, 1855-1859, doi: 10.1021/am300058j.

[195] H. Xie, X. Lai, H. Li, J. Gao, X. Zeng, X. Huang, S. Zhang, A sandwich-like flame retardant nanocoating for supersensitive fire-warning, *Chemical Engineering Journal*, 2020, **382**, 122929, doi: 10.1016/j.cej.2019.122929.

[196] X. Xu, Z. Liu, P. He, J. Yang, Screen printed silver nanowire and graphene oxide hybrid transparent electrodes for long-term electrocardiography monitoring, *Journal of Physics D: Applied Physics*, 2019, **52**, 455401, doi: 10.1088/1361-6463/ab3869.

[197] X. He, R. He, Q. Lan, W. Wu, F. Duan, J. Xiao, M. Zhang, Q. Zeng, J. Wu, J. Liu, Screen-printed fabrication of PEDOT: PSS/silver nanowire composite films for transparent heaters, *Materials*, 2017, **10**, 220, doi: 10.3390/ma10030220.

[198] D. Li, X. Liu, X. Chen, W.-Y. Lai, W. Huang, A simple strategy towards highly conductive silver-nanowire inks for screen-printed flexible transparent conductive films and wearable energy-storage devices, *Advanced Materials Technologies*, 2019, 4, 1900196, doi: 10.1002/admt.201900196.

[199] S. Yao, Y. Zhu, Wearable multifunctional sensors using printed stretchable conductors made of silver nanowires, *Nanoscale*, 2014, **6**, 2345, doi: 10.1039/c3nr05496a.

[200] S.-H. Ke, Q.-W. Xue, C.-Y. Pang, P.-W. Guo, W.-J. Yao, H.-P. Zhu, W. Wu, Printing the ultra-long Ag nanowires inks onto the flexible textile substrate for stretchable electronics, *Nanomaterials*, 2019, **9**, 686, doi: 10.3390/nano9050686.

[201] Y. Lin, W. Yuan, C. Ding, S. Chen, W. Su, H. Hu, Z. Cui, F. Li, Facile and efficient patterning method for silver nanowires and its application to stretchable electroluminescent displays, *ACS Applied Materials & Interfaces*, 2020, **12**, 24074-24085, doi: 10.1021/acsami.9b21755.

[202] J. Liang, K. Tong, Q. Pei, A water-based silver-nanowire screen-print ink for the fabrication of stretchable conductors and wearable thin-film transistors, *Advanced Materials*, 2016, **28**, 5986-5996, doi: 10.1002/adma.201600772.

[203] P. G. V. Sampaio, M. O. A. González, P. Oliveira Ferreira, P. Cunha Jácome Vidal, J. P. P. Pereira, H. R. Ferreira, P. C. Oprime, Overview of printing and coating techniques in the production of organic photovoltaic cells, *International Journal of Energy Research*, 2020, **44**, 9912-9931, doi: 10.1002/er.5664.

[204] M. Mohammed Ali, D. Maddipatla, B. B. Narakathu, A. A. Chlaihawi, S. Emamian, F. Janabi, B. J. Bazuin, M. Z. Atashbar, Printed strain sensor based on silver nanowire/silver flake composite on flexible and stretchable TPU substrate, Sensors and Actuators A: Physical, 2018, **274**, 109-115, doi: 10.1016/j.sna.2018.03.003.

[205] L. Song, A. C. Myers, J. J. Adams, Y. Zhu, Stretchable and reversibly deformable radio frequency antennas based on silver nanowires, ACS Applied Materials & Interfaces, 2014, **6**, 4248-4253, doi: 10.1021/am405972e.

[206] W. Xu, Q. Xu, Q. Huang, R. Tan, W. Shen, W. Song, Fabrication of flexible transparent conductive films with silver nanowire by vacuum filtration and PET mold transfer, *Journal of Materials Science & Technology*, 2016, **32**, 158-161, doi: 10.1016/j.jmst.2015.12.009.

[207] Y. R. Lee, H. Kwon, D. H. Lee, B. Y. Lee, Highly flexible and transparent dielectric elastomer actuators using silver nanowire and carbon nanotube hybrid electrodes, *Soft Matter*, 2017, **13**, 6390-6395, doi: 10.1039/c7sm01329a.

[208] A. Mushtaq, H. Cho, M. A. Ahmed, M. S. U. Rehman, J.-I. Han, A novel method for the fabrication of silver nanowires-based highly electro-conductive membrane with antifouling property for efficient microalgae harvesting, Journal of Membrane Science, 2019, **590**, 117258, doi: 10.1016/j.memsci.2019.117258.

[209] G.-W. Huang, H.-M. Xiao, S.-Y. Fu, Paper-based silver-nanowire electronic circuits with outstanding electrical conductivity and extreme bending stability, Nanoscale, 2014, **6**, 8495, doi: 10.1039/c4nr00846d.

[210] R. R. Kisannagar, P. Jha, A. Navalkar, S. K. Maji, D. Gupta, Fabrication of silver nanowire/polydimethylsiloxane dry electrodes by a vacuum filtration method for electrophysiological signal monitoring, *ACS Omega*, 2020, **5**, 10260-10265, doi: 10.1021/acsomega.9b03678.

[211] J. Liu, T. He, G. Fang, R. Wang, E. A. Kamoun, J. Yao, Z. Shao, X. Chen, Environmentally responsive composite films

fabricated using silk nanofibrils and silver nanowires, *Journal of Materials Chemistry C*, 2018, **6**, 12940-12947, doi: 10.1039/c8tc04549f.
[212] L. Shen, L. Du, S. Tan, Z. Zang, C. Zhao, W. Mai, Flexible electrochromic supercapacitor hybrid electrodes based on tungsten oxide films and silver nanowires, Chemical Communications, 2016, **52**, 6296-6299, doi: 10.1039/c6cc01139j.
[213] C. Liang, K. Ruan, Y. Zhang, J. Gu, Multifunctional flexible electromagnetic interference shielding silver nanowires/cellulose films with excellent thermal management and joule heating performances, ACS Applied Materials & Interfaces, 2020, **12**, 18023-18031, doi: 10.1021/acsami.0c04482.
[214] T.-B. Song, Y. Chen, C.-H. Chung, Y. M. Yang, B. Bob, H.-S. Duan, G. Li, K.-N. Tu, Y. Huang, Y. Yang, Nanoscale joule heating and electromigration enhanced ripening of silver nanowire contacts, *ACS Nano*, 2014, **8**, 2804-2811, doi: 10.1021/nn4065567.
[215] H. Lu, D. Zhang, J. Cheng, J. Liu, J. Mao, W. C. H. Choy, Locally welded silver nano-network transparent electrodes with high operational stability by a simple alcohol-based chemical approach, *Advanced Functional Materials*, 2015, **25**, 4211-4218, doi: 10.1002/adfm.201501004.
[216] X. Liang, T. Zhao, P. Zhu, Y. Hu, R. Sun, C.-P. Wong, Room-temperature nanowelding of a silver nanowire network triggered by hydrogen chloride vapor for flexible transparent conductive films, *ACS Applied Materials & Interfaces*, 2017, **9**, 40857-40867, doi: 10.1021/acsami.7b13048.
[217] S.-S. Yoon, D.-Y. Khang, Room-temperature chemical welding and sintering of metallic nanostructures by capillary condensation, *Nano Letters*, 2016, **16**, 3550-3556, doi: 10.1021/acs.nanolett.6b00621.
[218] W. Xiong, H. Liu, Y. Chen, M. Zheng, Y. Zhao, X. Kong, Y. Wang, X. Zhang, X. Kong, P. Wang, L. Jiang, Highly conductive, air-stable silver Nanowire@Iongel composite films toward flexible transparent electrodes, *Advanced Materials*, 2016, **28**, 7167-7172, doi: 10.1002/adma.201600358.
[219] T. Tokuno, M. Nogi, M. Karakawa, J. Jiu, T. T. Nge, Y. Aso, K. Suganuma, Fabrication of silver nanowire transparent electrodes at room temperature, *Nano Research*, 2011, **4**, 1215-1222, doi: 10.1007/s12274-011-0172-3.
[220] T. A. Celano, D. J. Hill, X. Zhang, C. W. Pinion, J. D. Christesen, C. J. Flynn, J. R. McBride, J. F. Cahoon, Capillarity-driven welding of semiconductor nanowires for crystalline and electrically ohmic junctions, *Nano Letters*, 2016, **16**, 5241-5246, doi: 10.1021/acs.nanolett.6b02361.
[221] Y. Liu, J. Zhang, H. Gao, Y. Wang, Q. Liu, S. Huang, C. F. Guo, Z. Ren, Capillary-force-induced cold welding in silver-nanowire-based flexible transparent electrodes, *Nano Letters*, 2017, **17**, 1090-1096, doi: 10.1021/acs.nanolett.6b04613.
[222] J. Lee, P. Lee, H. Lee, D. Lee, S. S. Lee, S. H. Ko, Very long Ag nanowire synthesis and its application in a highly transparent, conductive and flexible metal electrode touch panel, *Nanoscale*, 2012, **4**, 6408, doi: 10.1039/c2nr31254a.
[223] S. Hong, H. Lee, J. Yeo, S. H. Ko, Digital selective laser methods for nanomaterials: from synthesis to processing, *Nano Today*, 2016, **11**, 547-564, doi: 10.1016/j.nantod.2016.08.007.
[224] P. Lee, J. Ham, J. Lee, S. Hong, S. Han, Y. D. Suh, S. E. Lee, J. Yeo, S. S. Lee, D. Lee, S. H. Ko, Highly stretchable or transparent conductor fabrication by a hierarchical multiscale hybrid nanocomposite, *Advanced Functional Materials*, 2014, **24**, 5671-5678, doi: 10.1002/adfm.201400972.
[225] Y. Sun, M. Chang, L. Meng, X. Wan, H. Gao, Y. Zhang, K. Zhao, Z. Sun, C. Li, S. Liu, H. Wang, J. Liang, Y. Chen, Flexible organic photovoltaics based on water-processed silver nanowire electrodes, *Nature Electronics*, 2019, **2**, 513-520, doi: 10.1038/s41928-019-0315-1.
[226] S. J. Kim, H. G. Yoon, S. W. Kim, Extremely robust and reliable transparent silver nanowire-mesh electrode with multifunctional optoelectronic performance through selective laser nanowelding for flexible smart devices, *Advanced Engineering Materials*, 2021, **23**, 2001310, doi: 10.1002/adem.202001310.
[227] Y.-R. Chen, C.-C. Hong, T.-M. Liou, K. C. Hwang, T.-F. Guo, Roller-induced bundling of long silver nanowire networks for strong interfacial adhesion, highly flexible, transparent conductive electrodes, *Scientific Reports*, 2017, **7**, 16662, doi: 10.1038/s41598-017-16843-y.
[228] Y. Zhao, X. Wang, S. Yang, E. Kuttner, A. A. Taylor, R. Salemmilani, X. Liu, M. Moskovits, B. Wu, A. Dehestani, J.-F. Li, M. F. Chisholm, Z.-Q. Tian, F.-R. Fan, J. Jiang, G. D. Stucky, Protecting the nanoscale properties of Ag nanowires with a solution-grown SnO2 monolayer as corrosion inhibitor, *Journal of the American Chemical Society*, 2019, **141**, 13977-13986, doi: 10.1021/jacs.9b07172.
[229] Y. Xiong, R. E. Booth, T. Kim, L. Ye, Y. Liu, Q. Dong, M. Zhang, F. So, Y. Zhu, A. Amassian, B. T. O'Connor, H. Ade, Novel bimodal silver nanowire network as top electrodes for reproducible and high-efficiency semitransparent organic photovoltaics, *Solar RRL*, 2020, **4**, 2000328, doi: 10.1002/solr.202000328.
[230] G. A. dos Reis Benatto, B. Roth, M. Corazza, R. R. Søndergaard, S. A. Gevorgyan, M. Jørgensen, F. C. Krebs, Roll-to-roll printed silver nanowires for increased stability of flexible ITO-free organic solar cell modules, *Nanoscale*, 2016, **8**, 318-326, doi: 10.1039/c5nr07426f.
[231] Z. Wang, Y. Han, L. Yan, C. Gong, J. Kang, H. Zhang, X. Sun, L. Zhang, J. Lin, Q. Luo, C.-Q. Ma, High power conversion efficiency of 13.61% for 1 cm2 flexible polymer solar cells based

on patternable and mass-producible gravure-printed silver nanowire electrodes, *Advanced Functional Materials*, 2021, **31**, 2007276, doi: 10.1002/adfm.202007276.[LinkOut]

[232] C. Xie, X. Jiang, Q. Zhu, D. Wang, C. Xiao, C. Liu, W. Ma, Q. Chen, W. Li, Mechanical robust flexible single-component organic solar cells, *Small Methods*, 2021, **5**, 2100481, doi: 10.1002/smtd.202100481.

[233] Y. Wang, Q. Chen, G. Zhang, C. Xiao, Y. Wei, W. Li, Ultrathin flexible transparent composite electrode via semi-embedding silver nanowires in a colorless polyimide for high-performance ultraflexible organic solar cells, *ACS Applied Materials & Interfaces*, 2022, **14**, 5699-5708, doi: 10.1021/acsami.1c18866.

[234] K.-H. Ok, J. Kim, S.-R. Park, Y. Kim, C.-J. Lee, S.-J. Hong, M.-G. Kwak, N. Kim, C. J. Han, J.-W. Kim, Ultra-thin and smooth transparent electrode for flexible and leakage-free organic light-emitting diodes, *Scientific Reports*, 2015, **5**, 9464, doi: 10.1038/srep09464.

[235] J. Lee, K. An, P. Won, Y. Ka, H. Hwang, H. Moon, Y. Kwon, S. Hong, C. Kim, C. Lee, S. H. Ko, A dual-scale metal nanowire network transparent conductor for highly efficient and flexible organic light emitting diodes, *Nanoscale*, 2017, **9**, 1978-1985, doi: 10.1039/c6nr09902e.

[236] J. Sun, H. Wang, H. Shi, S. Wang, J. Xu, J. Ma, B. Ma, M. Wen, J. Li, J. Zhao, H. Liu, Y. Wang, L. Jiang, Large-area tunable red/green/blue tri-stacked quantum dot light-emitting diode using sandwich-structured transparent silver nanowires electrodes, *ACS Applied Materials & Interfaces*, 2020, **12**, 48820-48827, doi: 10.1021/acsami.0c15469.

[237] J. Liang, L. Li, K. Tong, Z. Ren, W. Hu, X. Niu, Y. Chen, Q. Pei, Silver nanowire percolation network soldered with graphene oxide at room temperature and its application for fully stretchable polymer light-emitting diodes, *ACS Nano*, 2014, **8**, 1590-1600, doi: 10.1021/nn405887k.

[238] A. G. Ricciardulli, S. Yang, G.-J A. H. Wetzelaer, X. Feng, P. W. M. Blom, Hybrid silver nanowire and graphene-based solution-processed transparent electrode for organic optoelectronics, Advanced Functional Materials, 2018, **28**, 1706010, doi: 10.1002/adfm.201706010.

[239] H. Shin, B. K. Sharma, S. W. Lee, J.-B. Lee, M. Choi, L. Hu, C. Park, J. H. Choi, T. W. Kim, J.-H. Ahn, Stretchable electroluminescent display enabled by graphene-based hybrid electrode, *ACS Applied Materials & Interfaces*, 2019, **11**, 14222-14228, doi: 10.1021/acsami.8b22135.

[240] X. Wu, Z. Zhou, Y. Wang, J. Li, Syntheses of silver nanowires ink and printable flexible transparent conductive film: a review, *Coatings*, 2020, **10**, 865, doi: 10.3390/coatings10090865.

[241] H. Yang, S. Bai, T. Chen, Y. Zhang, H. Wang, X. Guo, Facile fabrication of large-scale silver nanowire-PEDOT: PSS composite flexible transparent electrodes for flexible touch panels, *Materials Research Express*, 2019, **6**, 086315, doi: 10.1088/2053-1591/ab20d5.

[242] H. Yu, Y. Tian, M. Dirican, D. Fang, C. Yan, J. Xie, D. Jia, Y. Liu, C. Li, M. Cui, H. Liu, G. Chen, X. Zhang, J. Tao, Flexible, transparent and tough silver nanowire/nanocellulose electrodes for flexible touch screen panels, *Carbohydrate Polymers*, 2021, **273**, 118539, doi: 10.1016/j.carbpol.2021.118539.

[243] Z. Wang, B. Jiao, Y. Qing, H. Nan, L. Huang, W. Wei, Y. Peng, F. Yuan, H. Dong, X. Hou, Z. Wu, Flexible and transparent ferroferric oxide-modified silver nanowire film for efficient electromagnetic interference shielding, *ACS Applied Materials & Interfaces*, 2020, **12**, 2826-2834, doi: 10.1021/acsami.9b17513.

[244] F. Qin, Z. Yan, J. Fan, J. Cai, X. Zhu, X. Zhang, Highly uniform and stable transparent electromagnetic interference shielding film based on silver nanowire-PEDOT: PSS composite for high power microwave shielding, *Macromolecular Materials and Engineering*, 2021, **306**, 2000607, doi: 10.1002/mame.202000607.

[245] F. Fang, Y.-Q. Li, H.-M. Xiao, N. Hu, S.-Y. Fu, Layer-structured silver nanowire/polyaniline composite film as a high performance X-band EMI shielding material, *Journal of Materials Chemistry C*, 2016, **4**, 4193-4203, doi: 10.1039/c5tc04406e.

[246] J. Gu, S. Hu, H. Ji, H. Feng, W. Zhao, J. Wei, M. Li, Multi-layer silver nanowire/polyethylene terephthalate mesh structure for highly efficient transparent electromagnetic interference shielding, *Nanotechnology*, 2020, **31**, 185303, doi: 10.1088/1361-6528/ab6d9d.

[247] Z. Ma, S. Kang, J. Ma, L. Shao, Y. Zhang, C. Liu, A. Wei, X. Xiang, L. Wei, J. Gu, Ultraflexible and mechanically strong double-layered aramid nanofiber-Ti_3C_2Tx MXene/silver nanowire nanocomposite papers for high-performance electromagnetic interference shielding, *ACS Nano*, 2020, **14**, 8368-8382, doi: 10.1021/acsnano.0c02401.

[248] S. Li, K. Qian, S. Thaiboonrod, H. Wu, S. Cao, M. Miao, L. Shi, X. Feng, Flexible multilayered aramid nanofiber/silver nanowire films with outstanding thermal durability for electromagnetic interference shielding, *Composites Part A: Applied Science and Manufacturing*, 2021, **151**, 106643, doi: 10.1016/j.compositesa.2021.106643.

[249] F. Zhang, J. Hu, P. Zhao, P. He, H.-Y. Mi, Z. Guo, C. Liu, C. Shen, Multifunctional electromagnetic interference shielding films comprised of multilayered thermoplastic polyurethane membrane and silver nanowire, *Composites Part A: Applied Science and Manufacturing*, 2021, **147**, 106472, doi: 10.1016/j.compositesa.2021.106472.

[250] Z. Wang, Q.-Q. Kong, Z.-L. Yi, L.-J. Xie, H. Jia, J.-P. Chen,

D. Liu, D. Jiang, C.-M. Chen, Electromagnetic interference shielding material for super-broadband: multi-walled carbon nanotube/silver nanowire film with an ultrathin sandwich structure, *Journal of Materials Chemistry A*, 2021, **9**, 25999-26009, doi: 10.1039/d1ta08106c.

[251] Z. Zeng, T. Wu, D. Han, Q. Ren, G. Siqueira, G. Nyström, Ultralight, flexible, and biomimetic nanocellulose/silver nanowire aerogels for electromagnetic interference shielding, *ACS Nano*, 2020, **14**, 2927-2938, doi: 10.1021/acsnano.9b07452.

[252] Y. Yang, N. Wu, B. Li, W. Liu, F. Pan, Z. Zeng, J. Liu, Biomimetic porous MXene sediment-based hydrogel for high-performance and multifunctional electromagnetic interference shielding, *ACS Nano*, 2022, **16**, 15042-15052, doi: 10.1021/acsnano.2c06164.

[253] D. G. Kim, J. H. Choi, D.-K. Choi, S. W. Kim, Highly bendable and durable transparent electromagnetic interference shielding film prepared by wet sintering of silver nanowires, *ACS Applied Materials & Interfaces*, 2018, **10**, 29730-29740, doi: 10.1021/acsami.8b07054.

[254] X. Zhang, Y. Zhong, Y. Yan, Electrical, mechanical, and electromagnetic shielding properties of silver nanowire-based transparent conductive films, *Physica Status Solidi (a)*, 2018, **215**, 1800014, doi: 10.1002/pssa.201800014.

[255] J. H. Choi, K. Y. Lee, S. W. Kim, Ultra-bendable and durable Graphene-Urethane composite/silver nanowire film for flexible transparent electrodes and electromagnetic-interference shielding, *Composites Part B: Engineering*, 2019, **177**, 107406, doi: 10.1016/j.compositesb.2019.107406.

[256] W. Chen, L.-X. Liu, H.-B. Zhang, Z.-Z. Yu, Flexible, transparent, and conductive Ti_3C_2Tx MXene-silver nanowire films with smart acoustic sensitivity for high-performance electromagnetic interference shielding, *ACS Nano*, 2020, **14**, 16643-16653, doi: 10.1021/acsnano.0c01635.

[257] B. Zhou, M. Su, D. Yang, G. Han, Y. Feng, B. Wang, J. Ma, J. Ma, C. Liu, C. Shen, Flexible MXene/silver nanowire-based transparent conductive film with electromagnetic interference shielding and electro-photo-thermal performance, *ACS Applied Materials & Interfaces*, 2020, **12**, 40859-40869, doi: 10.1021/acsami.0c09020.

[258] G. Wang, L. Hao, X. Zhang, S. Tan, M. Zhou, W. Gu, G. Ji, Flexible and transparent silver nanowires/biopolymer film for high-efficient electromagnetic interference shielding, *Journal of Colloid and Interface Science*, 2022, **607**, 89-99, doi: 10.1016/j.jcis.2021.08.190.

[259] X. Zhu, A. Guo, Z. Yan, F. Qin, J. Xu, Y. Ji, C. Kan, PET/Ag NW/PMMA transparent electromagnetic interference shielding films with high stability and flexibility, *Nanoscale*, 2021, **13**, 8067-8076, doi: 10.1039/d1nr00977j.

[260] S. Yang, Y.-Y. Wang, Y.-N. Song, L.-C. Jia, G.-J. Zhong, L. Xu, D.-X. Yan, J. Lei, Z.-M. Li, Ultrathin, flexible and sandwich-structured PHBV/silver nanowire films for high-efficiency electromagnetic interference shielding, *Journal of Materials Chemistry C*, 2021, **9**, 3307-3315, doi: 10.1039/d0tc05266c.

[261] T.-W. Lee, S.-E. Lee, Y. G. Jeong, Highly effective electromagnetic interference shielding materials based on silver nanowire/cellulose papers, *ACS Applied Materials & Interfaces*, 2016, **8**, 13123-13132, doi: 10.1021/acsami.6b02218.

[262] H. Y. Choi, T.-W. Lee, S.-E. Lee, J. Lim, Y. G. Jeong, Silver nanowire/carbon nanotube/cellulose hybrid papers for electrically conductive and electromagnetic interference shielding elements, *Composites Science and Technology*, 2017, **150**, 45-53, doi: 10.1016/j.compscitech.2017.07.008.

[263] Z. Zeng, M. Chen, Y. Pei, S. I. Seyed Shahabadi, B. Che, P. Wang, X. Lu, Ultralight and flexible polyurethane/silver nanowire nanocomposites with unidirectional pores for highly effective electromagnetic shielding, *ACS Applied Materials & Interfaces*, 2017, **9**, 32211-32219, doi: 10.1021/acsami.7b07643.

[264] T. Tian, X. Huang, K. Cheng, Y. Liang, S. Hu, L. Yao, D. Guan, Y. Xu, P. Liu, Flexible and reconfigurable frequency selective surface with wide angular stability fabricated with additive manufacturing procedure, *IEEE Antennas and Wireless Propagation Letters*, 2020, **19**, 2428-2432, doi: 10.1109/lawp.2020.3034944.

[265] K. Sarabandi, N. Behdad, A frequency selective surface with miniaturized elements, *IEEE Transactions on Antennas and Propagation*, 2007, **55**, 1239-1245, doi: 10.1109/tap.2007.895567.

[266] Y. Yang, W. Li, K. N. Salama, A. Shamim, Polarization insensitive and transparent frequency selective surface for dual band GSM shielding, *IEEE Transactions on Antennas and Propagation*, 2021, **69**, 2779-2789, doi: 10.1109/tap.2020.3032827.

[267] H. J. Song, J. H. Schaffner, K. A. Son, J. S. Moon, Optically transparent Ku-band silver nanowire frequency selective surface on glass substrate. 2014 IEEE Antennas and Propagation Society International Symposium (APSURSI). July 6-11, 2014, Memphis, TN, USA. IEEE, 2014, 2100-2101, doi: 10.1109/APS.2014.6905377.

[268] W. Li, S. Yang, A. Shamim, Screen printing of silver nanowires: balancing conductivity with transparency while maintaining flexibility and stretchability, *Npj Flexible Electronics*, 2019, **3**, 13, doi: 10.1038/s41528-019-0057-1.

[269] M. Nogi, N. Komoda, K. Otsuka, K. Suganuma, Foldable nanopaper antennas for origami electronics, *Nanoscale*, 2013, **5**, 4395, doi: 10.1039/c3nr00231d.

[270] T. Rai, P. Dantes, B. Bahreyni, W. S. Kim, A stretchable RF antenna with silver nanowires, *IEEE Electron Device Letters*, 2013, **34**, 544-546, doi: 10.1109/led.2013.2245626.

[271] B. S. Kim, K.-Y. Shin, J. B. Pyo, J. Lee, J. G. Son, S.-S. Lee, J. H. Park, Reversibly stretchable, optically transparent radio-frequency antennas based on wavy Ag nanowire networks, *ACS Applied Materials & Interfaces*, 2016, **8**, 2582-2590, doi: 10.1021/acsami.5b10317.

[272] W. Li, A. Meredov, A. Shamim, Silver nanowire based flexible, transparent, wideband antenna for 5G band application. 2019 IEEE International Symposium on Antennas and Propagation and USNC-URSI Radio Science Meeting. July 7-12, 2019, Atlanta, GA, USA. IEEE, 2019, 275-276, doi: 10.1109/APUSNCURSINRSM.2019.8888371.

[273] L. Cai, S. Zhang, Y. Zhang, J. Li, J. Miao, Q. Wang, Z. Yu, C. Wang, Direct printing for additive patterning of silver nanowires for stretchable sensor and display applications, *Advanced Materials Technologies*, 2018, **3**, 1700232, doi: 10.1002/admt.201700232.

[274] X. Fan, N. Wang, F. Yan, J. Wang, W. Song, Z. Ge, A transfer-printed, stretchable, and reliable strain sensor using PEDOT: PSS/Ag NW hybrid films embedded into elastomers, *Advanced Materials Technologies*, 2018, **3**, 1800030, doi: 10.1002/admt.201800030.

[275] S.-H. Ke, P.-W. Guo, C.-Y. Pang, B. Tian, C.-S. Luo, H.-P. Zhu, W. Wu, Screen-printed flexible strain sensors with Ag nanowires for intelligent and tamper-evident packaging applications, *Advanced Materials Technologies*, 2020, **5**, 1901097, doi: 10.1002/admt.201901097.

[276] Y. Ko, D. Kim, G. Kwon, J. You, High-performance resistive pressure sensor based on elastic composite hydrogel of silver nanowires and poly(ethylene glycol), *Micromachines*, 2018, **9**, 438, doi: 10.3390/mi9090438.

[277] Z. Ma, H. Li, X. Jing, Y. Liu, H.-Y. Mi, Recent advancements in self-healing composite elastomers for flexible strain sensors: materials, healing systems, and features, *Sensors and Actuators A: Physical*, 2021, **329**, 112800, doi: 10.1016/j.sna.2021.112800.

[278] W. Pan, J. Wang, Y.-P. Li, X.-B. Sun, J.-P. Wang, X.-X. Wang, J. Zhang, H.-D. You, G.-F. Yu, Y.-Z. Long, Facile preparation of highly stretchable TPU/Ag nanowire strain sensor with spring-like configuration, *Polymers*, 2020, **12**, 339, doi: 10.3390/polym12020339.

[279] R. Cheng, J. Zeng, B. Wang, J. Li, Z. Cheng, J. Xu, W. Gao, K. Chen, Ultralight, flexible and conductive silver nanowire/nanofibrillated cellulose aerogel for multifunctional strain sensor, *Chemical Engineering Journal*, 2021, **424**, 130565, doi: 10.1016/j.cej.2021.130565.

[280] W. Hu, X. Niu, R. Zhao, Q. Pei, Elastomeric transparent capacitive sensors based on an interpenetrating composite of silver nanowires and polyurethane, *Applied Physics Letters*, 2013, **102**, 083303, doi: 10.1063/1.4794143.

[281] L. G. S. Albano, M. H. Boratto, O. Nunes-Neto, C. F. O. Graeff, Low voltage and high frequency vertical organic field effect transistor based on rod-coating silver nanowires grid electrode, *Organic Electronics*, 2017, **50**, 311-316, doi: 10.1016/j.orgel.2017.08.011.

[282] C. Kim, Y.-H. Kim, Y.-Y. Noh, S.-J. Hong, M. J. Lee, Improved charge injection of metal oxide thin-film transistors by stacked electrodes of indium tin oxide nanoparticles and silver nanowires, *Advanced Electronic Materials*, 2018, **4**, 1700440, doi: 10.1002/aelm.201700440.

[283] J. Liang, L. Li, D. Chen, T. Hajagos, Z. Ren, S.-Y. Chou, W. Hu, Q. Pei, Intrinsically stretchable and transparent thin-film transistors based on printable silver nanowires, carbon nanotubes and an elastomeric dielectric, *Nature Communications*, 2015, **6**, 7647, doi: 10.1038/ncomms8647.

[284] Z. Cui, Y. Han, Q. Huang, J. Dong, Y. Zhu, Electrohydrodynamic printing of silver nanowires for flexible and stretchable electronics, *Nanoscale*, 2018, **10**, 6806-6811, doi: 10.1039/c7nr09570h.

[285] W. Li, A. Meredov, A. Shamim, Coat-and-print patterning of silver nanowires for flexible and transparent electronics, *Npj Flexible Electronics*, 2019, **3**, 19, doi: 10.1038/s41528-019-0063-3.

[286] Z. Ma, X. Xiang, L. Shao, Y. Zhang, J. Gu, Multifunctional wearable silver nanowire decorated leather nanocomposites for joule heating, electromagnetic interference shielding and piezoresistive sensing, *Angewandte Chemie International Edition*, 2022, **61**, e202200705, doi: 10.1002/anie.202200705.

[287] S. Yao, J. Yang, F. R. Poblete, X. Hu, Y. Zhu, Multifunctional electronic textiles using silver nanowire composites, ACS *Applied Materials & Interfaces*, 2019, **11**, 31028-31037, doi: 10.1021/acsami.9b07520.

[288] Q. Sun, L. Wang, G. Ren, L. Zhang, H. Sheng, Y. Zhu, H. Wang, G. Lu, H.-D. Yu, W. Huang, Smart band-aid: Multifunctional and wearable electronic device for self-powered motion monitoring and human-machine interaction, *Nano Energy*, 2022, **92**, 106840, doi: 10.1016/j.nanoen.2021.106840.

[289] M. Zhao, D. Li, J. Huang, D. Wang, A. Mensah, Q. Wei, A multifunctional and highly stretchable electronic device based on silver nanowire/wrap yarn composite for a wearable strain sensor and heater, *Journal of Materials Chemistry C*, 2019, **7**, 13468-13476, doi: 10.1039/c9tc04252k.

[290] L.-X. Liu, W. Chen, H.-B. Zhang, Q.-W. Wang, F. Guan, Z.-Z. Yu, Flexible and multifunctional silk textiles with biomimetic leaf-like MXene/silver nanowire nanostructures for electromagnetic interference shielding, humidity monitoring, and self-derived hydrophobicity, *Advanced Functional Materials*, 2019, **29**, 1905197, doi: 10.1002/adfm.201905197.

[291] H. Kim, S.-K. Ahn, D. M. Mackie, J. Kwon, S. H. Kim, C.

Choi, Y. H. Moon, H. B. Lee, S. H. Ko, Shape morphing smart 3D actuator materials for micro soft robot, *Materials Today*, 2020, **41**, 243-269, doi: 10.1016/j.mattod.2020.06.005.

[292] P. Won, K. K. Kim, H. Kim, J. J. Park, I. Ha, J. Shin, J. Jung, H. Cho, J. Kwon, H. Lee, S. H. Ko, Transparent soft actuators/sensors and camouflage skins for imperceptible soft robotics, *Advanced Materials*, 2021, **33**, 2002397, doi: 10.1002/adma.202002397.

[293] H. Kim, H. Lee, I. Ha, J. Jung, P. Won, H. Cho, J. Yeo, S. Hong, S. Han, J. Kwon, K.-J. Cho, S. H. Ko, Biomimetic color changing anisotropic soft actuators with integrated metal nanowire percolation network transparent heaters for soft robotics, *Advanced Functional Materials*, 2018, **28**, 1801847, doi: 10.1002/adfm.201801847.

[294] H. Kim, J. Choi, K. K. Kim, P. Won, S. Hong, S. H. Ko, Biomimetic chameleon soft robot with artificial crypsis and disruptive coloration skin, *Nature Communications*, 2021, **12**, 4658, doi: 10.1038/s41467-021-24916-w.

[295] J. Han, J. Yang, W. Gao, H. Bai, Ice-templated, large-area silver nanowire pattern for flexible transparent electrode, *Advanced Functional Materials*, 2021, **31**, 2010155, doi: 10.1002/adfm.202010155.

[296] I. S. Jin, J. Choi, J. W. Jung, Silver-nanowire-embedded photopolymer films for transparent film heaters with ultra-flexibility, quick thermal response, and mechanical reliability, *Advanced Electronic Materials*, 2021, **7**, 2000698, doi: 10.1002/aelm.202000698.

[297] S. J. Lee, J.-W. Kim, J. H. Park, Y. Porte, J.-H. Kim, J.-W. Park, S. Kim, J.-M. Myoung, SWCNT-Ag nanowire composite for transparent stretchable film heater with enhanced electrical stability, *Journal of Materials Science*, 2018, **53**, 12284-12294, doi: 10.1007/s10853-018-2526-7.

[298] J.-H. Park, H.-J. Seok, E. Kamaraj, S. Park, H.-K. Kim, Highly transparent and flexible Ag nanowire-embedded silk fibroin electrodes for biocompatible flexible and transparent heater, *RSC Advances*, 2020, **10**, 31856-31862, doi: 10.1039/d0ra05990k.

[299] S. Duan, Z. Wang, L. Zhang, J. Liu, C. Li, A highly stretchable, sensitive, and transparent strain sensor based on binary hybrid network consisting of hierarchical multiscale metal nanowires, *Advanced Materials Technologies*, 2018, **3**, 1800020, doi: 10.1002/admt.201800020.

[300] D. T. Papanastasiou, A. Schultheiss, D. Muñoz-Rojas, C. Celle, A. Carella, J.-P. Simonato, D. Bellet, Transparent heaters: A review, *Advanced Functional Materials*, 2020, **30**, 1910225, doi: 10.1002/adfm.201910225.

[301] X. He, F. Duan, J. Liu, Q. Lan, J. Wu, C. Yang, W. Yang, Q. Zeng, H. Wang, Transparent electrode based on silver nanowires and polyimide for film heater and flexible solar cell, Materials, 2017, **10**, 1362, doi: 10.3390/ma10121362.

[302] J. Liu, Y. Ge, D. Zhang, M. Han, M. Li, M. Zhang, X. Duan, Z. Yang, J. Hu, Plasma cleaning and self-limited welding of silver nanowire films for flexible transparent conductors, *ACS Applied Nano Materials*, 2021, **4**, 1664-1671, doi: 10.1021/acsanm.0c03137.

[303] M. Patel, J. H. Seo, S. Kim, T. T. Nguyen, M. Kumar, J. Yun, J. Kim, Photovoltaic-driven transparent heater of ZnO-coated silver nanowire networks for self-functional remote power system, *Journal of Power Sources*, 2021, **491**, 229578, doi: 10.1016/j.jpowsour.2021.229578.

[304] B. Zheng, Q. Zhu, Y. Zhao, Fabrication of high-quality silver nanowire conductive film and its application for transparent film heaters, *Journal of Materials Science & Technology*, 2021, **71**, 221-227, doi: 10.1016/j.jmst.2020.07.021.

[305] H. Moon, H. Lee, J. Kwon, Y. D. Suh, D. K. Kim, I. Ha, J. Yeo, S. Hong, S. H. Ko, Ag/Au/polypyrrole core-shell nanowire network for transparent, stretchable and flexible supercapacitor in wearable energy devices, *Scientific Reports*, 2017, **7**, 41981, doi: 10.1038/srep41981.

[306] I. Chang, T. Park, J. Lee, M. H. Lee, S. H. Ko, S. W. Cha, Bendable polymer electrolyte fuel cell using highly flexible Ag nanowire percolation network current collectors, *Journal of Materials Chemistry A*, 2013, **1**, 8541, doi: 10.1039/c3ta11699a.

[307] L. Zeng, T. S. Zhao, L. An, A high-performance supportless silver nanowire catalyst for anion exchange membrane fuel cells, *Journal of Materials Chemistry A*, 2015, **3**, 1410-1416, doi: 10.1039/c4ta05005c.

[308] H. Lee, S. Hong, J. Lee, Y. D. Suh, J. Kwon, H. Moon, H. Kim, J. Yeo, S. H. Ko, Highly stretchable and transparent supercapacitor by Ag-Au core-shell nanowire network with high electrochemical stability, *ACS Applied Materials & Interfaces*, 2016, **8**, 15449-15458, doi: 10.1021/acsami.6b04364.

[309] I. Chang, T. Park, J. Lee, H. B. Lee, S. Ji, M. H. Lee, S. H. Ko, S. W. Cha, Performance enhancement in bendable fuel cell using highly conductive Ag nanowires, *International Journal of Hydrogen Energy*, 2014, **39**, 7422-7427, doi: 10.1016/j.ijhydene.2014.03.017.

[310] T. Park, I. Chang, H. B. Lee, S. H. Ko, S. W. Cha, Performance variation of bendable polymer electrolyte fuel cell based on Ag nanowire current collector under mixed bending and twisting load, *International Journal of Hydrogen Energy*, 2017, **42**, 1884-1890, doi: 10.1016/j.ijhydene.2016.08.022.

[311] H. Kim, K. R. Pyun, M.-T. Lee, H. B. Lee, S. H. Ko, Recent advances in sustainable wearable energy devices with nanoscale materials and macroscale structures, *Advanced Functional Materials*, 2022, **32**, 2110535, doi: 10.1002/adfm.202110535.

[312] J. Jung, H. Cho, R. Yuksel, D. Kim, H. Lee, J. Kwon, P. Lee, J. Yeo, S. Hong, H. E. Unalan, S. Han, S. H. Ko,

Stretchable/flexible silver nanowire electrodes for energy device applications, *Nanoscale*, 2019, **11**, 20356-20378, doi: 10.1039/c9nr04193a.
[313] H. Du, Y. Pan, X. Zhang, F. Cao, T. Wan, H. Du, R. Joshi, D. Chu, Silver nanowire/nickel hydroxide nanosheet composite for a transparent electrode and all-solid-state supercapacitor, *Nanoscale Advances*, 2019, **1**, 140-146, doi: 10.1039/c8na00110c.
[314] H. Li, X. Li, J. Liang, Y. Chen, Hydrous RuO_2-decorated MXene coordinating with silver nanowire inks enabling fully printed micro-supercapacitors with extraordinary volumetric performance, *Advanced Energy Materials*, 2019, **9**, 1803987, doi: 10.1002/aenm.201803987.
[315] X. Liu, D. Li, X. Chen, W.-Y. Lai, W. Huang, Highly transparent and flexible all-solid-state supercapacitors based on ultralong silver nanowire conductive networks, *ACS Applied Materials & Interfaces*, 2018, **10**, 32536-32542, doi: 10.1021/acsami.8b10138.
[316] J. Zhi, W. Zhao, X. Liu, A. Chen, Z. Liu, F. Huang, Highly conductive ordered mesoporous carbon-based electrodes decorated by 3D graphene and 1D silver nanowire for flexible supercapacitor, *Advanced Functional Materials*, 2014, **24**, 2013-2019, doi: 10.1002/adfm.201303082.
[317] S. Jeong, H. Cho, S. Han, P. Won, H. Lee, S. Hong, J. Yeo, J. Kwon, S. H. Ko, High efficiency, transparent, reusable, and active PM2.5 filters by hierarchical Ag nanowire percolation network, *Nano Letters*, 2017, **17**, 4339-4346, doi: 10.1021/acs.nanolett.7b01404.
[318] K. Park, S. Kang, J.-W. Park, J. Hwang, Fabrication of silver nanowire coated fibrous air filter medium via a two-step process of electrospinning and electrospray for anti-bioaerosol treatment, *Journal of Hazardous Materials*, 2021, **411**, 125043, doi: 10.1016/j.jhazmat.2021.125043.
[319] H. H. Khaligh, I. A. Goldthorpe, Failure of silver nanowire transparent electrodes under current flow, *Nanoscale Research Letters*, 2013, **8**, 235, doi: 10.1186/1556-276x-8-235.
[320] S. Ye, A. R. Rathmell, Z. Chen, I. E. Stewart, B. J. Wiley, Metal nanowire networks: the next generation of transparent conductors, *Advanced Materials*, 2014, **26**, 6670-6687, doi: 10.1002/adma.201402710.
[321] F. Cui, Y. Yu, L. Dou, J. Sun, Q. Yang, C. Schildknecht, K. Schierle-Arndt, P. Yang, Synthesis of ultrathin copper nanowires using tris(trimethylsilyl)silane for high-performance and low-haze transparent conductors, *Nano Letters*, 2015, **15**, 7610-7615, doi: 10.1021/acs.nanolett.5b03422.
[322] S. Ding, J. Jiu, Y. Gao, Y. Tian, T. Araki, T. Sugahara, S. Nagao, M. Nogi, H. Koga, K. Suganuma, H. Uchida, One-step fabrication of stretchable copper nanowire conductors by a fast photonic sintering technique and its application in wearable devices, *ACS Applied Materials & Interfaces*, 2016, **8**, 6190-6199, doi: 10.1021/acsami.5b10802.
[323] S. Han, S. Hong, J. Ham, J. Yeo, J. Lee, B. Kang, P. Lee, J. Kwon, S. S. Lee, M.-Y. Yang, S. H. Ko, Fast plasmonic laser nanowelding for a Cu-nanowire percolation network for flexible transparent conductors and stretchable electronics, *Advanced Materials*, 2014, **26**, 5808-5814, doi: 10.1002/adma.201400474.
[324] D. Zhang, R. Wang, M. Wen, D. Weng, X. Cui, J. Sun, H. Li, Y. Lu, Synthesis of ultralong copper nanowires for high-performance transparent electrodes, *Journal of the American Chemical Society*, 2012, **134**, 14283-14286, doi: 10.1021/ja3050184.

Author Information

Longxia Yang *received her bachelor's degree from the Nanjing University of Materials Chemistry in 2020. She is currently studying for a Ph.D. degree at General Research Institute for Nonferrous Metals of Materials Science and Engineering. Her research interests include nanocomposites, and electromagnetic functional materials.*

Xianjun Huang *received his Ph.D from University of Manchester in 2016, and obtained Bachelor and M.Sc degrees from National University of Defense Technology (NUDT), China in 2011 and 2013. He is now an Associate Professor in NUDT. His main research focuses on electromagnetic functional materials and devices.*

Huating Wu *received her master's degree from State key Laboratory of Advanced Materials for Smart Sensing, GRINM Group Co., Ltd. in 2018. She is now an engineer of Advanced Electronic Materials Division, GRIMAT Engineering Institute Co., Ltd.. Her research interests include nano-functional materials and vacuum maintenance materials.*

Yuanlong Liang *received his bachelor's degree from Xiamen University in 2015, and obtained master's degree from Lanzhou University in 2018. He is currently pursuing the Ph.D. degree in electronic science and technology at*

National University of Defense Technology. His research interest focuses on electromagnetic shielding materials.

***Mao Ye** received his master degree from the Institute of Advanced Materials (IAM), Nanjing University of Posts & Telecommunications in 2018. He is currently a PhD candidate fellow in Prof. Litao Sun's group in SEU-FEI Nano-Pico Center at Southeast University. His PhD research focuses on in-situ liquid cell TEM characterization.*

***Wencong Liu** received his bachelor's degree of Electronic Science and Engineering from National University of Defense Technology (NUDT) in 2018. He is now an MSc student in NUDT and his main research interest is microwave absorbing materials.*

***Faling Li** received her bachelor's degree from the Central South University in 2021. She is currently studying for a master's degree at General Research Institute for Nonferrous Metals. Her research focus on the design and fabrication of silver nanowires based electromagnetic shielding materials.*

***Tao Xu** received his BS(2009) PhD(2016) degree from Southeast University under the supervision of Prof. Litao Sun. He was appointed to the faulty after graduating from the School of Electronic Science and Engineering in 2016. His current research interests focus on nanoscale structural evolution of electronic materials under various stimuli, and the development of fabrication methodologies for nanoscale materials.*

***Haicheng Wang** received his Ph.D. from University of Science and Technology Beijing in 2008. He worked as a visiting professor in Lawrence Berkeley National Laboratory from 2014 to 2015. He is now a professor in General Research Institute for Nonferrous Metals. His research group focuses on multi-functional nanocomposites, electromagnetic materials and devices.*